

THESIS FOR THE DEGREE OF DOCTOR OF PHILOSOPHY

# Exploring functionalization of colloidal silica for nanoparticle-stabilized emulsions

Sanna Björkegren



Department of Chemistry and Chemical Engineering

CHALMERS UNIVERSITY OF TECHNOLOGY

Gothenburg, Sweden 2019

Exploring functionalization of colloidal silica for nanoparticle-stabilized emulsions

SANNA BJÖRKEGREN

ISBN: 978-91-7905-171-6

© SANNA BJÖRKEGREN, 2019.

Doktorsavhandling vid Chalmers tekniska högskola

Ny serie nr: 4638

ISSN: 0346-718X

Department of Chemistry and Chemical Engineering

Chalmers University of Technology

SE-412 96 Gothenburg

Sweden

Telephone + 46 (0)31-772 1000

Cover:

“Watercolor phase inversion”, by Elin Bergman

Printed by Chalmers Reproservice

Gothenburg, Sweden 2019

# Exploring functionalization of colloidal silica for nanoparticle-stabilized emulsions

SANNA BJÖRKEGREN

Department of Chemistry and Chemical Engineering  
Chalmers University of Technology

## ABSTRACT

The main objective of this thesis was to evaluate how surface functionalized colloidal silica can be utilized in emulsions stabilized solely by particles, so called Pickering emulsions. To achieve this, water-dispersed silica nanoparticles were functionalized with hydrophilic and hydrophobic groups. The surface coverage of the functional groups was studied using NMR spectroscopy, including diffusometry. To further explore the attained properties of the modified particles, these have been studied using zeta potential and surface charge measurements. In addition, studies of how pH affects the flocculation of the functionalized silica sols have been performed. Hydrophilic functionalization of the silica sols was achieved by attaching methyl poly(ethylene glycol) silane (mPEG silane) to the silica particle surface. This resulted in an efficient reduction of surface charge density, a pH dependent and controllable flocculation behavior and surface active particles. These properties are beneficial for emulsion formulation. In addition, temperature-dependent phase-separation of the silica suspensions was attained. The observed cloud-points were influenced by interparticle interactions and conformational changes of the grafted PEG-chains, and these could be controlled by electrolyte concentration and pH. To increase the particle-oil interaction, hydrophobic functionalization of the silica particles was performed by attaching organosilanes containing methyl, propyl and octyl groups.

Emulsification performance was evaluated by preparing emulsions using particles, functionalized with varying degrees and combinations of hydrophilic and hydrophobic groups, as stabilizers. It was found that colloidal silica functionalized with hydrophobic groups produced emulsions with smaller emulsion droplets compared to using unmodified silica. The emulsification performance was further improved by attachment of both mPEG silane and hydrophobic organosilanes such as a propyl silane. The balance between hydrophilic and hydrophobic groups is important, where a high degree of mPEG silane renders particles too hydrophilic to be efficient as emulsifiers. When studying the effect of silica particle size, it was found that smaller particles reduce the median emulsion droplet size, due to the larger surface area available for stabilization. The pH and the salt concentration are important for efficient emulsion droplet formation. Low pH conditions provide flocculated particles owing to the mPEG silane functionalization and the PEG-silica interactions. Pickering emulsions obtained display a high stability towards coalescence over a long period of time (from five weeks to at least five years).

By exploiting the clouding behavior observed for mPEG-grafted particles, phase inversions of butanol emulsions were observed, triggered through changing the temperature during emulsion preparation. Inversions were achieved in emulsions stabilized by particles modified with both mPEG and propyl silane, and the reversibility of the system was also studied. Electrolyte concentration and pH affect the phase inversion temperature, e.g. through salting-out effects and surface charge reductions, which decrease the inversion temperature. Understanding the phase inversion conditions of particle-stabilized emulsions could expand the use of these surfactant-free emulsions in industrial applications and facilitate emulsion fabrication.

Keywords: functionalized colloidal silica, Pickering emulsions, NMR spectroscopy, surface activity, clouding, thermo-responsive emulsions

## List of publications

This thesis is based on the following publications (referred to as Paper I, II, III and IV in the text):

- I. Surface activity and flocculation behavior of polyethylene glycol-functionalized silica nanoparticles  
Sanna Björkegren, Lars Nordstierna, Anders Törnecrona, Michael Persson and Anders Palmqvist, *Journal of Colloid and Interface Science*, 2015. 452: pp. 215-223
- II. Clouding observed for surface active, mPEG-grafted silica nanoparticles  
Sanna Björkegren, Lars Nordstierna, Andreas Sundblom and Anders Palmqvist  
*RSC Advances*, 2019. 9: pp. 13297-13303.
- III. Hydrophilic and hydrophobic modifications of silica particles for Pickering emulsions  
Sanna Björkegren, Lars Nordstierna, Anders Törnecrona and Anders Palmqvist,  
*Journal of Colloid and Interface Science*, 2017. 487: pp. 250–257
- IV. Thermo-responsive Pickering emulsions stabilized by surface functionalized, colloidal silica  
Sanna Björkegren, Maria Costa Artur Freixiela Dias, Kristina Lundahl, Lars Nordstierna and Anders Palmqvist  
Submitted for publication in *Langmuir*, under revision

## Additional publication not included in this thesis:

A new emulsion liquid membrane based on a palm oil for the extraction of heavy metals

Sanna Björkegren\*, Rose Fassihi Karimi\*, Anna Martinelli, Natesan Jayakumar and Mohammad Ali Hashim

*Membranes*, 2015. 5: pp. 168-179

\*Contributed equally in performing the experimental work

### Author's contribution to the listed publications:

- I. Planned the study, performed all experimental work, except for the NMR measurements, which were performed and analyzed together with co-author, and wrote the manuscript, with inputs from the other co-authors.
- II. Planned the study, performed all experimental work and wrote the manuscript, with inputs from the other co-authors.
- III. Planned the study, performed all experimental work and wrote the manuscript, with inputs from the other co-authors.
- IV. Planned the study and performed the experimental work together with co-author, and wrote the manuscript, with inputs from the other co-authors.



## Table of Contents

Introduction .....	1
Background .....	5
Emulsions.....	5
Particle-stabilized (Pickering) emulsions.....	6
Emulsion destabilization mechanisms .....	9
Emulsion properties .....	10
Amorphous colloidal silica.....	13
Colloidal silica by hydrolysis of alkoxy silanes.....	13
Fumed silica .....	14
Silica sols from sodium silicate.....	14
Surface chemistry of silica particles and stability aspects.....	16
Surface modification.....	18
Materials and methods.....	21
Materials.....	21
Methods for analysis .....	22
NMR spectroscopy.....	22
Dynamic light scattering.....	24
Titrations and surface charge .....	25
Emulsion droplet sizing .....	26
Surface and interfacial tension with the DuNoüy ring method .....	26
UV-Vis spectroscopy.....	27
Elemental analysis .....	27
Experimental procedures .....	27
Functionalization of silica nanoparticles.....	27
Determination of surface functionalization yield.....	27
Emulsion preparation.....	28
Cloud point and phase inversion studies.....	28
Results and discussion .....	29
Surface functionalized silica nanoparticles .....	29
Functionalization procedure.....	29
Colloidal properties of the functionalized particles .....	33
Silica particles with clouding behavior .....	41
Utilization of the surface functionalized silica nanoparticles in emulsions .....	43
General findings – emulsification .....	43
Exploring phase inversion conditions.....	47
Discussion and perspectives .....	55
Concluding remarks .....	57
Abbreviations.....	61
Acknowledgements.....	62
References .....	65





To Emy and Agnes  
You fill my life with happiness



# INTRODUCTION

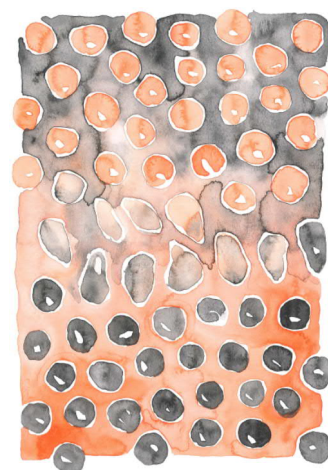


Figure 1. Examples of a successful emulsification, and a failed one. The homemade mayonnaise was made by adding oil to vinegar and egg, during continuous blending, creating a concentrated o/w emulsion stabilized by proteins and lecithin. Their containers are of glass – a material composed mainly of silica.

Emulsions have been used for thousands of years; emulsified paints were prepared already around 2000 BC when the ancient Egyptians used egg yolk to emulsify berry extracts. Today, a broad use of emulsions exists and examples include personal care products such as skin lotions and cosmetics, pharmaceutical products such as for topological skin creams<sup>1</sup> and drug delivery,<sup>2</sup> emulsion paints and coatings,<sup>3</sup> and food products such as margarine spreads.<sup>4, 5</sup> Emulsions can also be used as templates for producing e.g. porous materials<sup>6</sup> and foams<sup>7</sup>, and as reaction mediums.<sup>8</sup> A simple emulsion is composed of two immiscible liquids, mixed together to a kinetically stable blend, made possible through addition of an emulsifying agent. An efficient emulsifier has an affinity for both liquid phases, and stabilizes the mixture through adsorbing at the interface between these, which decreases the interfacial energy. The components are often oil and water, and the stabilizer can be

surface active agents (surfactant molecules), surface active polymers, proteins, solid particles, or combinations thereof.

The first scientific report on the formation of both emulsions and foams stabilized by solid particles was a paper written by Prof. Walter Ramsden in 1903.<sup>9</sup> Four years later, Prof. Spencer Pickering published a paper that further described the phenomena of particle-stabilized emulsions,<sup>10</sup> prepared with what he referred to as “insoluble emulsifiers”, such as lime and precipitated sulfate salts of copper, zinc and nickel. Pickering accurately cites the work of Ramsden several times, and he writes for example the following<sup>10</sup>: “That the formation of a pellicle of solid particles over the oil globules affords an explanation of emulsification, is, as has been mentioned, the conclusion to which Dr. Ramsden also was led, and the view that such a pellicle exists in the case of the oil globules in milk was advocated long ago”. Despite this, the term Pickering emulsion (instead of

Ramsden emulsion) was coined to denote particle-stabilized emulsions. Other important contributions were published during the 1920s, for example Briggs<sup>11</sup> who discussed weak flocculation of the colloids as a mean of enabling emulsification, and Finkle et al.<sup>12</sup> put forward the foundation for Finkle's rule, stating that the phase that more efficiently wets the solid will most likely constitute the continuous phase, and this is determined by the contact angle. During the last two decades, a renewed interest for particle-stabilized emulsions has emerged, seen for example in the vast number of reviews being published on the subject lately, of which a few are referred to here.<sup>1, 2, 4, 13-18</sup> There can be many advantages of Pickering emulsions compared to traditional emulsions stabilized by surfactants and various types of particles have been shown to be effective as emulsion stabilizers (examples in the right margin).<sup>1, 2, 16, 17, 19</sup> Particles of silicon dioxide, or silica for short, are probably the most studied in model systems of Pickering emulsions<sup>1</sup> and also the particles of interest in this thesis.

Silica is the major component of the crust of the earth. Rocks and soil are composed of silicate minerals; sand is mainly composed of silicates and silica.<sup>18, 19</sup> Most forms of silica materials are made up of tetrahedra  $\text{SiO}_4$  units, with shared oxygen atoms, forming a network. The materials have different structures that depend on the arrangement of the  $\text{SiO}_4$  units. Perfectly ordered arrangements of the tetrahedra results in crystalline silica material, such as quartz, whereas disordered arrangements are found in amorphous silicas, which is the type of silica studied in this thesis.<sup>20, 21</sup> Amorphous colloidal silica suspended in water, known as silica sols, has, in similarity to emulsion systems, a vast number of uses in industrial processes and exists in numerous commercial products. Examples are retention aids in paper making, additives in paints and ceramics, for beverage clarification, as binder for catalyst manufacture, in chromatography equipment and in polishing products.<sup>22</sup> There is a large particle size range of commercial colloidal silica available, and most sols have a relatively narrow particle size distribution. Silica particles are inherently hydrophilic and in order to promote adsorption at the interfaces of the emulsion droplets, functionalization of the silica surface may be performed. A typical functionalization reduces the concentration of the surface silanol groups, decreases the surface energy and surface charge density of the particles and makes the surface more hydrophobic.<sup>23</sup>

Examples of solid particles used for emulsion stabilization<sup>1, 2, 16, 17, 19</sup>

Silica particles, such as colloidal silica and fumed silica

Porous particles

Starch, natural or modified

Clay, bentonite, often disc-like structure

Fat particles, solid lipid nanoparticles

Aggregated proteins, proteins adsorbed on particles

Polymeric particles, e.g. polystyrene and chitosan

Microgels

Cellulose nanocrystals, nanocellulose

Carbon

Organic and inorganic pigments,

Silver and gold (nano)particles

Titania

Iron oxides

Calcium carbonate

Latex

Most hydrophilic particles are surface modified, often by adsorption of surfactants, and charged particles can be activated through e.g. salt addition.

## Purpose of the thesis

The research in this thesis is dedicated to surface functionalized silica nanoparticles and their use in emulsion formulations. By preparing emulsions stabilized by particles, which had been functionalized with varying degrees and combinations of hydrophilic and hydrophobic groups, evaluation of the emulsification performance could be performed, including studies of emulsion phase inversion conditions. Prior to emulsification studies, colloidal properties of the functionalized particles were evaluated, since these effect the properties of the emulsions obtained.

As indicated above, functionalization of the particles was required in order to gain control of the particle wettability, and, in the case of silica, increase the hydrophobic character of the particle, enabling adsorption at an oil-water interface and stabilization of an emulsion system. Subsequently, preparation and characterization of silica sols with hydrophilic and hydrophobic groups were the initiation of this work. The silica particles were characterized in various ways, in order to gain control of the functionalization process and to be able to elucidate the types and amounts of surface species required for obtaining functioning emulsifying agents. The amount of surface functionalization on the silica particles was determined, the stability of the colloidal system was evaluated and the obtained colloidal properties were further studied.

Subsequently, emulsification abilities were evaluated for particles with a broad range of surface functionalization. Thermo-responsiveness of the particles and temperature-induced phase inversions of the emulsions have been examined. Different emulsification conditions were employed, such as variations in salt concentration, pH conditions and temperature.

The work presented in this thesis has resulted in four scientific articles. In Paper I silica particles were functionalized with a methylated poly(ethylene glycol) silane (mPEG silane), with the aim to investigate the functionalization procedure, characterization methods and the altered surface chemical properties obtained, such as surface activity. Silica surfaces grafted with poly(ethylene oxide) (PEO) or poly(ethylene glycol) (PEG) have been frequently studied<sup>24-26</sup> and PEGylated particles exist in e.g. biomedical applications.<sup>27, 28</sup> However, PEG-grafted particles prepared through a process in purely aqueous conditions are not as recurrent. Paper II concerns the clouding behavior observed for the mPEG-functionalized particles, arising from the reverse solubility vs. temperature relationship of PEG-chains in water.<sup>3, 29-31</sup> Clouding in the mPEG-grafted silica particle-system will also depend on interparticle and PEG-silica interactions, studied through investigations at varying pH-conditions and salt concentrations.

Paper III reports on silica particles functionalized with both hydrophilic and hydrophobic species, also prepared in a water-based system, with the aim to produce efficient emulsifiers with controlled wettability. The mPEG silane constituted the hydrophilic part of the modification while the hydrophobic functionalization was accomplished by using organosilanes containing methyl, propyl or octyl groups. The hydrophilic mPEG group employed here provides additional properties beneficial for studying emulsification behavior, and the hydrophobic modifications are required to obtain stable o/w emulsions. The clouding behavior observed and studied in Paper II allowed investigations of phase inversion conditions, explored in Paper IV. Phase inversion temperatures, of emulsions stabilized by silica particles functionalized with propyl and mPEG silanes, were determined at varying emulsification conditions, a phenomenon well-studied in

surfactant systems.<sup>30-37</sup> Applying phase inversion studies in Pickering emulsions could broaden the applicability, facilitate emulsion preparation and contribute to the understandings of the particle-stabilized emulsion systems.

## BACKGROUND



## Emulsions

Emulsions are mixtures of two immiscible phases, with one phase dispersed in the other continuous phase. In the simple, two-phase, emulsion, oil droplets are dispersed in water, or water droplets are dispersed in oil, producing oil-in-water (o/w) or water-in-oil (w/o) emulsions, respectively. However, at a fluid-fluid interface, an interfacial tension exists, often explained as a consequence of a force imbalance, and this is exemplified in Figure 2; at an interface, an asymmetry of cohesive forces exists, which gives rise to a certain interfacial tension.<sup>3</sup> When the interface is the air-water interface, interfacial tension is referred to as surface tension. The magnitude of the surface tension is correlated to the cohesive energy in the fluid. Water has a high cohesive energy density and therefore also a relatively high surface tension.

Phase separation in for example mixtures of oil and water is driven by a minimization of the contact area between the phases, due to the existence of the interfacial tension, which is why a third component, an emulsifier, is added to the mixture and this enables creation of stable emulsions. Surface active species such as surfactants are commonly used as emulsifiers.<sup>3, 38</sup> These are amphiphilic molecules that consist of one hydrophilic and one hydrophobic part, providing a driving force for the molecule to assemble at interfaces. When added to water, surfactants will quickly cover all interfaces until the critical micelle concentration is

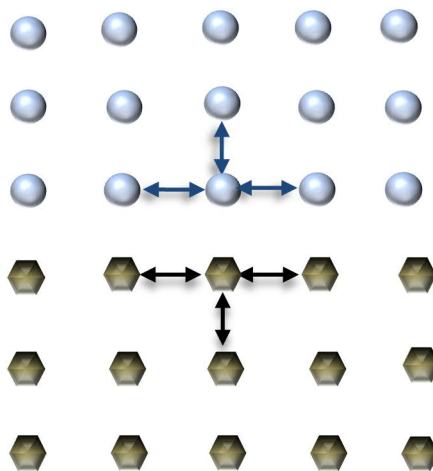


Figure 2. Upper image: Surface tension is what holds a drop of water together. Lower image: Schematic illustration of the imbalance of forces at an interface that causes interfacial tension: a molecule in the bulk liquid senses identical intermolecular forces in all directions, while a molecule at the interface lacks this attraction in one direction. Redrawn from Holmberg et. al.<sup>3</sup>

reached, resulting in a reduction of the surface tension.<sup>3</sup> Simultaneously, addition of surfactants to oil/water mixtures leads to a reduction of interfacial tension, which enables stabilization of small emulsion droplets, where the surface area between oil and water increases enormously.

The emulsifier will not only hinder fast phase-separation, it also affects which type of emulsion that forms, depending on the hydrophilic-lipophilic balance (HLB) of the system. An indication of the efficiency of the emulsifier is obtained through measuring the surface tension of the emulsifier in dissolved or suspended in water. Emulsions stabilized by surfactants are often referred to as traditional emulsions, but these are not the topic here. This thesis is dedicated to surfactant-free emulsions stabilized by solid particles.

## Particle-stabilized (Pickering) emulsions

Solid particles can work very well as emulsion stabilizers; a particle adsorbed at the oil/water interface will efficiently hinder emulsion droplet coalescence, through creation of a mechanical barrier between the phases.<sup>9-11, 39-41</sup> A remarkably high stability towards coalescence is a feature that characterizes particle-stabilized emulsions, and also a desirable property in many applications. Much research has been devoted to understand Pickering emulsion systems and develop their application areas since the first reports in the 1920s. Tambe and Sharma et al.<sup>41-43</sup> reported on emulsion stability aspects during the 1990s, and Midmore<sup>40, 44, 45</sup> investigated e.g. phase composition. Binks and colleagues<sup>19, 46, 47</sup> have, since the late 1990s, thoroughly investigated Pickering emulsion systems stabilized by particles of varying hydrophobicities, size ranges and shapes. The effects of various emulsification conditions such as salt concentration, oil-to-aqueous phase ratios, oil type and additives such as surfactants have been investigated,<sup>16, 39, 48-56</sup> as well as theoretical and experimental approaches to determine the particle contact angle at the interfaces.<sup>57, 58</sup> Chevalier, Frelichowska, and colleagues<sup>59-63</sup> have studied Pickering emulsion for e.g. pharmaceutical applications and emulsion polymerization. Another important application area is the food industry, studied for example by Dickinson<sup>4, 5</sup> and Murray et al.<sup>13, 64</sup> The mentioned groups are just a few examples, and the field has grown enormously in recent years and a vast amount of articles on the subject exist.

Emulsions prepared with particles acting as emulsifiers are similar to traditional (surfactant-stabilized) emulsions in many ways; however, a few differences exist. While the ability to reduce the interfacial tension is a vital parameter for the surfactants' effectiveness, it may not be a necessity in the case of particles. Surface-active particles exist, and these accumulate at interfaces<sup>19, 64</sup>, but long-lived emulsions can be produced without reduction of the interfacial tension.<sup>65</sup> Surfactants are always amphiphilic, while particles generally are not. Particles need, however, to be wetted by both phases, thus be partly hydrophilic and partly hydrophobic.<sup>17</sup> The liquid of higher wetting capacity will normally constitute the continuous phase of the emulsion, as illustrated in Figure 3.



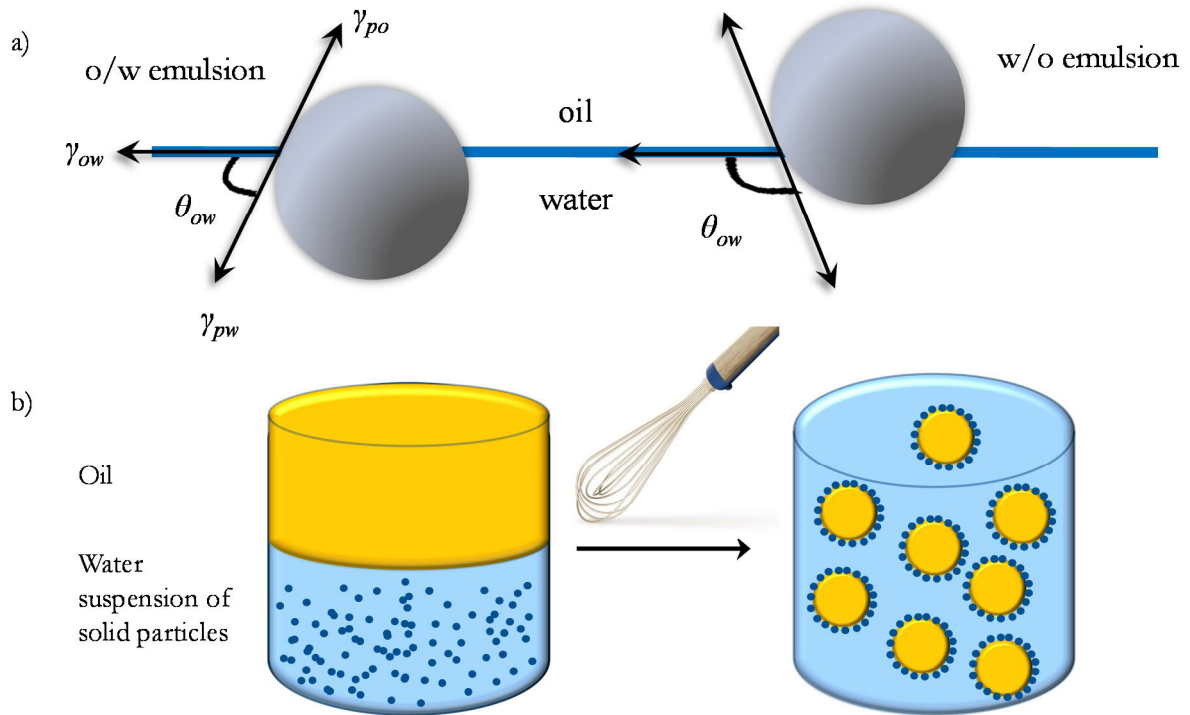


Figure 3. a) Simplified illustrations of solid particles at an oil-water interface. The wetting properties of the particle, quantified by the contact angle  $\theta_{ow}$ , depend on the oil-water, particle-water and particle-oil interfacial tensions:  $\gamma_{ow}$ ,  $\gamma_{pw}$  and  $\gamma_{po}$ , respectively. The magnitude of the contact angle affects the curvature of created emulsion droplets and the type of emulsion to be formed. b) A suspension of solid particles that is mixed with oil can form an emulsion. If nanoparticles are used, these are naturally not visible in the aqueous phase. If the formed emulsion droplets are of micron size, the emulsion appears as an opaque phase.

Surfactants, which are small ( $< 1$  nm), have low adsorption/desorption energies ( $< 10$  kT), and the emulsion system is dynamic. Particles, which are much larger (10 nm – several  $\mu\text{m}$ ) adsorb in principle irreversibly at the interface, if the three phase contact angle  $\theta$  is close to  $90^\circ$  (see Eq. 1).<sup>5</sup> The large adsorption energy for particles at the oil/water interface results in a high energy barrier for spontaneous desorption, resulting in the remarkably high stability of the system.

$$\Delta G_d = \pi r^2 \gamma_{ow} (1 - \cos \theta_{ow})^2 \quad \text{Eq. 1}$$

$$\cos \theta_{ow} = \frac{\gamma_{po} - \gamma_{pw}}{\gamma_{ow}} \quad \text{Eq. 2}$$

Eq. 1, valid for spherical particles with smooth and uniform surface structures, shows that the desorption energy,  $\Delta G_d$ , depends on the contact angle  $\theta_{ow}$ , the particle radius  $r$ , and the interfacial tension between the oil phase and the water phase  $\gamma_{ow}$ .<sup>5</sup> The contact angle is dependent on the particle-oil, particle-water and oil-water interfacial tensions  $\gamma_{po}$ ,  $\gamma_{pw}$  and  $\gamma_{ow}$  according to Young's equation (Eq. 2) and it describes the wettability of the particles.<sup>17</sup> When  $\theta$  is close to  $90^\circ$ , a large desorption energy is present, with  $\Delta G_d \gg 10k_B T$  also for small particles of radii around

5-10 nm.<sup>5, 52</sup> The size of the particles influences the system, and for efficient stabilization the particles should preferably be more than one magnitude smaller than the emulsion droplets.<sup>5</sup> This implies that nanoparticles are required in order to produce emulsions with droplets of sub-micron size. A rapid decrease in desorption energy is noted at either side of  $90^\circ$  and when  $\theta$  approaches  $0^\circ$  (hydrophilic particles) or  $180^\circ$  (hydrophobic particles) spontaneous desorption from the interface occurs ( $\Delta G_d < 10 k_B T$ ).<sup>19</sup> Figure 4 shows the influence of the interfacial tension on the desorption energy, at three different contact angles. An emulsion system where the oil/water interfacial tension is high, such as the system studied in Paper III, requires high energy for formation, but the emulsion stability is expected to be high. Low oil/water interfacial tension facilitates emulsion formation, but results in lower desorption energy and consequently a less stable emulsion, such as the butanol emulsions studied in Paper IV. The contact angles of the functionalized silica particles studied are expected to be below  $90^\circ$ , since the particles are dispersed in water and therefore hydrophilic.

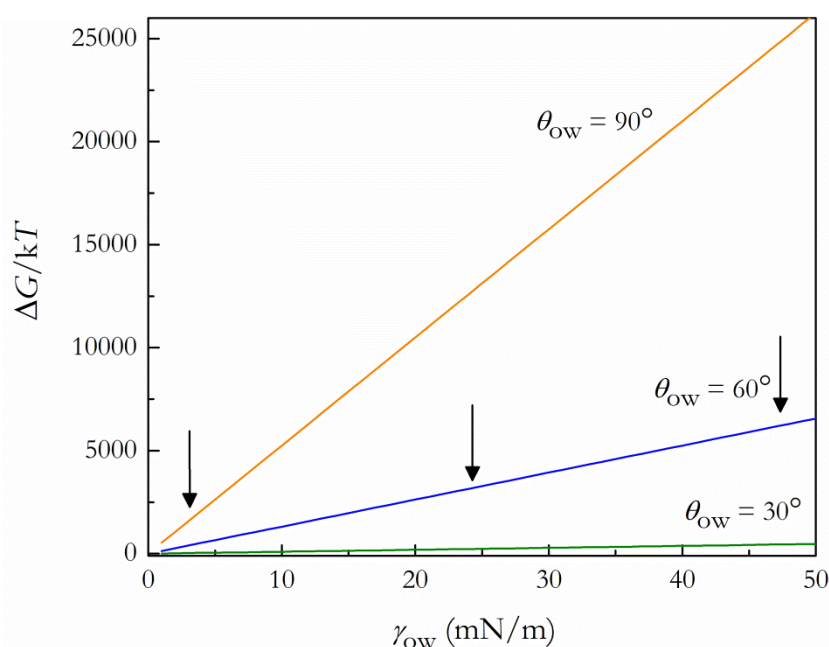


Figure 4. Desorption energy divided by the thermal energy ( $\Delta G/kT$ ) as a function of the oil-water interfacial tension ( $\gamma_{ow}$ ). The arrows indicate  $\gamma_{ow}$  at the butanol-water interface (around 2 mN/m), a typical vegetable oil-water interface such as olive oil (around 25 mN/m) and Exxsol D60-water (measured to 48 mN/m).

Particles are often pre-flocculated before emulsification, since weak flocculation has been found beneficial for emulsion formation.<sup>11, 15, 54, 66</sup> The structure of the continuous phase is important for the emulsion preparation and characteristics.<sup>67</sup> The presence of flocculated particles in the continuous phase would increase the viscosity, and thereby reduce the rate of creaming/sedimentation, which in turn could slow down emulsion breakage. Additional emulsion-stabilizing effects are achieved if a 3D network is created in the continuous phase. However, particles could therefore adsorb as larger aggregates or flocculates, not as a uniform monolayer and other factors besides the contact angle are therefore also important in practice, such as interfacial tension and degree of aggregation.<sup>4</sup> If the degree of particle aggregation is too high, it could instead result in emulsion destabilization.

Hydrophilic particles, such as silica, need to be hydrophobized in order to be suited as Pickering stabilizers. This can be achieved by physical adsorption or covalent attachment of surface species. A particle with  $\theta = 90^\circ$  is equally wet by both liquid phases, thereby strongly held at the interface, and an o/w emulsion is preferred for  $\theta < 90^\circ$  while a w/o emulsion for  $\theta > 90^\circ$ . The best stabilizing effects are therefore, in theory, achieved for Janus particles, that have two distinct areas differing from each other in terms of surface chemistry, and can be symmetrically positioned between the two liquid phases.<sup>68</sup>

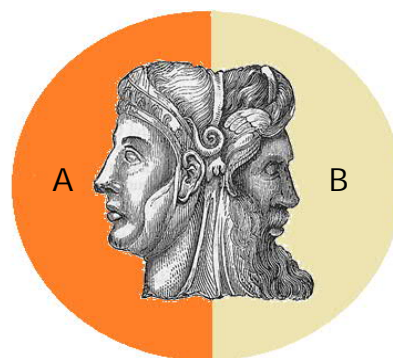


Figure 5. A Janus particle has two faces or regions A and B with e.g. differing surface chemistry.

The name comes from the two-faced Roman god Janus, since the particles are said to have two faces or regions; one region being polar and one being non-polar, providing a true amphiphilic character of the particle (see Figure 5).<sup>69</sup> It has been theoretically predicted that a three-fold increase in adsorption energy can be achieved, if the ratio of the polar to non-polar region is 50:50, compared to a homogeneous particle.<sup>68</sup> This has also been studied experimentally, where increased adsorption energy was achieved.<sup>70, 71</sup> Simultaneously, a more effective steric barrier towards coalescence is created if the particles are positioned in a way that they extend out into the continuous phase,<sup>4</sup> with the contact angle deviating from  $90^\circ$ . Janus particles are often tedious to produce and therefore not yet suitable for industrial applications. The particles discussed in this thesis do not have a Janus character, but since they have been surface modified with both hydrophobic and hydrophilic groups, a heterogeneous surface modification exists.

## Emulsion destabilization mechanisms

Control of emulsion stability is vital in industrial applications. Depending on the application, different degrees of instability may be tolerated. As an example, creaming or sedimentation of the emulsion may not be tolerated in cosmetics, food applications or paints while it is a desired feature in for example production of cream from un-homogenized milk. Through a gentle shake of a creamed or sedimented emulsion its original appearance is regained; this type of separation is reversible and a result of gravity acting on the emulsion droplets, due to density differences between the dispersed and continuous phases.<sup>3</sup> Small emulsion droplets reduce the rate of creaming/sedimentation. When droplets merge together through coalescence, whereby they increase in size and decrease in number, is a much more severe, and irreversible, destabilization mechanism.<sup>3, 15</sup> At low concentrations of emulsifying agent, initially formed emulsion droplets normally coalesce until the oil/water interface of each droplet is covered with a sufficiently large amounts of particles for stabilization.<sup>5, 72, 73</sup> The driving force for increased droplet size is described by Laplace pressure difference  $\Delta P$  (Eq. 3), where  $r$  is the droplet radius.

$$\Delta P = 2\gamma_{ow}/r \quad \text{Eq. 3}$$

If the emulsion droplets are completely covered by particles they are sterically hindered from coalescence. On the other hand, Vignati et al,<sup>65</sup> have shown that stable emulsions can be obtained

when the emulsion droplets are not fully covered with particles. This obtained stability could be explained by bridging monolayers with emulsion droplets sharing particles.<sup>39</sup> In addition, large droplets do not necessarily result in unstable Pickering emulsions, in contrast to surfactant-stabilized emulsions, where small droplets are key for stable emulsions.<sup>3</sup> Production of large, but stable emulsion droplets broaden industrial applicability; emulsions with millimeter-sized droplets that are stable towards coalescence have been successfully obtained.<sup>74</sup> Very small droplets are on the other hand not as frequent in the field of Pickering emulsions. Stable nano-sized emulsion droplets have been obtained,<sup>75</sup> but micron-sized droplets are the most frequently appearing. One reason is the choice of particles; as mentioned in the introduction they need to be of nano-size to obtain such small droplets. Another explanation originate in the oil-water interfacial tension; Dickinson<sup>4</sup> suggests that, since particles are seldom surface active, the normally high oil-water interfacial tension makes it difficult to create small, stable droplets.

## Emulsion properties

The type of emulsion formed from an oil-water-emulsifier system describes the spatial organization of the constituents and is also referred to as the emulsion morphology.<sup>76</sup> Oil-in-water and water-in-oil emulsions are two simple, and common, morphologies. During a phase inversion, a change in emulsion morphology occurs, into a more favorable one, for example an o/w emulsion changes to w/o. The phase inversion conditions and the type of emulsion depend on several variables such as type of oil, type of emulsifier, oil volume fraction, electrolyte concentration, pH, temperature and the type of emulsification process. By tuning the formulation variables, defined morphologies can therefore be obtained. An understanding of the expected emulsion properties is thereby important for emulsion preparation and control of emulsion stability.

## Phase inversions

Emulsion phase inversion is a desired process in some applications, for example butter production, while undesired in others, such as emulsions used in pharmaceuticals. Two distinct types of inversions are discussed: catastrophic phase inversion and transitional phase inversion.<sup>76, 77</sup> Catastrophic phase inversion is distinguished by a sudden change in behavior at the inversion point, such as significant changes in viscosity or conductivity. The inversion is induced by addition of dispersed phase, and at a certain volume phase ratio, the inversion point is found. This volume phase ratio depends on various parameters, for example emulsification conditions, emulsification equipment, type of emulsifier and temperature; catastrophic phase inversions are normally not reversible and have the characteristics of a catastrophe.<sup>37, 78</sup> Catastrophic phase inversions in surfactant systems are distinguished by hysteresis (the inversion point depends on previous treatment), a sudden jump, bimodality (an emulsion with almost similar volume phase ratios can exist as both o/w and w/o), divergence (only a small difference in preparation results in change of morphology) and an inability to capture a stable stage during the inversion.<sup>76, 78</sup>

A change in the chemical conditions, for instance by altering the surface affinity of the emulsifier at a fixed oil/water ratio, gives rise to transitional phase inversion.<sup>76</sup> The preferred emulsion type changes during the transitional phase inversion, and can be achieved for example by addition of salt or by changing the pH. The stabilities of the emulsion before and after

inversion are often comparable, and a continuous change in e.g. conductivity is observed when the emulsion passes through the inversion region.

Non-ionic surfactants that contain PEG-chains possess cloud points, due to the inverse solubility vs. temperature relationship in water, where polar molecular conformations dominate at low temperatures, and non-polar conformations dominate at higher temperatures. By changing the temperature of emulsions stabilized by non-ionic surfactants, phase inversion is induced at a specific temperature known as phase inversion temperature (PIT),<sup>31</sup> and the mentioned conformational change drives the phase inversion (see Figure 6).<sup>3, 79</sup>

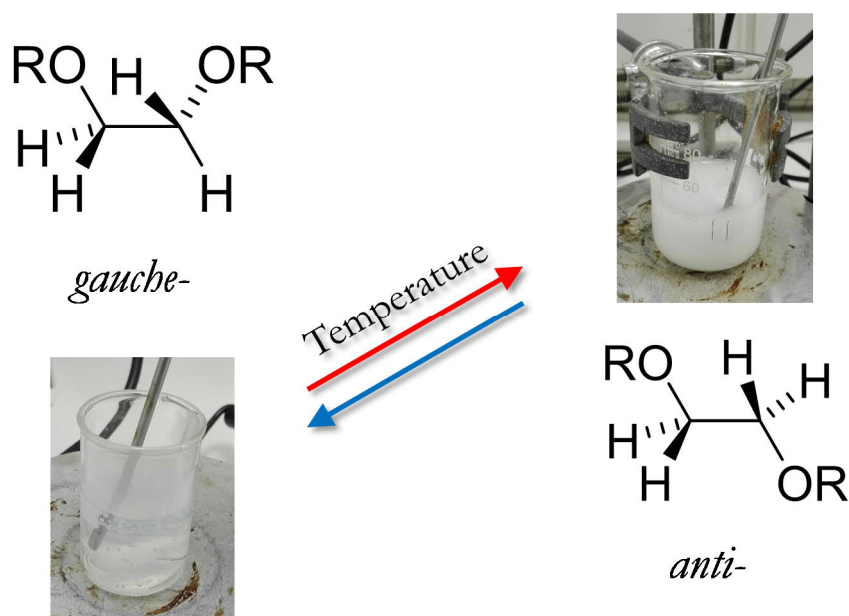


Figure 6. During clouding, separation of the solution into one polymer-rich and one polymer-poor phase occurs, which results formation of aggregates that scatter the incoming light, which makes the solution appear cloudy. The phenomenon originates in the conformational change of the PEG chains, from the polar anti-gauche-anti conformation to the left (lower energy, present at low temperatures) to the anti-anti-anti conformation to the right, which is less polar with a higher energy.

The correlation between the PIT and the cloud point as well as with the hydrophilic/lipophilic balance (HLB) of non-ionic surfactants was reported by Shinoda and colleagues.<sup>30, 34</sup> PIT was later proposed as a useful classification method used for these types of non-ionic surfactants.<sup>80</sup> Preparation of emulsions close to their inversion temperature reduces the energy demand, since ultralow interfacial tension is found here, facilitating creation of small emulsion droplets but simultaneously resulting in low emulsion stability. By quickly cooling the system to the application temperature, fine, more stable and monodispersed emulsion droplets are obtained.<sup>37</sup> The PIT varies depending on conditions such as the type of hydrocarbon and electrolyte concentration, but linear relations to the cloud point, the critical packing parameter (CPP) and/or the HLB are normally found.<sup>30, 81, 82</sup>

## Phase inversions and emulsion types in Pickering systems

The type of particle-stabilized emulsions to be formed may be controlled in the same manner as for surfactant-stabilized emulsions, however instead of HLB, the contact angle is the relevant parameter to describe the preferred emulsion type by a wetting perspective. The simple o/w and w/o emulsion types are frequently reported, where hydrophobic particles stabilize o/w emulsions, and hydrophilic particles stabilize w/o emulsions.<sup>12, 41, 83</sup> Creation of bi-continuous phases and bi-continuous emulsion gels ('bijels') of Pickering systems have also been investigated by e.g. Clegg et al.<sup>84-86</sup> A convenient way of controlling the wetting properties of the particle is through addition of surfactants that adsorb onto the particle surface, which in turn influence which type of emulsion that is preferred (e.g. oil- or water- continuous).<sup>53, 83</sup> Antagonistic effects between adsorbed surfactants and particles are also possible, which may be exploited for controlled phase separation.<sup>87</sup> Controlled phase separation can likewise be obtained by using for example stimuli-responsive surfactants, which generates switchable Pickering emulsions.<sup>14, 88, 89</sup>

Catastrophic phase inversions in Pickering emulsions have been reported, achieved through varying the oil-to-aqueous phase ratio, without altering particle wettability.<sup>50, 90</sup> The catastrophic inversions reported by Binks et al were found to occur without hysteresis; the inversion occurred at the same oil-to-water ratio, irrespective of the route of phase addition, i.e. if oil was added to an o/w emulsion, or if water was added to a w/o emulsion.<sup>47, 50</sup> However, it has also been found that the inversion point can be dependent on the initial particle-fluid interaction; a w/o emulsion prepared with particles initially dispersed in the oil phase required a higher water fraction for inversion, compared to the same system, but with the particles initially dispersed in the water phase.<sup>91</sup>

Transitional phase inversion has been achieved in Pickering systems, by using mixtures of particles as well as of particles and surfactants.<sup>53, 55, 92</sup> Temperature can be an important tool to control the type of emulsion and the emulsion stability.<sup>93, 94</sup> As an example, temperature dependence was utilized to induce phase inversions in batch Pickering emulsions, stabilized by polymer-modified latex particles.<sup>95</sup>

The studies presented in this thesis concern silica particles that have been surface functionalized with mPEG silane, and are thereby given clouding properties (Paper II), which are further explored for phase inversions occurring at specific temperatures (Paper IV).

## Amorphous colloidal silica

Emulsions may be stabilized by several types of particles, but silica is one of the most studied materials and also what this work pivots around. Colloidal silicas are dispersions, often concentrated, of discrete amorphous silica particles in a liquid. The colloidal state comprises particles in the size range from 1 nm to 1  $\mu\text{m}$ , made up of colonies of approximately  $10^3$  to  $10^9$  atoms.<sup>22</sup> As an example, a silica particle of 26 nm has a molar mass of around 10 million g/mol. These particles are small enough not to settle through gravitational forces, their movement due to Brownian motion dominates over the gravitational one.<sup>22</sup> Colloidal particles scatter incoming light, but since they are dispersed,

not dissolved, no change in e.g. in freezing point of the liquid occurs, in contrast to molecular solutions. Other physical parameters are instead affected, such as viscosity and density of the suspension. If the liquid in which the silica particles are maintained is organic, the suspension is referred to as an organosol and when the liquid is water it is called an aquasol or hydrosol.<sup>22</sup> The colloidal systems used in the work presented in this thesis are water-based and are referred to simply as silica sols. Silica sols that were stable and concentrated became available in the 1960s. However, other types of silica, besides the aqueous dispersions employed in this work, have been frequently employed as emulsion stabilizers. A brief description of relevant colloidal silica, including the preparation processes, is therefore provided. Most of the information has been retrieved from the two books "The Chemistry of Silica" from 1979, written by Ralph K Iler<sup>96</sup> and "Colloidal Silica: Fundamentals and Applications" from 2006, edited by Horacio E. Berna and William O. Roberts.<sup>22</sup>

### Colloidal silica by hydrolysis of alkoxysilanes

Spherical silica particles, of uniform size can be prepared through a sol-gel process, developed by Stöber et al,<sup>97</sup> in which a silica precursor, often tetraethylorthosilicate (TEOS) is reacted in an alcohol solvent, with ammonia as catalyst. Particles, often referred to as Stöber silica, are obtained in suspension and have diameters ranging from 50 – 2000 nm. The particles have a very narrow size distribution, but the production is time-consuming, since the particles are prepared at low concentrations. Stöber silica, including modified Stöber methods, have been used frequently to prepare silica particles for Pickering emulsions stabilization,<sup>65, 98, 99</sup> some specific examples are French et al,<sup>100, 101</sup> who studied particle sharing between the formed emulsion droplets and Hertzig et al,<sup>84</sup> who prepared bi-continuous Pickering emulsions.

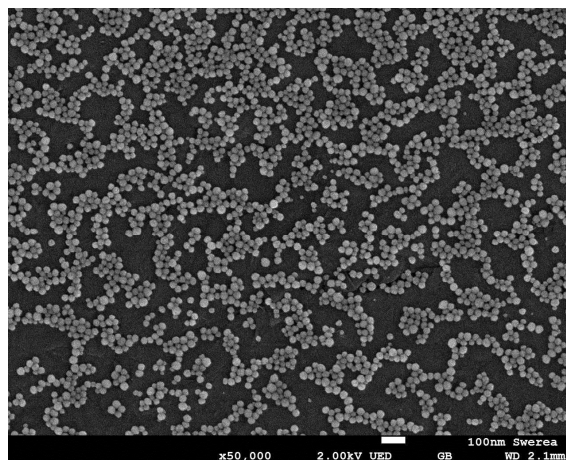


Figure 7. Transmission electron microscopy image of colloidal silica particles. The scale-bar represents 100 nm.

## Fumed silica

Fumed or pyrogenic silica exists in powder-form and is prepared by reacting  $\text{SiCl}_4$  in a hydrogen flame, in the presence of oxygen, to obtain spherical droplets of  $\text{SiO}_2$ .<sup>22</sup> The process yields particles with small primary radii, typically 5 – 50 nm. As the silica droplets cool, and the primary particles form, they continue to aggregate and form agglomerates. Fumed silica can be obtained with different degree of hydrophilic/hydrophobic character, distinguished by the ratio of silanol (Si-OH, hydrophilic) to siloxane (Si-O-Si, hydrophobic) groups present at the surface, see Figure 8. The ratio is controlled through heat treatment of the silica.<sup>102</sup> Surface modification of fumed silica is also employed to hydrophobize the particles, for example by attaching methyl silanes such as chloromethyl silane, to the hydrophilic silica surface. Fumed silica, of varying hydrophobicity, is a commonly used material for studying particles at interfaces and for emulsion stabilization. For example, the work by Binks et al.<sup>46, 48, 49, 51, 56, 91, 103-105</sup> includes fumed silica, and many other examples utilizing the material exist,<sup>106-108</sup> including studies by Frelichowska et al.<sup>59, 61</sup>

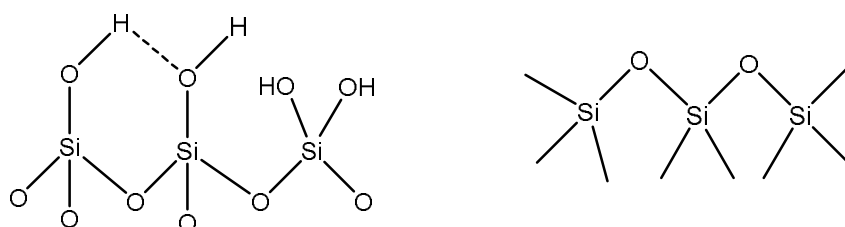


Figure 8. Examples of groups involving Si-O bonds identified on the surface of amorphous silica: vicinal and geminal silanol groups (left) and surface siloxanes (right).

## Silica sols from sodium silicate

Spherical silica particles, of both narrow and broad size distributions, with sizes ranging from 5 – 100 nm, can be prepared as aqueous dispersions from alkali silicates. The most common raw material, sodium silicate (lump water-glass), is obtained by melting sodium carbonate ( $\text{Na}_2\text{CO}_3$ ) and quartz sand ( $\text{SiO}_2$ ), in proportions to obtain a molar ratio  $\text{SiO}_2:\text{Na}_2\text{O} > 3$ . The production process that follows is shown schematically in Figure 9 and involves several steps, summarized below:<sup>109, 110</sup>

- 1) Dissolving lump water-glass to obtain sodium silicate solution, which is diluted to 2-6 wt%  $\text{SiO}_2$
- 2) Cation-exchange, to remove sodium and obtain dilute silicic acid. Polymerization of silicic acid monomers is initiated.
- 3) Addition of silicic acid to dilute sodium silicate at elevated temperature. Polymerization and nucleation occur, and particles begin to form. Particle growth and size distribution are mainly controlled by the temperature and the  $\text{SiO}_2:\text{Na}_2\text{O}$  ratio.
- 4) Concentration of the silica sol, to around 15-50 wt%  $\text{SiO}_2$ .

Modifications, such as surface functionalization, may be added as a subsequent step following the concentration of the sol.



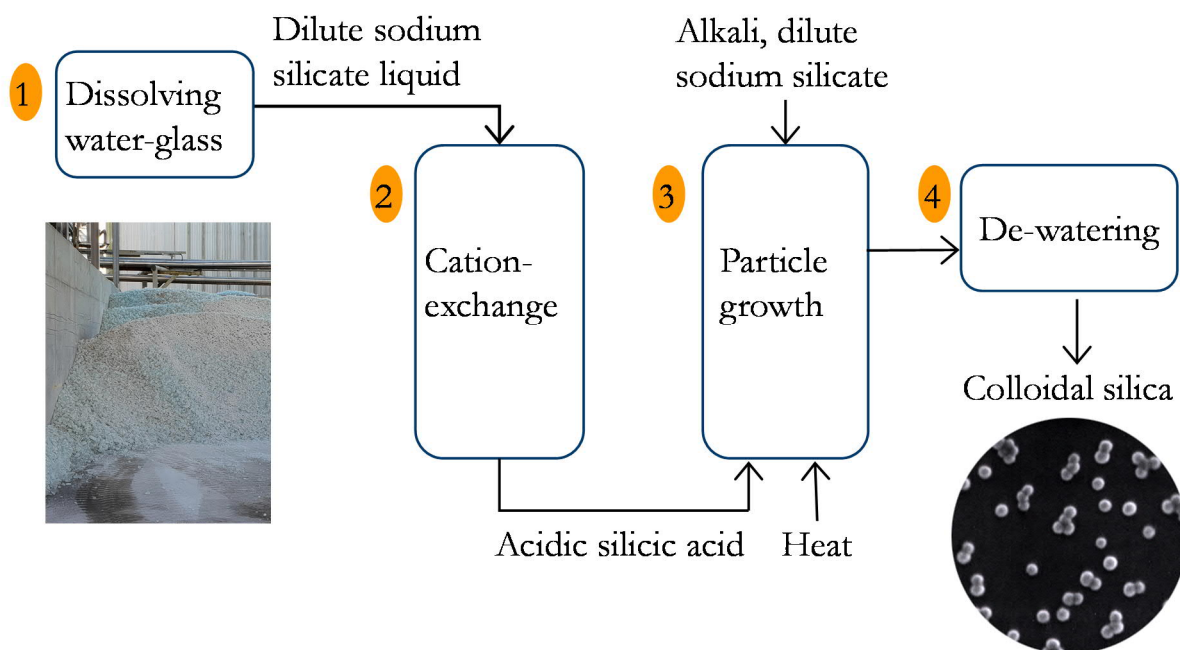
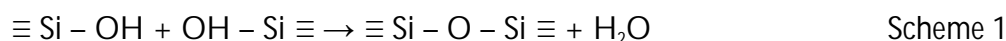


Figure 9. Schematic representation of the different production stages involved in production of colloidal silica from sodium silicate. The inset images are water-glass lumps (left) and a SEM micrograph of colloidal silica (right).

Polymerization of silicic acid,  $\text{Si}(\text{OH})_4$ , occurs through condensation reactions (see Scheme 1), where monomers turn into dimers, which polymerize into oligomers (Step 2 in Figure 9). Cyclic structures tend to form, because the formation of siloxane bonds (Si-O-Si) is maximized and uncondensed silanol groups are disfavored. The spherical units, constituted of 3-4 silicon atoms, are linked together and subsequently constitute the nuclei that grow into larger particles.<sup>110</sup>



Smaller and larger particles will be present, and further growth of larger particles follows by deposition of silicic acid dissolving from smaller ones (Step 3 in Figure 9). At pH around 2, where the ionic charge of the silica surface is low, collisions of particles result in aggregation to chains and gel networks. At pH 5-6, the monomer grows fast into particles, but aggregation and gelling occur simultaneously. At higher pH conditions, up to pH 10.5, the negative surface charge causes repulsions and the particles can grow without aggregation, wherefore production of commercial silica sols normally occurs at alkali conditions. Addition of salt will reduce the repulsion, resulting in gelling and aggregation.<sup>111</sup> The growth process will thereby determine what type of particle structure that is obtained. The process is adjusted for the desired particle size distribution, followed by adjustment of the solid concentration, typically through heat treatment and evaporation of water (Step 4 in Figure 9).

One of the driving forces for this work was to achieve a readily usable, easily manufactured silica particle, functionalized through a water-based route that could be directly utilized as emulsifiers through simple dilution. Examples of emulsion studies utilizing silica sols include Saleh et al,<sup>73</sup> where both hydrosol and organosol, with high grafting density of polymer are employed, and Saigal et al<sup>112</sup> who explored the use organosols grafted with relatively large

thermo-responsive polymers, and Persson et al.<sup>75</sup> studied a commercial silica hydrosol with hydrophilic surface modification, and others.<sup>113-115</sup>

## Surface chemistry of silica particles and stability aspects

The nature of colloidal silica depends on the status of its functional groups at the surface. The relevant surface functional groups of silica nanoparticles present in silica sols are silanol groups, since the surface in water is fully hydroxylated and surface siloxane is normally not present. Physically adsorbed water molecules are hydrogen-bonded to all types of silanol groups building up the hydrate cover.<sup>22</sup> The silanol number,  $\alpha_{\text{OH}}$ , of fully hydroxylated amorphous silica lies within the range 4.2-5.7 OH groups per square nm.<sup>116</sup> According to Zhuravlev,<sup>116</sup> the average value  $\alpha_{\text{OH}} = 4.9$  OH groups per nm<sup>2</sup> is considered a physicochemical constant and is independent of origin and surface characteristics of the particles, such as specific surface area. The value corresponds to 8  $\mu\text{mol}$  of silanol groups per m<sup>2</sup> surface. These can in water be ionized bearing a charge density that increases with pH;  $\text{pK}_a$  of the SiOH is found between pH 6.5 and 9.2.<sup>22, 96, 116</sup> Silicic acid has a relatively high  $\text{pK}_a$ , and polymerization leads to a decrease in  $\text{pK}_a$ ; the silica surface has a lower  $\text{pK}_a$  and is more acidic compared to monomeric silicic acid.

### Stability of colloidal particles

A dispersion of colloidal particles that remain separated over long periods of time (at least several days) is considered stable. Figure 10 shows a schematic illustration of three types of stabilizing options relevant for the discussions in this thesis: electrostatic, steric and electrosteric stabilization.

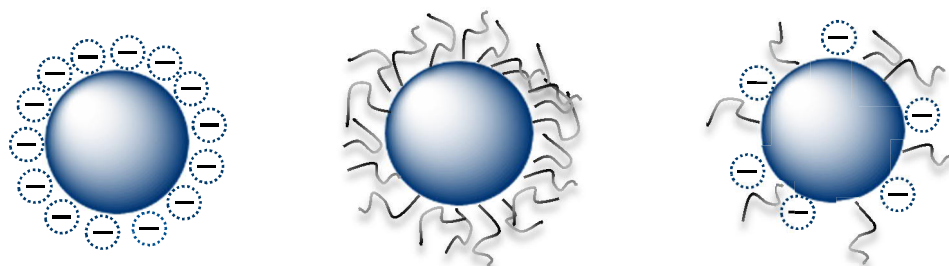


Figure 10. Schematic illustration of electrostatic, steric and electrosteric stabilization of colloids, from left to right, respectively.

Unmodified colloidal silica particles, in waterborne silica sols, are stabilized through electrostatic repulsion. Electrostatic stabilization can be described through the DLVO theory as an interplay between electrostatic repulsive forces and attractive van der Waal forces.<sup>117, 118</sup> A colloid in contact with a polar medium will attain a surface charge, and ions will be distributed at the interface, forming a layer that can be described as the electrical double layer.<sup>3</sup> The strength of the electrostatic stabilization is dependent on the potential resulting from the surface charge density of the distributed ions, where a compact layer of adsorbed ions exist close to the surface and a diffuse layer of Boltzmann distributed ions exist outside the compact layer.<sup>117</sup> The thickness of the electric double layer, referred to as the Debye screening length, is decreased by increased electrolyte concentration. The decay of the potential as a function of the distance from the surface is schematically shown in Figure 11. As two colloids approach, an overlap of their

electrical double layer occurs, and this causes the repulsive forces. At very close proximities, when van der Waals forces dominate, aggregation occurs.

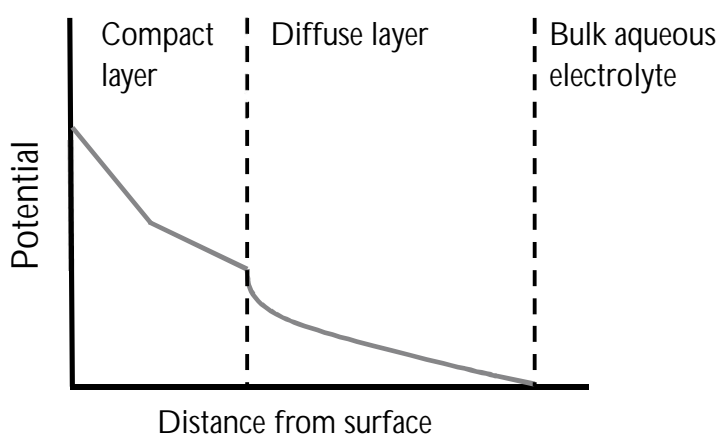


Figure 11. Schematic representation of the electric double layer at a charged surface, with the surface potential as a function of distance from the surface. The compact layer is composed of tightly bound counter ions and may be divided into the inner and outer Helmholtz planes. The shear plane exist between the compact and the diffuse layer, where the diffuse layer consists of Boltzmann distributed ions.

The electrostatic stability of a silica sol is dependent on the salt concentration in the suspension, and addition of salt will compress the electrical double layer. The stability is also affected by the pH of the suspension, see Figure 12. Above pH 7, the surface charge concentration is sufficient to cause the mutual repulsion between the particles, providing stability towards gelling of the sol.<sup>22,96</sup> A silica sol is also stable around the isoelectric point, reported to be found between pH 2 and 4. The stability of the uncharged silica particles around pH 2 most likely originates in a highly structured hydration-layer around the particles, causing short-range repulsive forces.<sup>119</sup>

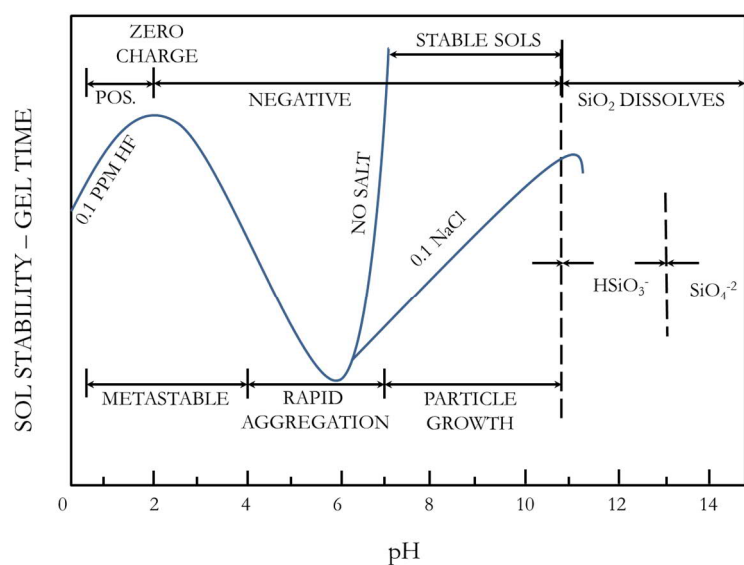


Figure 12. Influence of pH on sol stability or gel time of the water-colloidal silica systems. Reproduced from Iler.<sup>120</sup>

Steric stabilization of colloidal particles is achieved through adsorption or chemical grafting of functional groups. Several different stabilizing mechanisms are possible, which may be enthalpic and/or entropic.<sup>121</sup> For example, steric stabilization is achieved when grafted groups have a stronger interaction with the solvent, compared to the chain-chain interaction, and repulsion between particles will occur as the grafted groups approach each other. Steric stabilization may broaden the application of silica sols and enable utilization in broader pH conditions and at higher salt concentrations.

Aggregation of silica particles in a sol involves formation of 3D networks of particles linked together, and the aggregation can, according to Iler, be distinguished into gelling, flocculation and coagulation.<sup>120</sup> Gelling occurs when the particles are linked in branched chains, with the solid phase filling the volume of the sol and resulting in viscosity increase which eventually solidifies the sol into a gel. There is no macroscopic increase in silica concentration in the network of particles that is formed.<sup>20, 120</sup> Flocculation may occur through charge neutralization, patching and bridging, depending on the characteristics of the system. As an example, during bridge flocculation, particles are linked by a flocculation agent long enough to allow the aggregated structure to remain open and voluminous. However, in patching, the flocculation agent is of lower molecular weight and patch-wise flocculation therefore occurs, with more dense aggregates. Coagulation leads to the formation of compact aggregates, that are macroscopically separated and in which the silica concentration increases.<sup>120</sup> When a silica sol is electrostatically stabilized and the counter ion is, for example, sodium, these systems can be denoted as sodium-stabilized for short; low concentration of counter-ions decreases the hydrodynamic radius of the particles through compression of the diffuse layer and reduces Ostwald ripening.

## Surface modification

Silica materials functionalized with silane derivatives has been on the market since the 1950s; one example is glass-fibers for use in composite materials.<sup>122, 123</sup> Amorphous silica sols may be surface modified using silanes, which are available with a range of different functional groups. Modification of the surface through chemical grafting is in many cases preferred over physical adsorption, since release of adsorbed molecules may occur upon a shift in equilibrium conditions, i.e. upon dilution, changes in pH or in electrolyte concentrations.

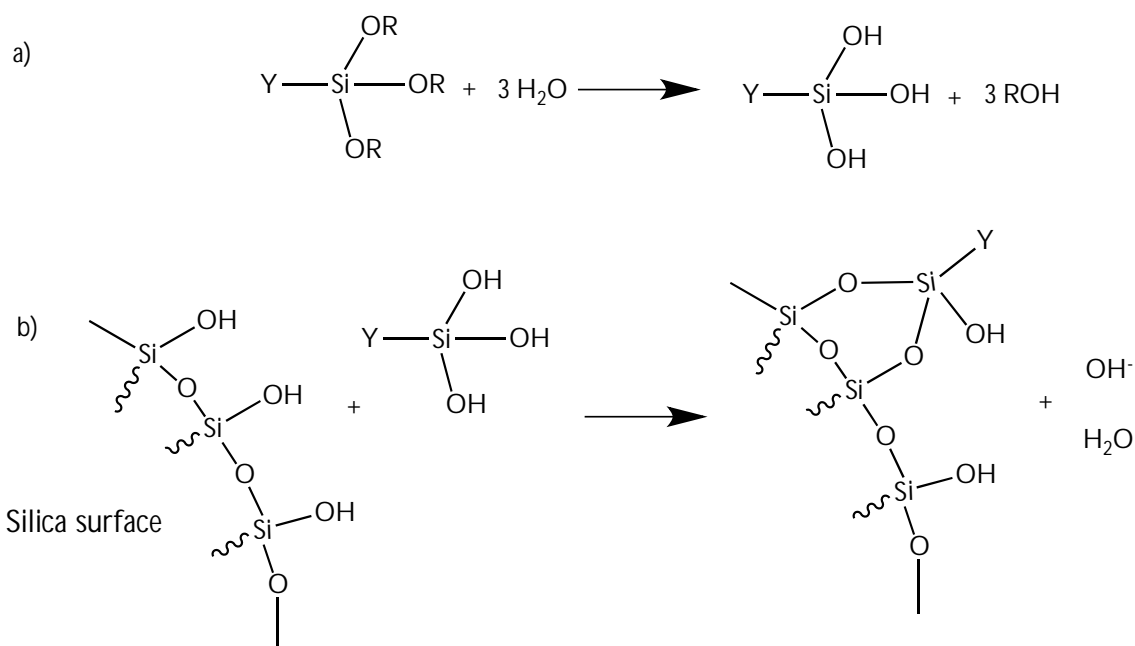
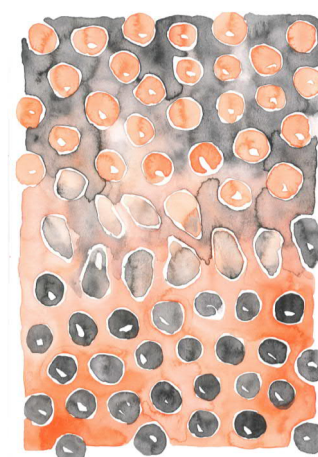


Figure 13. Silylation of the silica surface. a) Silanol groups become available for condensation to the silica surface through silane hydrolysis. b) The hydrolyzed silane may react with both protonated and deprotonated silanol groups, releasing either water or hydroxyl ions.

The work presented in this thesis comprises functionalization of colloidal silica by silylation of the surface, illustrated in Figure 13. The silanes employed consist of hydrolysable (R) and organofunctional (Y) groups, e.g.  $(\text{RO})_3\text{SiY}$ . Alcohol is released during hydrolysis, normally methanol or ethanol, depending on the silane used. During silane functionalization a decrease in the measured Sears<sup>124</sup> specific surface area (SSA) and an increase in pH occurs.<sup>125</sup> The methodology employed in Sears titration relates the SSA to the volume of sodium hydroxide solution added to a silica sol saturated with sodium chloride, during titration between pH 4 and 9, via an empiric function. The obtained SSA is thereby proportional to the number of available silanol groups on the particle surface. Sears titration is therefore not applicable for measuring SSA on functionalized sols, since the silanes react with a fraction of the silanol groups. But, by comparing the Sears SSA before and after functionalization, a measure of the change in available silanol groups is obtained, providing an indication of the effect of the functionality on the silica surface. The pH is affected since release of  $\text{OH}^-$  ions occurs, see Figure 13. The hydrolysis reaction has a minimum in reaction rate around pH 6-7, but is fast at both sides: below pH 4 and above pH 8.<sup>123</sup> The condensation reaction, which attaches the silane to the silica surface, has its minimum around pH 4 and is very fast around pH 9. The functionalization can therefore conveniently be carried out in alkaline silica sols.



## MATERIALS AND METHODS



### Materials

All of the colloidal silicas used in this work have been obtained from Nouryon and are dispersed in water. The sols are electrostatically stabilized at high pH conditions, and the counter ion is sodium, wherefore the sols are denoted sodium-stabilized. In Paper III, a few experiments were performed using de-ionized (DI) sols, and a few different sizes of the particles were explored. Apart from this, the sols used in Paper I, II and IV have been Levasil CS 40-213 (the old name Bindzil 40/130 is used in Paper I) or Levasil SP2138, where the latter is a slightly purified version of the former, resulting in a slightly lower inherent ionic strength. The sols have a particle size of 26 nm, as measured with DLS, and a Sears specific surface area (SSA) of 130 m<sup>2</sup>/g. The silanes used for the functionalization, are seen in Table 1. The technical oil Exxsol D60, consisting of a mixture of alkanes and cyclic hydrocarbons, was used in Paper III for exploration of emulsifying properties. Butanol was used as oil phase in Paper IV, to enable phase inversion studies.

Table 1. Silanes used for the functionalization of silica presented in this thesis (for product names and suppliers, see Paper I and III).

Silane type	Chemical structure	Character	Used in
Trimethoxy(mPEG) silane	$(\text{H}_3\text{CO})_3\text{Si}(\text{CH}_2)_3(\text{OCH}_2\text{CH}_2)_{11}\text{OCH}_3$	Hydrophilic	Paper I, II, III, IV
Ethoxy(trimethyl)silane	$\text{H}_5\text{C}_2\text{OSi}(\text{CH}_3)_3$	Hydrophobic	Paper III
Dimethoxy(dimethyl) silane	$(\text{H}_3\text{CO})_2\text{Si}(\text{CH}_3)_2$	Hydrophobic	Paper III
Triethoxy(propyl)silane	$(\text{H}_5\text{C}_2\text{O})_3\text{Si}(\text{CH}_2)_2\text{CH}_3$	Hydrophobic	Paper III, IV
Trimethoxy(propyl) silane	$(\text{H}_3\text{CO})_3\text{Si}(\text{CH}_2)_2\text{CH}_3$	Hydrophobic	Paper III
Triethoxy(octyl)silane	$(\text{H}_5\text{C}_2\text{O})_3\text{Si}(\text{CH}_2)_7\text{CH}_3$	Hydrophobic	Paper III

## Methods for analysis

### NMR spectroscopy

Nuclear magnetic resonance (NMR) spectroscopy has, in this work, been a useful technique for analysis of the functionalized particles and enabled determination of the amounts of bound surface species. NMR diffusometry was employed in Paper I, the relaxation behavior was analyzed in Papers I and II, and the amounts of free silane species was determined with the help of  $^1\text{H}$  NMR in Papers II, III and IV.

NMR spectroscopy utilizes the ability of the nuclei of atoms to absorb and reemit electromagnetic radiation due to a change of the nuclei spin states. The NMR spectrum is a plot of the intensity of absorption on the vertical axis against frequency on the horizontal axis and provides information about the chemical and physical properties of the atoms or molecules in the sample. In order for a nucleus to be detected with NMR it must possess a nuclear spin. Nuclei possess a nuclear spin if they have i) odd number of protons and odd number of neutrons ii) odd number of protons and even number of neutrons or iii) even number of protons and odd number of neutrons. Examples relevant for this work are  $^1\text{H}$ ,  $^{13}\text{C}$  and  $^{29}\text{Si}$ . However, the natural abundance of both  $^{13}\text{C}$  and  $^{29}\text{Si}$  is low (1.08 % and 4.67 %, respectively),<sup>126</sup> and  $^1\text{H}$  NMR has been the technique mainly used.

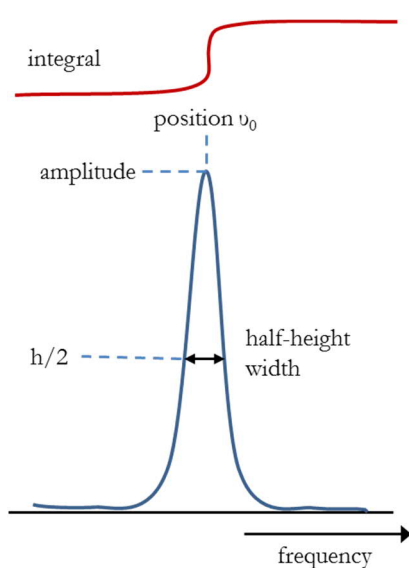


Figure 14. A typical lineshape of an NMR signal.

Figure 14 shows the typical Lorentzian lineshape of an NMR signal, where the peak is centered at position  $\nu_0$  in Hz and has got amplitude of height  $h$ . The width is measured at half of the peak height,  $h/2$ . The separation between two peaks relative to their linewidth, and also their lineshape, will determine whether the peaks are resolved or not.<sup>127</sup> The position of the peak is usually

given as the chemical shift in ppm, relative to the position of a reference peak from a reference compound, as this scale is independent of the magnetic field strength. The chemical shift of the nuclei in the sample is dependent on its specific chemical environment, wherefore different nuclei in a molecule give rise to different chemical shifts.<sup>127</sup> The intensity of the signal is directly proportional to the amount of nuclei that give rise to the signal, which enables quantification of the amount (concentration) of molecules (nuclei) in the sample.

### NMR spin relaxation and signal detection

When a sample is put in an NMR spectrophotometer, a static magnetic field,  $B_0$ , is applied to the sample. This makes the magnetic moments of the spins in the sample interact with the magnetic field ( $B_0$ ) and align along a given z-axis, while the x- and y-components are distributed randomly, resulting in no net transverse magnetization. To record a spectrum, a short radio-frequency (RF) pulse is applied, which generates an oscillating second magnetic field  $B_1$  perpendicular to  $B_0$ . The length of the RF-pulse can be tuned to transfer the magnetization of the nuclear spins into the xy-plane, where experimental detection can be carried out. Such RF-pulse is denoted as a  $90^\circ$ -



pulse and all magnetic z-components are rotated onto the same axis in the xy-plane. Figure 15 uses the descriptive vector model to show how the magnetization affects the magnetic moments of the spins, e.g. the net z-magnetization ( $M_z$ ) is the sum of the z-components of the magnetic moment of each spin. NMR spin relaxation is the phenomenon that describes how the bulk magnetization from the spins in a sample, after an RF-pulse has been applied, returns to its thermal equilibrium value. The rate of relaxation is sensitive to the physical environment of the nuclei and the nature of motion that the molecule is undergoing.

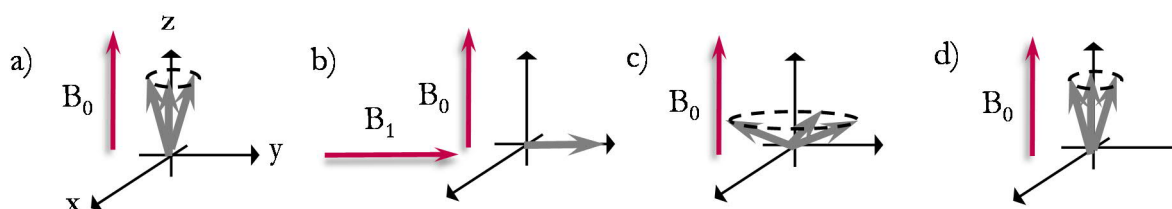


Figure 15. Using the descriptive vector model, showing magnetization from magnetic moments of the nuclear spins in a sample: a) The magnetic moments align with the applied magnetic field  $B_0$  and precess about the z-axis with net magnetization along the z-direction; b) An RF pulse has been applied, creating the magnetic field  $B_1$ , the magnetic moments align coherently in the xy-plane; c) Relaxation in both the z-direction and the xy-plane; d) Back at thermal equilibrium.

Relaxation involves the flow of energy between spins due to molecular motion. Longitudinal relaxation or spin-lattice relaxation is the process when the z-magnetization is returned to its equilibrium value. Transverse relaxation is the process by which transverse magnetization decays to its decoherence equilibrium value of zero net magnetization in the xy-plane. The longitudinal and transverse relaxations can be expressed as first order equations with rate constants  $R_1$  and  $R_2$ , where  $R_1$  is the longitudinal relaxation rate and  $R_2$  is the transverse relaxation rate. The inverse of the relaxation rates gives the relaxation times  $T_1$  and  $T_2$ , see Eq. 4 and Eq. 5.

$$\frac{dM_z}{dt} = -(M_z - M_0)R_1 ; T_1 = 1/R_1 \quad \text{Eq. 4}$$

$$\frac{dM_{xy}}{dt} = -M_{xy}R_2 ; T_2 = 1/R_2 \quad \text{Eq. 5}$$

### NMR diffusometry

NMR diffusometry is normally used to obtain the self-diffusion coefficient of specific nuclei in a sample, by following the loss of intensity during a magnetic field gradient pulse experiment. The intensity decrease provides information on the physical movement of the molecules during a certain time, and thereby the self-diffusion can be obtained. In this work, NMR diffusometry is employed to obtain the functionalization yields of mPEG-grafted particles, the fractions of bound and free mPEG silanes present in the samples, respectively. Although diffusion coefficients are obtained, these values are not of main interest here. These values, as well as the relaxation times, are however required to obtain the fractions of bound and free mPEG species

in the samples. Eq. 6 below describes the decayed intensity  $I$  compared to equilibrium intensity  $I_0$ , where  $\Delta$  is the diffusion time,  $\delta$  is the gradient pulse length,  $\tau_r$  is the gradient ringing delay,  $T_1$  and  $T_2$  are the longitudinal and transverse relaxation times, respectively,  $D$  is the diffusion coefficient,  $\gamma$  is the  $^1\text{H}$  gyromagnetic ratio and  $G$  is the gradient field strength. The equation can be simplified into Eq. 7. If the stimulated spin echo profile ( $\log I$  vs.  $k$ ) is bi-exponential, it suggests two distinct diffusion rates, and the intensity follows Eq. 8, where  $p$  represents the fraction of free species in the sample, i.e. fast diffusing species.

$$I = \frac{1}{2} I_0 \exp\left\{-\frac{\Delta - \tau_r}{T_1}\right\} \exp\left\{-\frac{2\delta - \tau_r}{T_2}\right\} \exp\{-D(\gamma\delta G)^2(\Delta - \delta/3)\} \quad \text{Eq. 6}$$

$$I = C \exp\{-Dk\} \quad \text{Eq. 7}$$

$$I(k) = pC_{\text{free}} \exp\{-kD_{\text{free}}\} + (1-p)C_{\text{bound}} \exp\{-kD_{\text{bound}}\} \quad \text{Eq. 8}$$

$D_{\text{free}}$ ,  $D_{\text{bound}}$  and  $p$  can be extracted by calculating  $C_{\text{free}}$  and  $C_{\text{bound}}$  and by fitting the equations in MatLab or similar, if the relaxation times  $T_1$  and  $T_2$  for both free and bound species are measured. The relaxation times can be obtained by standard inversion recovery and CPMG pulse sequences, while the pulsed gradient stimulated spin-echo (PGSTE) method<sup>128</sup> can be employed to measure diffusion. The NMR diffusometry measurements, including measurements of relaxation times, were conducted on a Bruker Avance 600 spectrometer. Other NMR measurements were performed on a Varian 400 MHz spectrometer equipped with an auto-sampler (mainly  $^1\text{H}$  NMR) and on a Varian 500 MHz spectrometer (when the temperature was altered).

## Dynamic light scattering

Functionalization of silica nanoparticles could result in particle aggregation and an undesired increase in particle size distribution. The particle size distributions of the functionalized silica particles were therefore measured using dynamic light scattering (DLS) with a Zetasizer Nano-ZS from Malvern Instruments. DLS is a widely used technique for determining particle size distributions, generally within the range of a few nm up to around 1  $\mu\text{m}$ . The method employs determination of the Brownian motion of the particles in the system, referred to as the translational diffusion coefficient. The diffusion coefficient,  $D$ , is related to the size, or more specifically the hydrodynamic radius,  $R_H$ , of the particles in a fluid of dynamic viscosity  $\eta$  via the Stokes-Einstein equation (Eq. 9), where  $k_B$  is the Boltzmann's constant and  $T$  is the absolute temperature.

$$D = \frac{k_B T}{6\pi\eta R_H} \quad \text{Eq. 9}$$

The size obtained is the radius of a sphere having the same translational diffusion coefficient as the particle. A particle in motion scatters light that is frequency-shifted, referred to as the Doppler shift. The frequency spectrum is Fourier transformed by a so called correlator, from

which a correlation curve and correlation function is obtained. The correlation function is analyzed using cumulant analysis.

Zeta potential,  $\zeta$ , of colloidal particles in liquids often determines the stability of the system, where a low absolute value leads to aggregation. As a rule of thumb, the zeta potential of an electrostatically stabilized system should be  $\geq \pm 30$  mV. A surface functionality could affect the zeta potential and the range where colloidal stability is present. Measurements of the zeta potential of functionalized particles were therefore performed, also on the Zetasizer from Malvern. Determination of zeta potential can be achieved by applying an electric field on the sample in a capillary cell, making the particles undergo electrophoresis. Zeta potential is measured at the shear plane of the diffuse electric double layer (see Figure 11) and calculated from the velocity of the particles in the electric field.

## Titration and surface charge

Silica particles in water with a pH above 2 have a negative charge that increases with pH. By functionalizing the silica surface, a reduction in surface charge should be observed. In addition, less sensitivity towards changes in pH and salt concentration could be achieved, since the attachment of functional groups can induce steric stabilization of the silica particles. This was assessed by analyzing apparent surface charge through polyelectrolyte titration (Paper I), by studying reduction of available surface silanol groups through Sears titration<sup>124</sup> (all samples), and by performing potentiometric titrations (Paper II), as complements to the zeta potential measurements.

Polyelectrolyte titration was conducted on a particle charge detector, equipped with an oscillating piston that detects the current between two electrodes. The titration was performed with polybrene ( $C_{13}H_{30}Br_2N_2$ ), which is a cationic polyelectrolyte that has two equivalent charges per mole. The required volume of added polybrene to reach zero charge depends on the amount of available groups on the silica surface and this value enables calculation of the equivalent charge per mass (eq/g), denoted as apparent surface charge (ASC). The ASC obtained originates in the potential outside the compact ion layer surrounding the particles, and its' absolute value is decreased by addition of salt, in similarity to the zeta potential, but in contrast to potentiometric titrations (see Figure 11).<sup>129</sup>

Potentiometric titrations provide the surface charge density (SCD) per unit surface area, and the SCD is obtained through comparing the volume of acid required to obtain a certain pH in the silica suspensions, to the volume required in salt-solutions without particles.<sup>130, 131</sup> The SCD obtained from this method depends on the reactions at the surface that occur upon addition of potential determining ions ( $H^+$  and  $OH^-$ ), and therefore gives the charge at the particle surface inside the compact layer. Addition of salt results in surface relaxation, due to screening of the particle surface charge, and therefore gives a higher absolute value of the SCD. The potentiometric titrations were conducted with acid (0.1 M HCl), which results in less steric restrictions compared to titrations with the bulkier polyelectrolyte.

## Emulsion droplet sizing

Laser diffraction, conducted on a Malvern Mastersizer Micro Plus, was used for determination of the emulsion droplet size distributions. This technique is used for sizing from the submicron range up to several millimeters and is therefore suitable for analyzing the sizes of the emulsion droplets obtained in this work. The emulsion droplets are dispersed in a liquid media (water for o/w emulsions) and laser is passed through the sample. The laser is diffracted by the particles, and the diffraction pattern is characteristic of the particle size, which is transformed to a particle size distribution. Emulsion droplets were also studied using optical microscopy.

## Surface and interfacial tension with the DuNoüy ring method

The surface activity of the particles was assessed using the DuNoüy ring method, conducted on a Sigma 70 Tensiometer. In this method, a platinum ring is hung on a balance and submerged below the interface being tested. The interface is either the surface of a liquid (measuring surface tension) or the interface between e.g. oil and water (measuring interfacial tension), as seen in Figure 16. The ring will carry a meniscus of the liquid upwards. The meniscus will eventually tear from the ring, however, prior to this event it will carry a maximum volume, thus a maximum force  $F_{max}$  is detected. The ring is returned to its original position just before the meniscus tears and the process can be repeated until the values of surface or interfacial tension level out. The surface or interfacial tension,  $\gamma$ , is calculated from the maximum force experienced by the balance as the ring is raised according to Eq. 10, where  $d$  is the diameter of the ring and  $f$  is a correction factor accounting for an additional volume of liquid being raised due to the proximity of one side of the ring to the other.<sup>132</sup>

$$\gamma = f \frac{F_{max}}{2\pi d} \quad \text{Eq. 10}$$

In Paper I, the measured surface tensions of diluted suspensions of mPEG functionalized silica particles are discussed. The interfacial tensions of oil and functionalized silica sols have also been assessed and are discussed in this thesis but have not been included in the appended papers.

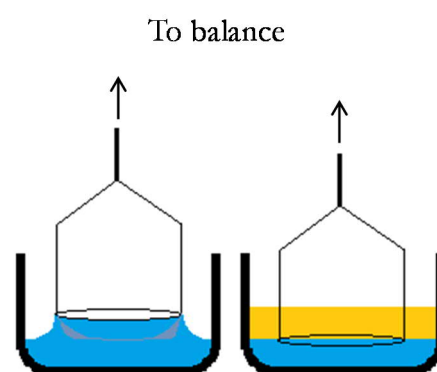


Figure 16. The DuNoüy ring method, used for assessment of surface tension and interfacial tension. A platinum ring is submerged into the liquid with highest density and the tension at the interface is measured.

## UV-Vis spectroscopy

UV-Vis spectroscopy was used to study turbidity, as a mean of characterizing particle flocculation. When light is passed through a suspension, light is scattered due to interactions with the particles. The turbidity of a suspension of particles increases with the particle size. In order to qualitatively study the aggregation behavior of a suspension, a UV-Vis spectrophotometer can be used, which operates at the UV and visible spectra (light of wavelength 200-800 nm). If the absorbance of the suspension is recorded where the molecular absorbance of the system is low, an increase in absorbance, i.e. increased scattering of light is therefore due to an increase in turbidity.

## Elemental analysis

Elemental analysis was performed using an Elementar Vario MICRO cube for determination of the carbon content in functionalized silica nanoparticles. The dried suspensions are, with this method, incinerated at 1100 °C in a tin vial and the carbon content is determined from the amount of CO<sub>2</sub> gas developed. Elemental analysis of solutions containing free silane species was also performed.

## Experimental procedures

### Functionalization of silica nanoparticles

The silane-grafted silica nanoparticles were prepared via a direct, water-based route and at silica concentrations of between 20 to 40 wt% SiO<sub>2</sub>. The silanes, pre-hydrolyzed or as received, were added to the silica sols at controlled temperature and stirring. A slow addition rate is required, to minimize self-condensation of the silane and to reduce gelling or precipitation of the sol. For further details regarding the functionalization procedure, the reader is referred to the methods sections of Paper I, III and IV.

### Determination of surface functionalization yield

The mPEG-grafted particles in Paper I were analyzed using NMR diffusometry, described in the previous section. The particles used in Paper II, III and IV were analyzed by depletion method. Functionalized silica sols were ultra-centrifuged, whereby a gel of concentrated silica particles was obtained in the bottom of the tube, and the supernatant solution could be carefully extracted, which contains the free, unreacted silanes which are not associated to the silica particles. The ratios between the different types of free silanes in the supernatants were obtained by <sup>1</sup>H NMR spectroscopy and were recalculated into carbon weight ratios. Elemental analysis of dried, purified particles provided the carbon contents arising from bound silanes in the samples. This allowed calculation of the amounts of each type of free silanes in the samples and thereby also the amounts of each type of bound silanes, from which the yields are obtained. In Paper II and IV, elemental analysis (to obtain the carbon content) and HPLC (to obtain the alcohol content) were instead performed on the supernatant, to simplify the method. The amounts of each type

of free silanes were determined in the supernatant and thereby also the amounts of each type of bound silanes, from which the yields could be calculated.

## Emulsion preparation

A common way to obtain an emulsion is through homogenization. This may be accomplished by using for example a kitchen hand blender for preparation of home-made mayonnaise. In lab scale, an Ultra Turrax (Figure 17) and similar devices such as a Silent Crusher are frequently employed. For the creation of Pickering emulsions a relatively high energy input is required to achieve small emulsion droplets, which could result in undesired foam formation. Emulsification can also be performed using a Magic Lab device, which recirculates the product (Figure 17). The recirculation provides efficient shearing thus a high input energy but still gives low generation of foam. In Paper III Magic Lab was used, while in Paper IV, homogenization was executed using Ultra Turrax and Silent Crusher.

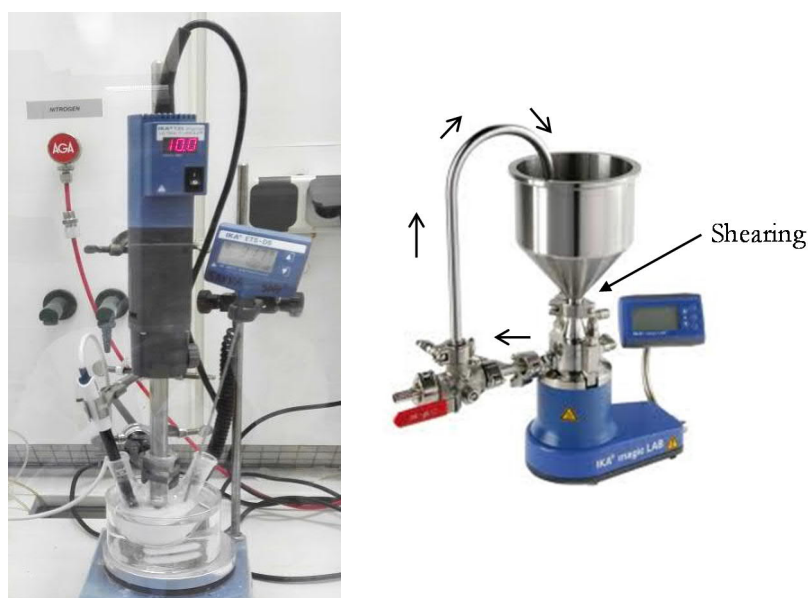
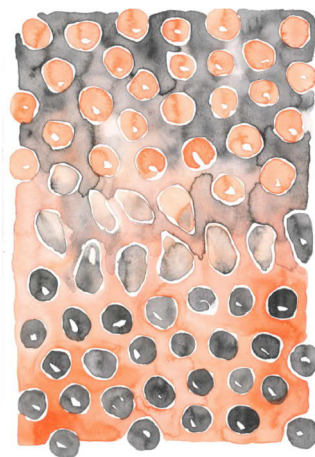


Figure 17. Right: Emulsification setup for phase inversion studies, where conductivity and temperature were followed during the homogenization, using an Ultra Turrax homogenizer. Left: Magic Lab emulsification device.

## Cloud point and phase inversion studies

The cloud points of mPEG-grafted silica nanoparticles, distinguished by an increase in turbidity upon heating, were determined by visual inspection. Phase inversion temperatures (PITs) were determined by following the electrical conductivity of the emulsion system, while heating it in an oil bath with the homogenization turned on. Any existence of PIT could thereby be defined, since a difference in conductivity indicates an inversion, where a water-continuous emulsion has a high conductivity and an oil-continuous emulsion has a low conductivity.<sup>49, 90</sup>

## RESULTS AND DISCUSSION



This chapter summarizes the results obtained in the appended papers, and is divided into two parts, wherein the first part concerns the colloidal silica suspensions, functionalization of these and characterization from a colloidal chemistry perspective (Paper I, II and parts of Paper III). The second part concerns the utilization of the particles in emulsion systems (Paper III and IV).

### Surface functionalized silica nanoparticles

#### Functionalization procedure

*Hydrophilic functionalization:* Particles modified with only mPEG silane were studied in Paper I and II. Several batches of mPEG-grafted particles were prepared, where the reaction conditions were varied. Because the mPEG silane is soluble in water, relatively high amounts could be added to the silica sol without the occurrence of particle aggregation during the synthesis, although a relatively large fraction remains unreacted and present as free mPEG silane in the sample. Between 0.3 and 4  $\mu\text{mol}$  silane per  $\text{m}^2$  of  $\text{SiO}_2$  was added to the silica sol during the functionalization process. The particle surface coverages were determined to 0.068 – 0.315  $\mu\text{mol m}^{-2}$  using NMR diffusometry, while particles surface coverages of up to 0.85  $\mu\text{mol m}^{-2}$  were obtained with the method including elemental analysis. The synthesis yields were between 20 – 50 %, and were improved by a slow addition rate, preferably below 0.25  $\mu\text{mol per m}^2$  and hour.

*Hydrophobic functionalization:* The propyl silane has been the most frequently employed hydrophobic functionality in this work. In contrast to the mPEG silane, addition of high amounts of hydrophobic silanes readily results in gelling of the sol. But, due to the low water solubility, almost all added silane attaches to the silica surface, as long as the total added amount was around or below 1  $\mu\text{mol silane m}^{-2} \text{SiO}_2$ .

*Combining hydrophilic and hydrophobic functionalization:* Particles modified both with mPEG silane, used as the hydrophilic functionality, and with hydrophobic groups were prepared by first adding pre-hydrolyzed hydrophobic silane, with the exception of the methylsilanes used, which were added without pre-hydrolysis. This was followed by addition of the mPEG silane. Adding the mPEG silane first was disadvantageous for the emulsification properties, probably due to a more homogeneous distribution of the silane functionalities, resulting in a more hydrophilic character of the particles.

### Determination of silane surface coverage

The hydrophilic nature of the mPEG silane and the relatively long (poly)ethylene oxide chains that, in alkaline conditions, protrude out from the particle surface result in a  $T_2$  relaxation time long enough to detect the chain signals with NMR spectroscopy. The repeating EO-units of the PEG chain give rise to a signal of high sensitivity, but which overlaps for both free and bound species. The relaxation times  $T_1$  and  $T_2$  were obtained by inversion recovery and CPMG pulse sequence experiments, and strict bi-exponential behavior was noted in both cases. Thus the signal could be analyzed, and two distinct rates could be obtained for both longitudinal and transverse relaxation. The measured longitudinal relaxation times  $T_1$  were 336 ms and 1 960 ms, while the transverse relaxation times  $T_2$  were measured to 259 ms and 16 ms, respectively. The relaxation times provide information on the local molecular mobility (see Figure 18a).<sup>133</sup> The significantly reduced value of  $T_2$  and the increased value of  $T_1$  indicate reduced mobility, wherefore these values ( $T_1 = 1\,960$  ms and  $T_2 = 16$  ms) are the relaxation times of species that are bound to the silica surface.

A strict two-component attenuation of the logarithmic NMR signal intensity versus  $k = (\gamma G \delta)^2 (\Delta - \delta / 3)$  was obtained for all samples also from the NMR diffusometry experiments, which enables determination of the fractions of fast- and slow-moving species, or the free and bound mPEG silanes, respectively. Subsequently, calculation of the yield is possible, defined as the amount of bound silane compared to the amount of added silane.

Figure 18b shows the stimulated spin echo profile from free, aqueous mPEG silane, with one diffusion component, and from particles grafted with mPEG silane, where the bi-exponential profile is seen. The latter profile corresponds to two diffusion components, subsequently containing both bound and unreacted (free) mPEG silane.

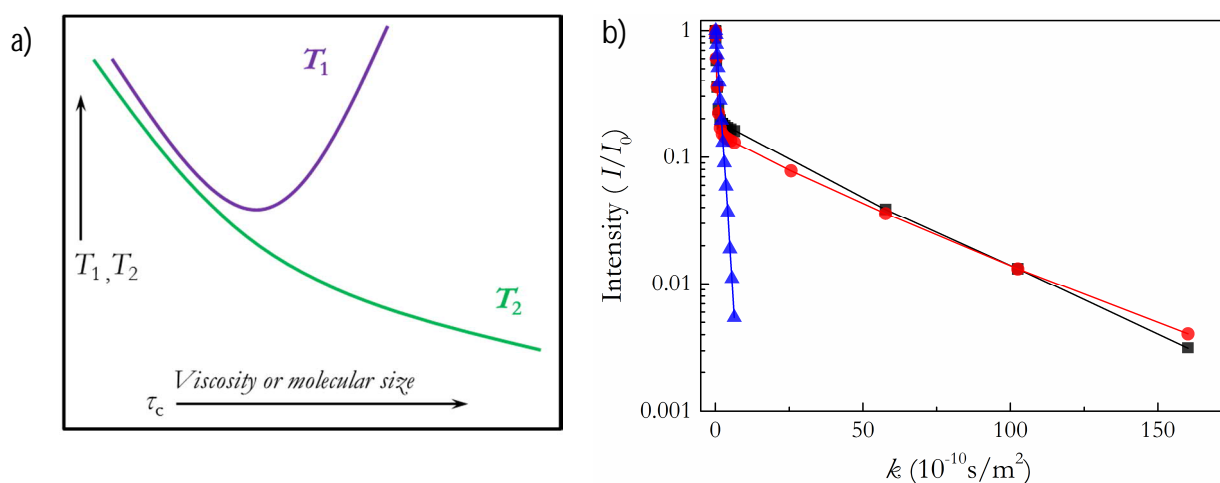


Figure 18. a) Typical variations in the transverse and longitudinal relaxation times,  $T_1$  and  $T_2$ , respectively, with the rotational correlation time  $\tau_c$ . b) Stimulated spin echo profile from NMR diffusometry measurements of silica particles grafted with 0.21 (black ■) and 0.31 (red ●)  $\mu\text{mol}$  mPEG silane/ $\text{m}^2$ , having bound fractions of 22 and 17 %, respectively. Free aqueous mPEG silane (blue ▲) is shown for comparison.

Experiments with varying diffusion times were performed to substantiate covalent linkage. Identical results were obtained, and it can therefore be concluded that the residence time of the species was more than several hundreds of milliseconds, most likely discarding the possibility of non-covalent adsorption since it would most likely result in shorter residence times. The self-diffusion coefficients obtained are in the order of  $10^{-10} \text{ m}^2 \text{ s}^{-1}$  for free silane, and  $10^{-12} \text{ m}^2 \text{ s}^{-1}$  for bound silane, with variations due to differences in concentrations, viscosity and obstruction. In principal, the yields could be obtained by measuring the relaxation times and analyzing the



relaxation profiles, but the higher relative difference of the self-diffusion coefficients, compared to the relaxation times, provides superior sensitivity of diffusometry for quantification of the functionalization yield.

The yields, and consequently the surface coverages, of the particles grafted with only mPEG silane used in Paper I was determined using NMR diffusometry. However, when other types of modifications are introduced, such as the propyl silane with a shorter hydrophobic group, immobilization of the silane species occurs when bound to a particle surface. This leads to very short  $T_2$  and in turn a non-detectable NMR signal, discarding diffusometry as an analysis tool. Another method, containing several experimental steps, was therefore developed to obtain the surface compositions of the particles with combined surface functionalities. The steps include ultra-centrifugation, elemental analysis and NMR spectroscopy analysis (see Experimental procedures). This method may therefore be less accurate compared to NMR diffusometry.

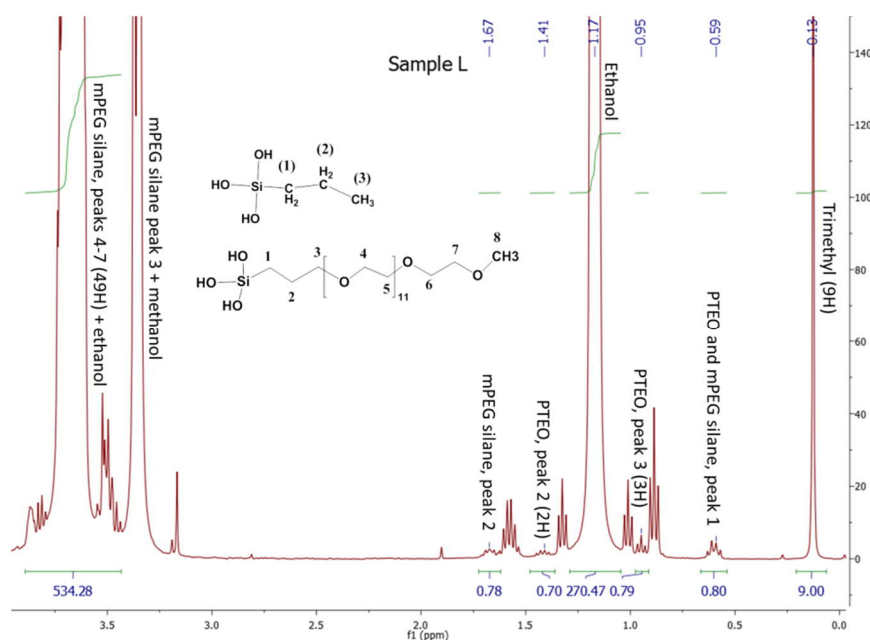


Figure 19. HR (H) PRESAT NMR spectrum of the supernatant taken from sample methyl<sub>0.5</sub>/propyl<sub>0.5</sub>/mPEG<sub>0.27</sub>-SiNP (sample L in Paper III), with integral relative values given. Reprinted from Paper III ©2017 with permission from Elsevier.

The NMR spectrum seen in Figure 19 is an example of a spectrum that was used for obtaining the molar ratios of the different silane species. It shows the NMR signals detected in a supernatant solution from ultracentrifugation of sample methyl<sub>0.5</sub>/propyl<sub>0.5</sub>/mPEG<sub>0.27</sub>-SiNP, where the subscripts indicate the grafting degree in  $\mu\text{mol per m}^2$  silica surface, and SiNP denotes silica nanoparticle (see also Table 2). An overlap of the signal of ethanol and the EO-units of the PEG-polymer exists, wherefore this was compensated for in the calculations. It can also be seen that the signals of the propyl silane are relatively weak – only the species not bound to the surface can be detected. Figure 20 shows the spectra of the purified suspension of sample

propyl<sub>0.93</sub>/mPEG<sub>0.27</sub>-SiNP, where most of the free silane species and alcohol residues have been removed.

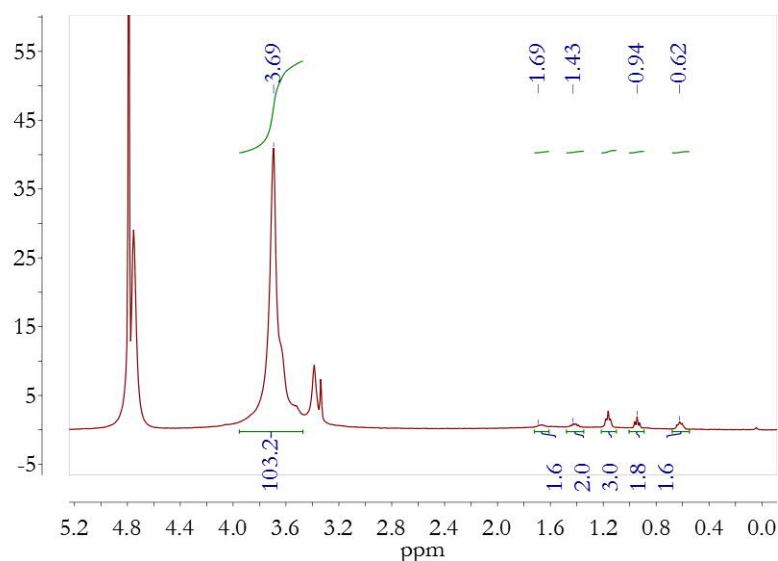


Figure 20. NMR spectrum of surface functionalized silica sol (propyl<sub>0.93</sub>/mPEG<sub>0.27</sub>-SiNP, see Table 2 for sample information) that has been purified by ultrafiltration. It can be seen that the signals from the alcohols and the propyl silanes are weak, indicating that most of the alcohols as well as free silane species have been removed.

Surface compositions and DLS particle size of a selected portion of the particles used are presented in Table 2 (for other samples, see appended papers). By performing Sears titration<sup>124</sup> before and after the surface functionalization, a change in SSA on account of the surface functionalization was obtained. Unless significant particle aggregation has occurred during the functionalization process, the change in the obtained SSA does not correspond to an actual change in the particle surface area, but instead to a change in available silanol groups, and thereby a change in the silanol number.<sup>125</sup> This provides an indication of the achieved silane surface coverage and the expected effect on the silica surface charge.

Table 2. Examples of samples used. The subscripts in the sample name denote the amounts of attached silanes, in  $\mu\text{mol}$  per  $\text{m}^2$   $\text{SiO}_2$ , and SiNP denotes silica nanoparticle. The reduction in silanol number was obtained through comparing the Sears SSA obtained before and after the functionalization procedure.

Samples	Levasil silica sol Sears SSA	Functionalization ( $\mu\text{mol}$ silane per $\text{m}^2$ $\text{SiO}_2$ )			$D_{p, vol}$ (nm)	Reduction in silanol no.	<i>Sample names in appended papers</i>
		Silane	Amounts				
			added	bound			
mPEG <sub>0.74</sub> -SiNP <sub>130</sub>	CS 40-213* 130 $\text{m}^2/\text{g}$	mPEG	4.00	0.74	33	78 %	Paper II: sample i
mPEG <sub>0.31</sub> -SiNP <sub>130</sub>	CS 40-213 130 $\text{m}^2/\text{g}$	mPEG	1.81	0.31	32	57 %	Paper I: 0.31mPEG
mPEG <sub>0.16</sub> -SiNP <sub>130</sub>	CS 40-213 130 $\text{m}^2/\text{g}$	mPEG	0.90	0.16	31	35 %	Paper I: 0.16mPEG, Paper II: sample iii
Propyl <sub>0.82</sub> -SiNP <sub>130</sub>	SP2138 130 $\text{m}^2/\text{g}$	Propyl	0.98	0.82	28	19 %	Paper IV: mPEG- SiNP
Propyl <sub>0.93</sub> /mPEG <sub>0.27</sub> - SiNP <sub>130</sub>	SP2138 130 $\text{m}^2/\text{g}$	Propyl mPEG	1.00 0.50	0.93 0.27	27	39 %	Paper IV: Propyl/mPEG- SiNP
Propyl <sub>1</sub> -SiNP <sub>130</sub>	CS 40-213 130 $\text{m}^2/\text{g}$	Propyl	1.06	1.0	27	-	Paper III: Sample B
Propyl <sub>0.93</sub> /mPEG <sub>0.27</sub> - SiNP <sub>130</sub>	CS 40-213 130 $\text{m}^2/\text{g}$	Propyl mPEG	1.00 0.50	0.99 0.21	30	39 %	Paper III: Sample G
Propyl <sub>1.9</sub> /mPEG <sub>0.2</sub> - SiNP <sub>200</sub>	CS 34-720** 200 $\text{m}^2/\text{g}$	Propyl mPEG	2.00 0.50	1.90 0.20	73	-	Paper III: Sample J
Propyl <sub>1.9</sub> /mPEG <sub>0.2</sub> - SiNP <sub>360</sub>	CS 30- 236*** 360 $\text{m}^2/\text{g}$	Propyl mPEG	1.0 0.59	1.0 0.17	13		Paper III: Sample P

\* Old name: Bindzil 40/130

\*\* Old name: Bindzil 2034D1

\*\*\* Old name: Bindzil 30/360

## Colloidal properties of the functionalized particles

Attaching silanes onto the silica particle surface enables reduction of the silica surface charge, control of the colloidal stability and the wettability of the particles, at various salt concentrations, pH conditions, and in different media. The following sections describe the observed colloidal behaviors, starting with the effects on the silica particle surface and how the colloidal system is affected by changes in pH and electrolyte concentrations.

### Silica surface charge and zeta potential

The decrease in the silanol number seen in Table 2 can be ascribed to all types of functionalities employed here, although the mPEG silane functionality most efficiently reduces the silica surface charge. As a complement to Sears titration, zeta potential was analyzed, and polyelectrolyte as well as potentiometric titrations were performed. Figure 21 shows the zeta potential and the apparent surface charge density (ASC) of dialyzed, mPEG-grafted SiNPs as functions of mPEG surface coverage. The decrease in ASC, obtained from particle charge density measurements through polyelectrolyte titration, and also in the absolute value of zeta potential, can be correlated to the surface coverage of mPEG silane. However, sample mPEG<sub>0.74</sub>-SiNP (used in Paper II), which has a higher degree of mPEG coverage, shows no further decrease in ASC. This suggests a steric effect where silica surface, at around  $0.3 \mu\text{mol}$  mPEG per  $\text{m}^2$ , is covered with sufficiently high

amounts of mPEG silane to hinder full polyelectrolyte adsorption. However, the yield of sample mPEG<sub>0.74</sub>-SiNP was not determined with NMR diffusometry, but with the analysis method including elemental analysis. The latter method could overestimate the amount of mPEG silane attached to the silica surface, since unreacted mPEG silane that may be associated with the particle could end up in the precipitate.

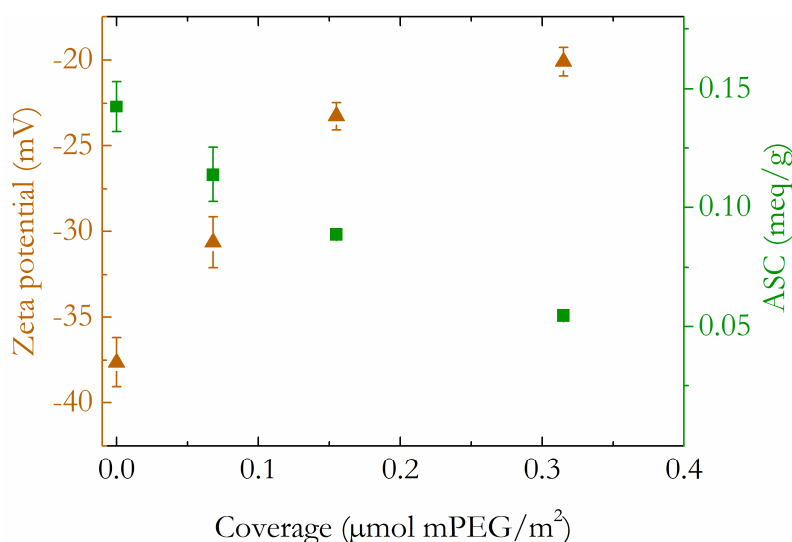


Figure 21. Zeta potential in mV (orange  $\blacktriangledown$ ) and apparent surface charge (ASC) in meq/g (green  $\bullet$ ) as measured with PCD polyelectrolyte adsorption, as a function of the mPEG silane surface coverage in  $\mu\text{mol mPEG m}^{-2}$  of the particles. Reproduced from Paper I ©2015 with permission from Elsevier.

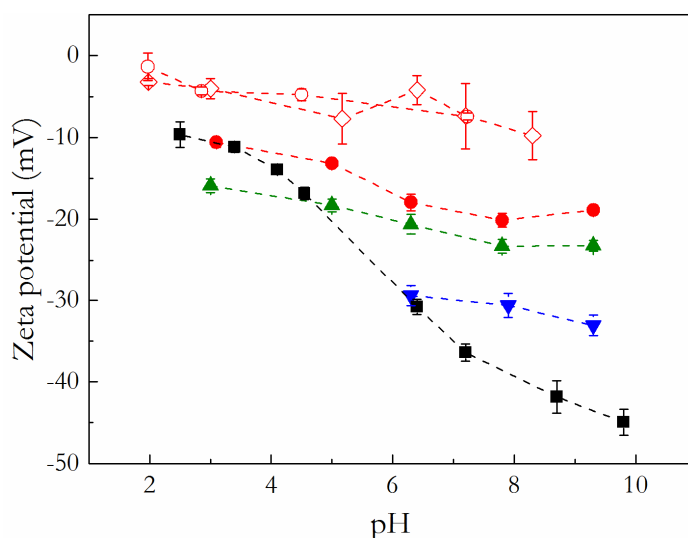


Figure 22. Zeta potential of dialyzed PEGylated samples as a function of pH, with varying salt concentrations and surface coverages: samples with 0.068 (blue  $\blacktriangledown$ ), 0.155 (green  $\blacktriangle$ ) and 0.315 (red  $\bullet$ )  $\mu\text{mol mPEG silane m}^{-2}$  are measured at 7 mM salt. Unmodified particles (black  $\blacksquare$ ) are shown for comparison and have  $\sim 10$  mM salt. For high surface coverage it was possible to measure at higher salt concentrations; 100 mM (red  $\circ$ ) and 200 mM (red  $\diamond$ ). Reprinted from Paper I ©2015 with permission from Elsevier.

The zeta potential is the measured potential in the shear plane between the particle and the bulk solution that is created when the particle moves through an electric field.<sup>134</sup> When polymers are adsorbed to the particles and extend out into the diffuse layer, a movement of the shear plane

further out from the particle surface occurs, which decreases the zeta potential.<sup>134</sup> The mPEG silane is very short (11 EO units, a couple of nm long) compared to the thickness of diffuse double layer at low salt concentrations, wherefore such effect may be negligible. At high salt concentrations on the other hand, where the diffuse double layer is compressed, such an effect might have been captured (see Figure 22 where zeta potentials close to zero are obtained upon addition of salt).

The measurements shown in Figure 22 also demonstrate that the functionalization with mPEG makes the particles less affected by changes in pH, when the surface coverage is 0.155  $\mu\text{mol mPEG silane m}^{-2}$  and above. An increased salt concentration to  $\geq 100$  mM leads to severe aggregation of the particles in all samples apart from the high coverage one (0.315  $\mu\text{mol mPEG silane m}^{-2}$ ). For the latter, only moderate aggregation was noted through an increase in average particle diameter from 32 nm at alkaline conditions to  $\sim 40$  nm at 100 mM salt and  $\sim 90$  nm at 200 mM salt. These results demonstrate that steric and electrosteric stabilization effects have been achieved, which will be discussed further in correlation to the flocculation behavior of the functionalized particles.

#### Potentiometric titrations

Surface charge densities (SCDs) per unit surface area of mPEG-grafted samples are seen in Figure 23. The point of zero charge (PZC) was put to pH = 3 (Fig. 4 in Paper II), but for sample mPEG<sub>0.74</sub>-SiNP the curve obtained with PZC at pH 4 is more similar to the other samples (Figure 23), wherefore a higher PZC is more likely. The measured SCD of mPEG<sub>0.74</sub>-SiNP is around 30 % lower than that of non-modified sol at pH 9. The effect of the functionalization appears small compared to the polyelectrolyte titration, where a reduction in ASC of around 60 % was observed. This probably originates in different steric effects, since H<sup>+</sup>-ions (i.e. H<sub>3</sub>O<sup>+</sup>) are smaller than polybrene used in the latter case.

As mentioned in the Materials and methods-section, addition of salt leads to screening of the silica surface charge and results in a higher SCD. Consequently, when CaCl<sub>2</sub> is added, the silica particle surface hold a higher SCD (see Figure 23b). At the high mPEG surface coverage employed, particle aggregation is avoided through steric stabilization, wherefore e.g. clouding properties can be explored at relatively high salt concentrations. Salt addition also results in a reduction of pH; a diluted silica suspension with 1.5 M CaCl<sub>2</sub> had a measured pH of 7.7, compared to pH 9.8, which was obtained when the suspension was diluted without salt. The reduction of pH can be explained by adsorption of OH<sup>-</sup>-ions onto the silica surface,<sup>135</sup> or by the release of H<sup>+</sup>-ions from the surface, where both these processes should be facilitated by surface charge screening. The screening of surface charges is a way to activate charged particles, if the desired use is adsorption at interfaces and as Pickering stabilizers.<sup>16</sup>

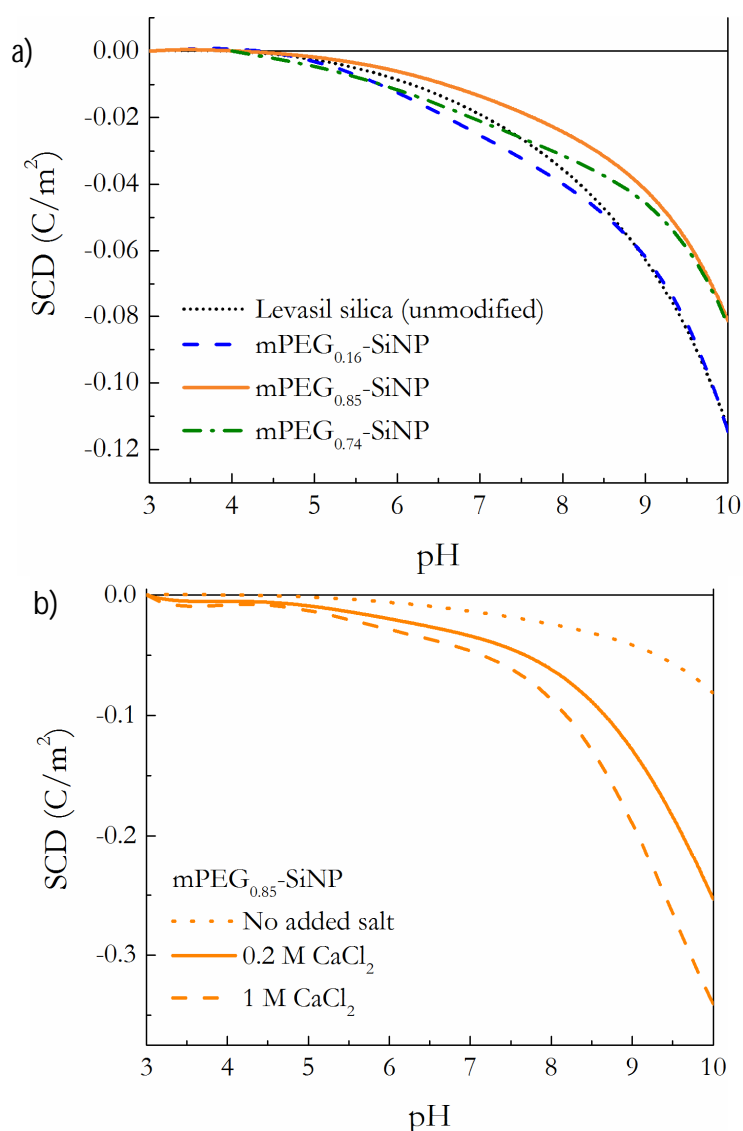


Figure 23. Surface charge densities (SCDs), per square meter of silica: a) As a function of measured pH and b) at varying concentrations of calcium chloride. Reproduced from Paper II, but with the point of zero charge (PZC) changed to pH 4 for sample mPEG<sub>0.74</sub>-SiNP. The subscripts in the sample name denote the amounts of attached silanes, in  $\mu\text{mol per m}^2 \text{SiO}_2$ , and SiNP denotes silica nanoparticle.

### Surface activity of functionalized silica nanoparticles

Species added to water are surface active if a reduction in the surface tension, compared to the surface tension of pure water (72 mN/m), is observed, and the lower the surface tension, the higher is the surface activity. Surface tension measurements are therefore a common way to characterize surfactants. The relevant parameter for quantifying particle wettability is the three-phase contact angle (illustrated in Figure 3a). However, there is yet no simple way of direct measurements of the mentioned contact angle for particles of nano-scale at an oil/water interface. The surface tension provides an indication of the wettability, and the interfacial tension is another possible way of characterizing the particles. Charged particles can only be depleted from a suspension, and thus adsorb at the interface, if the energy gain compensates for the energy barrier due to e.g. concentrating charged particles at the interface, and for the entropy loss.<sup>136</sup> Surface active species adsorb at interfaces, and decrease the interfacial energy. A lower

particle charge density will therefore lead to a higher surface activity, since a reduction of surface charge facilitates the adsorption at the air-water interface.<sup>136</sup> Figure 24 shows the effect of the functionalized particles on surface tension, measured with the D unouy ring method. A very small effect on the surface tension ( $\sim 2$  mN/m of reduction) in the presence of unmodified silica particles is observed, consistent with other findings.<sup>137-139</sup> Particles modified with only hydrophobic groups show very small, or no, effects on the surface tension. The PEGylated particles, on the other hand, have a larger effect on the surface tension. The samples were purified through ultrafiltration, which removes the major part of the unreacted mPEG species and alcohol residues from the functionalization reaction, and contained less than 0.7 mM free mPEG silane. A solution of 0.7 mM mPEG silane and methanol residues from the hydrolysis reaction has a surface tension of  $\sim 62$  mN/m. The surface tension observed for both high and medium surface coverage samples is below that of the free silane solution;  $\sim 56$  mN/m for mPEG<sub>0.15</sub>-SiNP and  $\sim 51$  mN/m for mPEG<sub>0.31</sub>-SiNP. This shows that the PEGylated particles are, to some extent, surface active, where a higher degree of surface functionalization, associated with a larger reduction of surface charge density, was found to result in a more pronounced decrease of the surface tension.

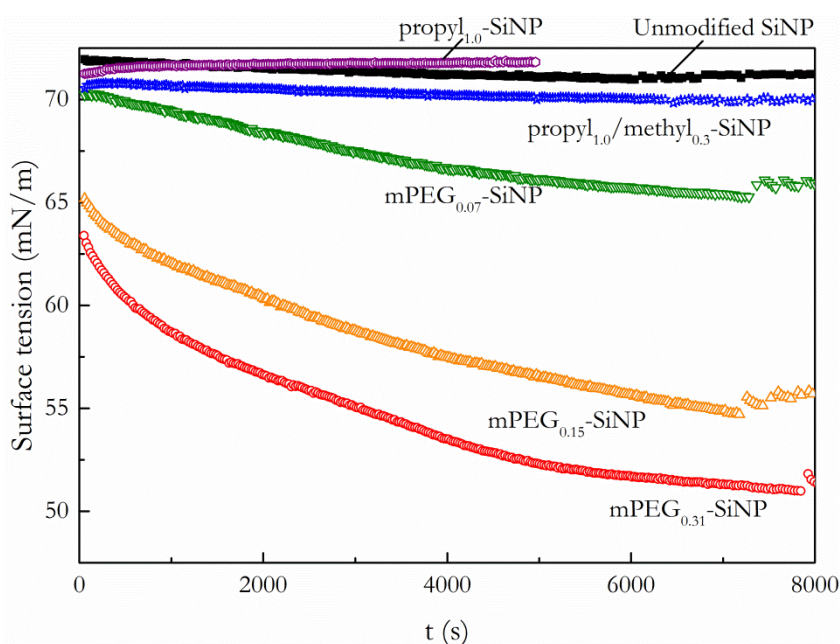


Figure 24. Surface tension as a function of time, for functionalized silica particles at a concentration of 5 wt% SiO<sub>2</sub>. The particles have been functionalized with mPEG silane, propyl silane and trimethyl silane, respectively. The subscripts in the sample name denote the amounts of attached silanes, in  $\mu\text{mol}$  per m<sup>2</sup> SiO<sub>2</sub>, and SiNP denotes silica nanoparticle. Unmodified particles are shown for comparison. The samples have been purified through ultrafiltration prior to the measurements.

Interfacial tension measurements at the Exxsol D60-silica suspension interface also revealed effects arising from the presence of the particles, both modified and unmodified ones, seen in Figure 25, with the pH of the silica suspensions adjusted to 10 and 4.7 - 3.5, respectively. The interfacial tension at the Exxsol D60-distilled water interface was measured to be 48 mN/m. A decrease in interfacial tension of more than 10 mN/m was observed at the Exxsol D60-silica suspension interface, and further reduction was observed for the functionalized particles, compared to the Exsol D60-water interfacial tension. A decreased pH, which decreases the silica



particle charge, is expected to facilitate particle interfacial adsorption. This was observed for the samples not containing mPEG: the measured interfacial tension was lower at pH 3.5 compared to at pH 10. Addition of the mPEG silane increases the surface activity at pH 10, since further reduction in the interfacial tension is observed compared to particles without the mPEG functionality. However, the same effect is not seen at low pH. The behavior most likely originates in the pH- and temperature dependent attractive forces that exist between silica and poly(ethylene oxide).<sup>79, 140, 141</sup> The attraction exists below, but not above, pH 8. Any free mPEG silane present in the sample at high pH conditions will therefore be expelled from the silica surface and is available for adsorption at the interface, while at low pH conditions free mPEG is more likely to be adsorbed onto the silica surface and the surface activity is reduced. An increased amount of mPEG in the sample leads to increased surface activity at high pH conditions, but not at low pH. The sample  $\text{prop}_{1.0}/\text{mPEG}_{0.17}\text{-SiNP}_{360}$  has the highest concentration of mPEG silane (both free and bound), since the particle has the highest SSA, and the amount of mPEG silane in the sample is proportional to the SSA. The interfacial tension is low at pH 10, where the free mPEG contributes to an increased surface activity, but at pH 4.7 where a large silica surface area is available for mPEG adsorption, a higher interfacial tension, corresponding to a lower surface activity, is observed. The mentioned PEG-silica interaction has brought other important features, such reversible flocculation.

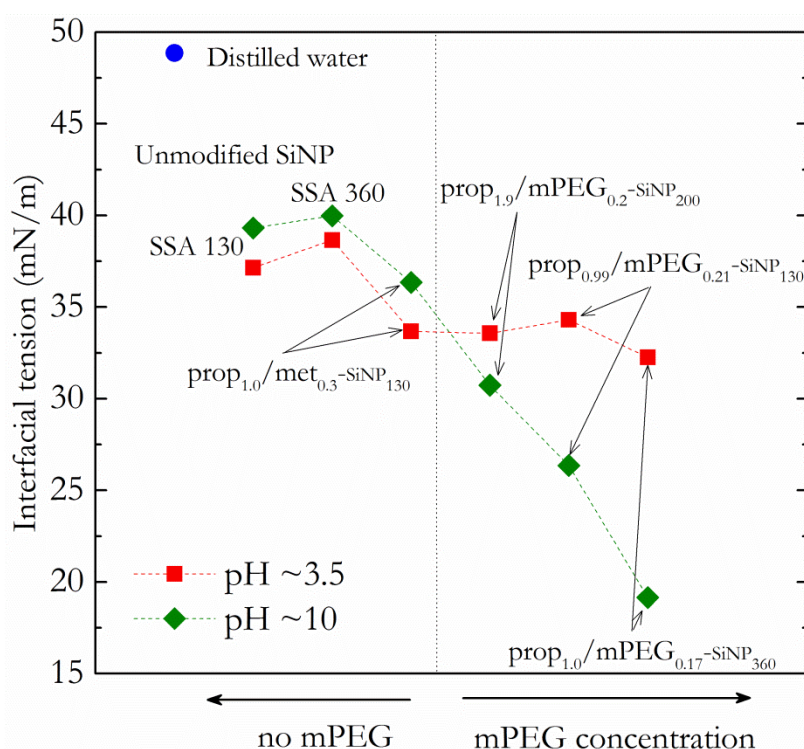


Figure 25. Interfacial tensions at the silica suspension-Exxsol D60 interface, of unmodified particles: Levasil CS 40-213 (SSA 130) and Levasil CS 30-236 (SSA 360), and of functionalized particles (samples D, J, G and P in Paper III, respectively) at 2.5 wt%  $\text{SiO}_2$ . The subscripts in the sample name denote the amounts of attached silanes, in  $\mu\text{mol per m}^2 \text{SiO}_2$ , and the SSA of the silica particle in  $\text{m}^2/\text{g}$ . The values for the interfacial tension were collected at two pH values of the suspensions and after measuring for at least 4000 s (for sample  $\text{prop}_{1.0}/\text{mPEG}_{0.17}\text{-SiNP}_{360}$  the low pH value was 4.7, since at lower pH the viscosity was too high). For comparison the interfacial tension of distilled water-Exxsol D60 is shown (blue ●).



## Reversible flocculation behavior

It is now known that weak flocculation of particles utilized as emulsifiers is beneficial for emulsion formation.<sup>11, 15, 54, 66</sup> mPEG-grafted particles, with medium and low amounts of mPEG silane ( $< 0.3 \mu\text{mol mPEG silane m}^{-2} \text{SiO}_2$ ) display a pH dependent flocculation behavior. Figure 26 shows the absorbance (i.e. turbidity) as a function of pH, and a distinct increase in turbidity is seen below pH 6. Decreasing the pH of the suspension increases interaction between the mPEG and the silica particle surface,<sup>140</sup> and flocculation of silica due to adsorption of PEO polymers on the silica surface is known to depend on ionic strength, pH and the amount of polymer adsorbed.<sup>142</sup> mPEG-grafted particles with surface coverages below  $0.3 \mu\text{mol mPEG silane/m}^2 \text{SiO}_2$  display a distinct increase in turbidity below pH 6. The results suggest a weak flocculation due to inter-particle patch-flocculation at low pH conditions and low mPEG surface coverages. At higher surface coverages ( $> 0.3 \mu\text{mol mPEG silane/m}^2 \text{SiO}_2$ ), the attached mPEG silane sterically hinders such interaction and no flocculation occurs. While the pH clearly influences the flocculation, similar experiments were performed using ion-exchange instead of adding acid (see Fig 4C, Paper I), resulting in a lower ionic strength of the suspension. Flocculation occurred also at these conditions, but the process was slower and the turbidity increase was lower. Free mPEG present in the samples also influences the system, but the effect was not captured by flocculation studies (it does, however, influence the cloud point, as is discussed in the coming section). The flocculation is reversible; increasing the pH of an acidic suspension returned the flocculated system to its original turbidity. Likewise, the DLS particle size was regained. The mPEG functionalization thus provides electrosteric stabilization, and mPEG-grafted particles are apparently very efficient in achieving controllable flocculation below pH, especially if the ionic strength is high.

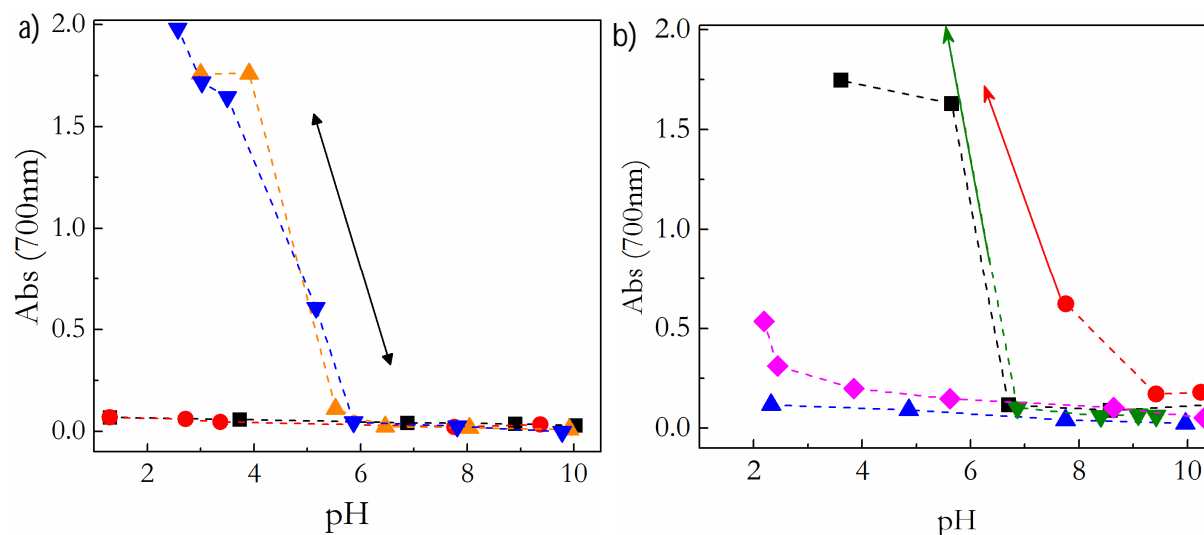


Figure 26. Absorbance (abs) at 700 nm measured with UV/Vis spectroscopy, showing the variations in turbidity as a function of pH: a) mPEG-grafted particles: with 0.068 (blue ▼), 0.155 (orange ▲) and 0.315 (red ●)  $\mu\text{mol mPEG silane m}^{-2}$ , respectively, and without functionalization (black ■). b) Surface functionalized particles: propyl<sub>1.0</sub>/dimethyl<sub>0.9</sub>/mPEG<sub>0.27</sub>-SiNP<sub>200</sub> (red ●), propyl<sub>1.6</sub>/mPEG<sub>0.15</sub>-SiNP<sub>130</sub> (green ▼), propyl<sub>0.99</sub>/mPEG<sub>0.21</sub>-SiNP<sub>130</sub> (black ■), propyl<sub>1.0</sub>-SiNP<sub>130</sub> (pink ◆) and trimethyl<sub>0.2</sub>-SiNP<sub>130</sub> (blue ▲). Reproduced from Paper I ©2015 (a) and Paper III ©2016 (b), with permission from Elsevier.

Figure 27 shows the  $^1\text{H}$  NMR signal from the poly(ethylene oxide) units of the mPEG silane grafted on silica particles with (a) 0.155 and (b) 0.315  $\mu\text{mol}$  mPEG silane/ $\text{m}^2$   $\text{SiO}_2$ , respectively. Ultra-filtrated samples were diluted in  $\text{D}_2\text{O}$  and ion-exchanged using a cation-exchange resin, and the spectra were collected as a function of pH. The spectra provide information regarding the mobility of the mPEG polymer chain; immobilization of a molecule leads to reduction of the transitional relaxation time,  $T_2$ , and the signal eventually become non-detectable due to severe broadening of the peak. In Figure 27 a decrease in intensity is seen for (a), most probably due to the mentioned broadening of the peaks, a consequence of mPEG silane adsorption to the silica surface during patch flocculation. For (b), no decrease in intensity is observed, in coherence with the turbidity results. It demonstrates that even though the surface coverage of mPEG is relatively far from the theoretical maximum of 8  $\mu\text{mol}$  OH groups per  $\text{m}^2$   $\text{SiO}_2$ , it has a large influence on the surface properties. Apparently, at 0.315  $\mu\text{mol}$  mPEG silane/ $\text{m}^2$   $\text{SiO}_2$ , no further pH-dependent PEG-silica interactions that result in reduced PEG-chain mobility are present, which indicates that the surface is relatively well covered with the functionality.

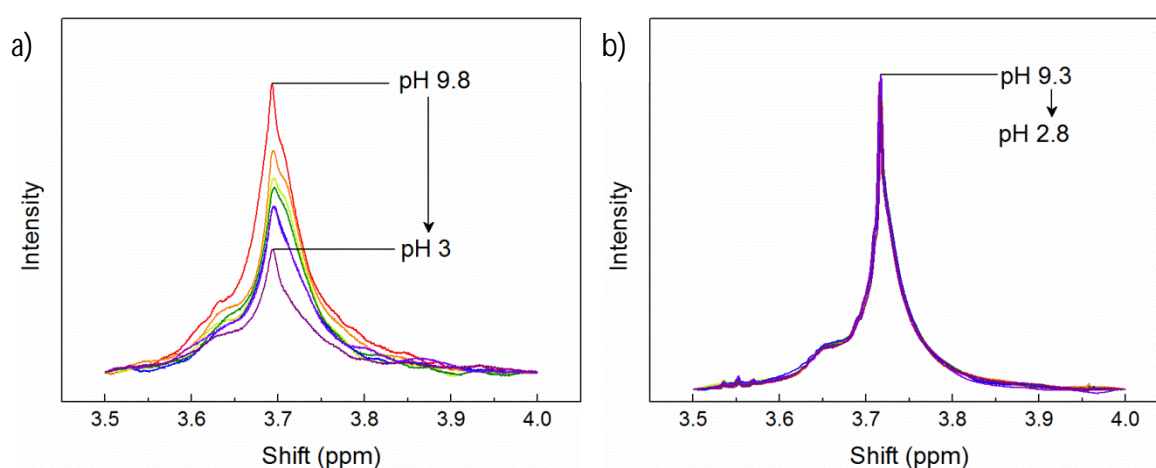


Figure 27. NMR spectra showing the peak arising from the poly(ethylene oxide) units of the mPEG silane grafted on silica particles with a) 0.155  $\mu\text{mol}$  mPEG silane/ $\text{m}^2$   $\text{SiO}_2$  and b) 0.315  $\mu\text{mol}$  mPEG silane/ $\text{m}^2$   $\text{SiO}_2$ , as the pH is decreased. The experiments were conducted on a Varian 400 MHz spectrometer. Reprinted from Paper I ©2015 with permission from Elsevier.

The particles modified with only hydrophobic modifications, shown in Figure 26b, display very little or no flocculation upon a decrease in pH. Particles with both hydrophobic and hydrophilic surface species provide the desired flocculation behavior on account of the presence of mPEG, and high amounts of hydrophobic groups display a hydrophobic effect that accelerates the flocculation. The zeta potential measurements, surface charge determinations, flocculation behavior and NMR measurements show that by grafting colloidal silica with mPEG silane, a stabilization of the particles is achieved in such a way that a controllable flocculation is obtained at low surface coverages, while at higher surface coverages steric stabilization is achieved. It also shows the importance of pH, for controlling both colloidal stability and emulsification abilities, as will be discussed further in relation to emulsion studies.

## Silica particles with clouding behavior

The steric stabilization achieved at high mPEG surface coverages enabled studies of clouding behavior, since  $\text{CaCl}_2$  could be added to suspensions of mPEG-grafted silica particles at room temperature, without particle aggregation occurring, in contrast to unmodified silica particles where severe aggregation occurs immediately. The addition of salt leads to salting out effects on the PEG-chains, which in turn reduce the cloud point.<sup>3, 143</sup> This allowed clouding to be observed below 100 °C.



Figure 28. a) Diluted suspensions of  $\text{mPEG}_{0.74}$ -SiNP with no added salt, with 1 M  $\text{CaCl}_2$  and with 1.5 M  $\text{CaCl}_2$ , from left to right, at 3.5 wt% of  $\text{SiO}_2$ . The samples have been heated to 110 °C and clouding was observed for the two samples containing  $\text{CaCl}_2$ . b) Shows the sample with 1.5 M  $\text{CaCl}_2$  cooled to room temperature, and the original turbidity was regained.

Figure 28 shows the visual appearance of diluted suspensions of mPEG-grafted silica particles, at varying electrolyte concentrations, where the distinct increase in turbidity that signifies clouding is observed for the two samples containing  $\text{CaCl}_2$ . The observed cloud points were clearly dependent on the electrolyte concentrations, where a lower cloud point is observed for high  $\text{CaCl}_2$  concentrations, see Figure 29a. This is in agreement to the behavior of nonionic surfactants.<sup>143, 144</sup> But, in contrast to surfactant systems, a non-linear relationship is observed, suggesting that the addition of salt is more effective at low salt concentrations.<sup>145</sup> It seems that, at low salt concentration, the effect on the screening of the silica particle surface charge is dominating, whereas at increased  $\text{CaCl}_2$  concentration salting out effects of the PEG-chains become increasingly important. Also, an effect of pH was found, but only when the concentration of free mPEG is reduced; clouding of  $\text{mPEG}_{0.74}$ -SiNP, having the highest amount of free mPEG of the samples studied, was not pH dependent, while a sample with lower free mPEG-concentration displayed a decreased cloud point at lower pH conditions. Purification of the sample using ultra filtration (UF), which removed major part of the free mPEG silanes, reduced the cloud points further and lead to irreversible aggregation at high pH and high salt concentrations. The pH of the suspension affects the particle surface charge and the PEG-silica interaction, promoting flocculation of sparsely covered particles at pH below 6-8. At the higher free mPEG content, this effect is suppressed.

Although pH is important, the intensity of the NMR signal from the EO units of the PEG polymer shown in Figure 29b demonstrates the strong salting-out effect that  $\text{CaCl}_2$  has on the mPEG silane. The intensity at varying pH conditions (pH 9, 7, 4 and 2), recorded at increasing temperatures did not affect the mobility of the PEG chain. This is in coherence with the discussions in Paper I and with Figure 27: at high enough mPEG coverage steric stabilization is present, the silica particle surface is fully covered with mPEG and therefore not affected by changes in pH. The intensities from the sample containing 1 M  $\text{CaCl}_2$  show a distinct decrease of the mobility of the PEG chain. When water becomes a poorer solvent for the PEG polymer, due

to the addition of salt, the PEG chains will seek each other and possibly adsorb in thicker layers around the particle, a clear salting out effect. At the cloud point, where PEG rich and particle rich domains are created, further reduction of the intensity is seen, due to further reduction of the mobility during clouding. The clouding behavior found opens new routes for studying emulsion properties and emulsification performance of Pickering emulsions stabilized with mPEG-grafted particles. This was explored in Paper IV.

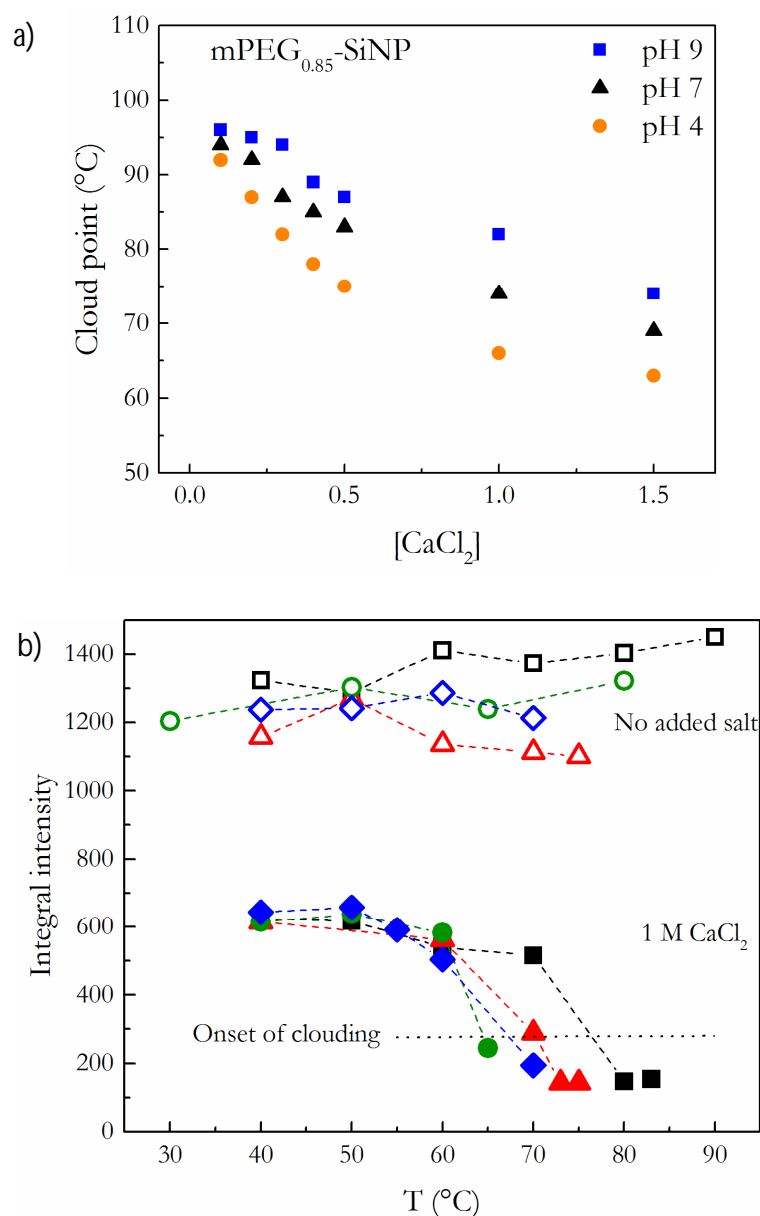


Figure 29. a) Cloud point observed in suspensions with mPEG<sub>0.85</sub>-SiNP<sub>130</sub>, at 2 wt% of SiO<sub>2</sub>, as a function of  $CaCl_2$  concentration in M, and at varying pH conditions. b) Integral intensities, obtained from <sup>1</sup>H NMR spectroscopy, of the peak arising from the poly(oxy ethylene) units in the mPEG silane in mPEG<sub>0.85</sub>-SiNP<sub>130</sub>, at 1 M  $CaCl_2$  and without added salt, at varying pH conditions (pH 9: black ■/□; pH 7 red ▲/△; pH 4 green ●/○; pH 2 blue ◆/◇). Reprinted from Paper II.

## Utilization of the surface functionalized silica nanoparticles in emulsions

Emulsification properties of an emulsifier can be discussed in different ways, depending on what features that are important for the application of interest. These could be fast or spontaneous emulsification, low energy demand, high stability towards coalescence, controlled phase separation, controlled phase inversion and possibility to load the emulsion with substances that are to be released. Possibility to control the emulsion droplet size is also important but is mainly influenced by the emulsification equipment. Emulsions stabilized by surfactants are dynamic systems, where spontaneous emulsification is possible at e.g. ultralow surface tension. Large reductions of interfacial tension normally occur upon addition of surfactant, facilitating the formation of very small emulsion droplets, and type of emulsion may be controlled through the choice of surfactant. mPEG-grafted silica particles possess both clouding behavior and are surface active, making these particles potential candidates to achieve similar features in Pickering emulsions. Pickering emulsions also offer the possibility of preparing large emulsion droplets that are stable towards coalescence, in contrast to surfactant-stabilized emulsions, where large emulsion droplets usually result in poor coalescence stability. The coalescence stability is mainly determined by the nature of the repulsive interactions of the emulsion droplets, where the thickness of the stabilizing layer plays an important role.<sup>4</sup> In this aspect, particles offer superior stabilizing characteristics compared to surfactants, especially if polar oils are of interest. PEGylated particles can be used to stabilize emulsions,<sup>107</sup> but by adding a hydrophobic group in addition to the hydrophilic mPEG silane, superior emulsification abilities are expected due to increased interaction with the oil-phase, resulting in contact angles closer to 90°.

### General findings – emulsification

Paper III reports on a comparative study, where the main purpose was to produce particles with suitable combinations of hydrophobic and hydrophilic functionalization and utilize these for emulsion stabilization. In addition, salt concentration, silica particle-to-oil phase ratio and pH dependence were investigated. A summary of the findings is given here. The emulsions prepared were o/w, and most had an oil content of 40 wt% (45.7 vol%) and an aqueous suspension containing 2.5 wt% SiO<sub>2</sub>, giving 0.0375 grams of SiO<sub>2</sub> per gram oil. The pH of the aqueous phase was adjusted to 3.9 ± 0.3, to achieve flocculated particles with low surface charge, and facilitate adsorption at the interface.

#### Effect of type of surface modification

Figure 30 shows the median emulsion droplet diameter as a function of time of emulsions stabilized by unmodified particles, particles with hydrophobic groups attached, and particles functionalized with both hydrophilic and hydrophobic groups. The emulsions were prepared using Magic Lab, which efficiently supplies a high shear rate during the emulsification. Relatively stable emulsions could therefore be obtained using unmodified particles, which are inherently hydrophilic. Unmodified silica has been used by Frelichowska et al<sup>59</sup> to emulsify butanol and ethyl acetate in water, and hydrophilic silica sol has been used by Persson et al<sup>75</sup> to prepare o/w

emulsions with various types of oils. However, the mPEG-modified particles employed here displayed poor emulsifying abilities: o/w emulsions prepared with butanol, ethyl acetate and Exxsol D60 underwent complete phase-separation within 0.5-5 days at the investigated conditions, suggesting poor interaction between the PEG-chains and the oil-phases. Emulsions stabilized by particles functionalized with only hydrophobic groups show good coalescence stability, as can be seen in Figure 30, the median emulsion droplet size is not increasing at a significant rate over the course of more than four years, although the fraction of larger droplets is slightly increased, which can be seen in Figure 31. It is obvious that a higher rate of coalescence occurs in the emulsions stabilized with unmodified particles, and the use of particles with the combined functionalization, of both hydrophobic and hydrophilic groups, enables preparation of emulsions with slightly smaller emulsion droplets (Figure 30 and Figure 31). The interfacial tension between Exxsol D60 and water is relatively high, but through mPEG silane functionalization, a reduction of interfacial tension is achieved. It is also probable that the presence of free, surface active mPEG silane in the suspensions aids the emulsification, through further reduction of the interfacial tension, which facilitates formation of smaller emulsion droplets.

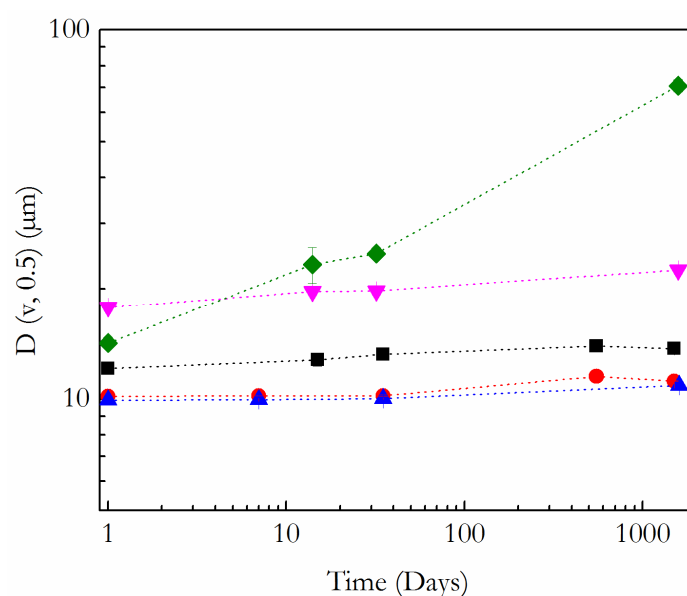


Figure 30. Median emulsion droplet diameter ( $D$ ) as a function of time as measured with laser diffraction, of emulsions containing 40 wt% Exxsol D60 and 2.5 wt% silica particles in the water phase. Emulsions stabilized by unmodified Levasil CS 40-213 show a remarkably high stability towards coalescence (pink  $\blacktriangle$ ), while the use of a smaller particle, Levasil CS 30-236 (green  $\blacklozenge$ ) results in coalescence of the emulsion droplets. Surface modified particles; propyl<sub>1</sub>-SiNP<sub>130</sub> (black  $\blacksquare$ ), propyl<sub>0.99</sub>/mPEG<sub>0.21</sub>-SiNP<sub>130</sub> (red  $\bullet$ ) and propyl<sub>1.0</sub>/mPEG<sub>0.17</sub>-SiNP<sub>360</sub> (blue  $\blacktriangledown$ ) display a high coalescence stability. Reproduced from Paper III ©2016 with permission from Elsevier.



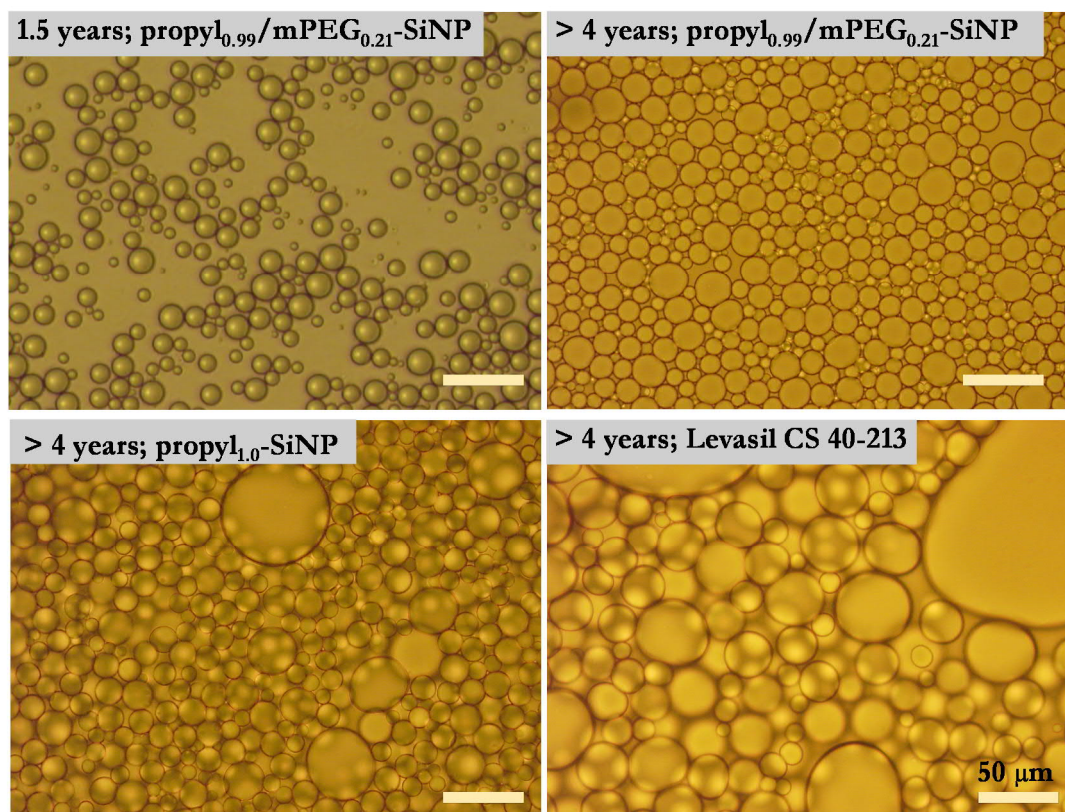


Figure 31. Microscope images of emulsions stabilized by surface functionalized silica particles, taken 1.5 and more than 4 years after preparation (the time and the particle used as emulsifier are indicated in the upper left corner of the micrograph). It is clear that the emulsion stabilized by unmodified particles has large emulsion droplets and that coalescence or Ostwald ripening has occurred. The scale bars represent 50  $\mu\text{m}$ .

Functionalization conditions as well as the relative amounts of functionalization of the particles used as emulsifiers influence the emulsion droplet size obtained. For example, addition of mPEG before the hydrophobic species during the functionalization process lead to an increase in droplet size, of emulsions with these particles as emulsifiers, most likely due to a more hydrophilic character of the particles. Adding large amounts of hydrophobic groups also results in larger emulsion droplets, this because of particle aggregation and less surface area available to stabilize the droplets. Figure 32 shows how the emulsion droplet size depends on the available surface area to stabilize the droplets and demonstrates the importance of considering particles size. Thus, proper balance between the amounts of hydrophilic and hydrophobic groups is of high importance. The emulsification behavior is thereby affected by the nature of the silica surface and may also be controlled by the pH conditions and salt concentration in the aqueous phase.

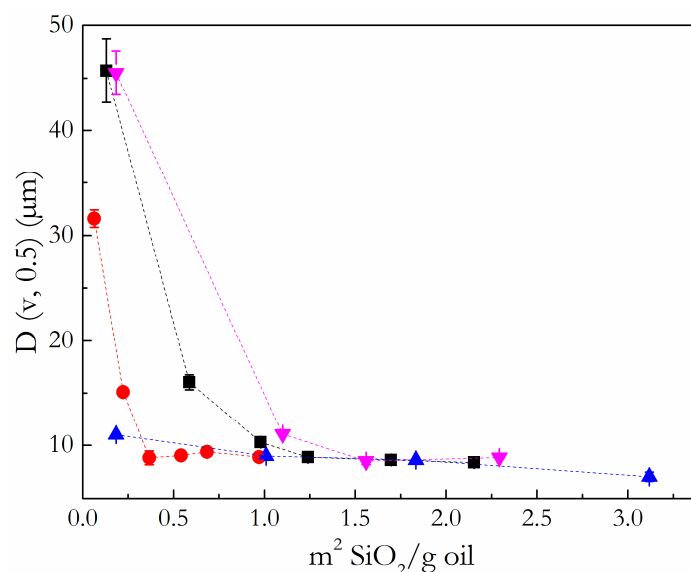


Figure 32. Emulsion droplet diameter as a function of surface area silica-to-oil content. The emulsions contain 19 wt% oil and were prepared at pH 4 using the following particles as emulsifiers: propyl<sub>0.99</sub>/mPEG<sub>0.21</sub>-SiNP<sub>130</sub> (black ■), propyl<sub>1.0</sub>/mPEG<sub>0.17</sub>-SiNP<sub>360</sub> (blue ▲), propyl<sub>1.0</sub>/dimethyl<sub>0.9</sub>/mPEG<sub>0.27</sub>-SiNP<sub>200</sub> (red ●) and propyl<sub>0.5</sub>/octyl<sub>0.5</sub>/mPEG<sub>0.2</sub>-SiNP<sub>130</sub> (pink ▼). The silica surface area was calculated assuming a contact angle of 90° and not taking into account flocculation due to the low pH. Reproduced from Paper III ©2016 with permission from Elsevier.

#### Effect of pH and salt concentration

Emulsion droplet size was monitored as a function of pH and a clear effect of pH exists, which can be correlated to the pH-dependent flocculation behavior of the silica sols discussed previously. Figure 33 shows that more efficient stabilization of the oil droplets occur at low pH conditions, especially below pH 6 and 8, for sample propyl<sub>1.6</sub>/mPEG<sub>0.15</sub>-SiNP and propyl<sub>1.0</sub>/dimethyl<sub>0.9</sub>/mPEG<sub>0.27</sub>-SiNP, respectively. The pH at which the reduced emulsion droplet size is observed coincides with the pH conditions at which flocculation occurs for the respective silica sol. Flocculation can also be achieved by addition of salt to the suspensions before emulsification, another way to control emulsification properties.

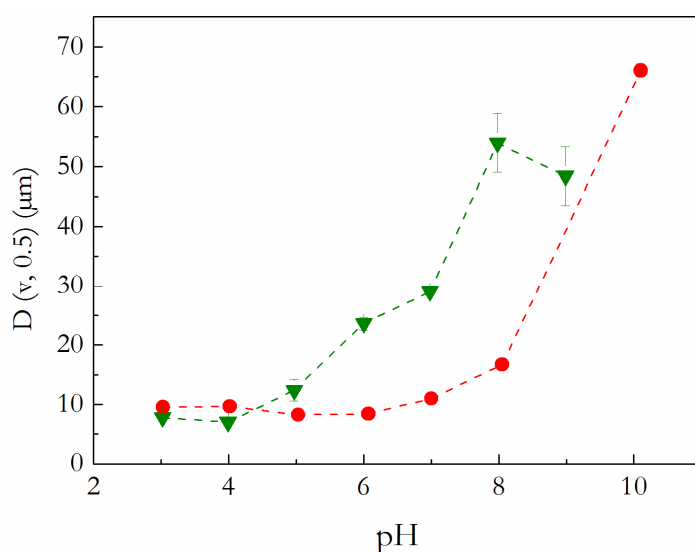


Figure 33. Median emulsion droplet diameter as a function of pH of emulsions stabilized by propyl<sub>1.0</sub>/dimethyl<sub>0.9</sub>/mPEG<sub>0.27</sub>-SiNP (red ●), propyl<sub>1.6</sub>/mPEG<sub>0.15</sub>-SiNP (green ▼). At pH conditions where flocculation starts to occur (compare Figure 26), small emulsion droplets are produced. Reproduced from Paper III ©2016 with permission from Elsevier.



## Exploring phase inversion conditions

Paper IV explores phase inversion, from o/w to w/o, of emulsions stabilized by functionalized silica particles. mPEG functionalization provides electrosteric stabilization towards changes in pH and salt concentrations, controllable particle flocculation, surface charge reduction and clouding behavior. By functionalizing the particles with propyl groups, interaction with the oil-phase is increased and an increase in the three-phase contact angle is expected. Thus, propyl/mPEG-SiNPs have high potential as emulsifiers for studying phase inversions, including exploration of the effects of salt and pH. The system studied contains several components, which are affected by the emulsification conditions in different ways. The most relevant interactions are the PEG-PEG, PEG-silica, particle-particle, particle-water and particle-oil interactions. PEG-PEG interactions become evident when salt concentration and temperature are varied through salting-out effects and clouding phenomena. Particle-particle interactions are also largely influenced by the salt concentration as well as the pH of the suspension prior emulsification. This is manifested through particle aggregation at high salt concentrations, where the zeta potential is reduced and particle-particle collisions increase, unless steric stabilization is employed. PEG-silica interactions exist below pH 8, wherefore low pH conditions flocculate the particles. Adsorption of particles at the oil-water interface is facilitated by low surface charge, achieved through adjustments of pH conditions or degree of surface modification, affecting both particle-oil and particle-water interactions. Paper IV attempts to assess the effects of all these aspects on emulsion phase inversion, and a summary is given in the following subsections.

### Temperature-induced phase inversions of the silica-stabilized emulsions

The modified silica particles used were all relatively hydrophilic and initially dispersed in water. Consequently, o/w emulsions were obtained at room temperature.<sup>19</sup> Contact angle measurements on dried samples, either pressed into pellets or distributed on double-sided tape, verified the hydrophilic nature of the particles; all angles were below 90 ° (unpublished data). The morphology of the emulsions was characterized through conductivity measurements, and a high conductivity of the same magnitude as that of the aqueous phase was initially obtained, characteristic of the o/w emulsion. When the temperature was increased, an increase in conductivity occurred, presumably due to increased electric mobility and possible dissociation of ions in the solution<sup>146</sup> and not due to phase changes of the emulsion. If an inversion from o/w to w/o would occur, a drop in conductivity to a value at least one order of magnitude below that of the aqueous phase is expected. Zero conductivity was not expected, since butanol, which was used as oil phase, is partially mixable with water; the solubility of butanol in water is around 7 % at 25 °C. Consequently, some water/salt solution dissolves in the oil phase. The conductivities of butanol in contact with water and salt solutions can be seen in Supporting information, Paper IV.

Phase inversions were observed in butanol emulsions stabilized by silica particles functionalized with mPEG silane. A reduced phase inversion temperature (PIT) is observed for heterogeneously modified particles with both mPEG silane and propyl silane attached. Figure 34 shows the conductivity, measured during the homogenization, as a function temperature. Particles modified with only mPEG silane display a PIT of 85 °C, higher than the cloud point of 75 °C at corresponding conditions (pH 4 and 500 mM CaCl<sub>2</sub>) revealing poor interaction of the PEGylated particles with the butanol oil phase at elevated temperatures. In addition, the emulsion phase separated immediately when the homogenizer was turned off. The observed PIT

of an emulsion stabilized by propyl<sub>0.93</sub>/mPEG<sub>0.27</sub>-SiNPs has a PIT that is reduced by > 30 °C (at 500 mM CaCl<sub>2</sub>), due to an increased particle-oil interaction, owing to the propyl silane modification. As is seen in Figure 34, no inversion occurs in an emulsion stabilized by particles modified with only propyl silane, since no thermo-responsiveness exists in this system; the thermo-responsiveness comes from the mPEG silane alone. It does, however, demonstrate the robustness of the Pickering emulsions obtained, since the o/w emulsion obtained was relatively stable towards coalescence, despite being exposed to very high temperatures during the preparation. Emulsions prepared without CaCl<sub>2</sub> and stabilized by propyl<sub>0.93</sub>/mPEG<sub>0.27</sub>-SiNPs required higher temperatures for inversion, while no phase inversions were observed in emulsions prepared without added CaCl<sub>2</sub> using mPEG<sub>0.85</sub>-SiNPs particles as stabilizers.

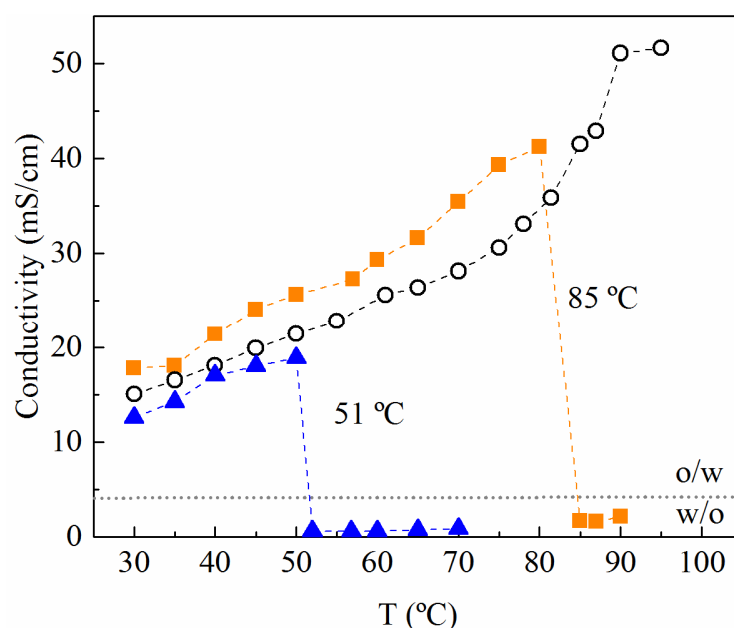


Figure 34. Conductivity as function of temperature during emulsification of butanol using functionalized silica particles as emulsifiers, with 500 mM CaCl<sub>2</sub> and pH 4 in the aqueous phase. The emulsions had a 50/50 vol% oil-to-aqueous phase ratio and 0.075 g/g silica-to-oil ratio. Particles with varying modifications were examined; mPEG<sub>0.85</sub>-SiNPs (orange ■); propyl<sub>0.82</sub>-SiNPs (black ○) and propyl<sub>0.93</sub>/mPEG<sub>0.27</sub>-SiNPs (blue ▲).

#### Effects of salt concentration and pH on emulsion phase inversion and emulsification

Figure 35 exemplifies how the PIT of the butanol emulsions is reduced by addition of CaCl<sub>2</sub>. The salting-out effects on the mPEG functionality leads to reduction of its solubility, mobility and clouding temperature, contributing to the reduced PITs.<sup>3, 31, 33, 34, 147, 148</sup> In addition, at an increased salt concentration, the particle-oil interaction is increased, through decreased particle dispersibility in the aqueous phase,<sup>66</sup> facilitating the formation of w/o emulsions. However, large o/w emulsion droplets are created at 500 mM CaCl<sub>2</sub>, since the high degree of particle aggregation that occurs diminishes the capacity to cover the emulsion droplets. The severe particle aggregation could also result in unavailability of the mPEG and propyl functionalities to enforce emulsion stabilization. Lower electrolyte concentration contributes to formation of smaller emulsion droplets and increased stability towards coalescence, but simultaneously, an increase in PIT is observed.

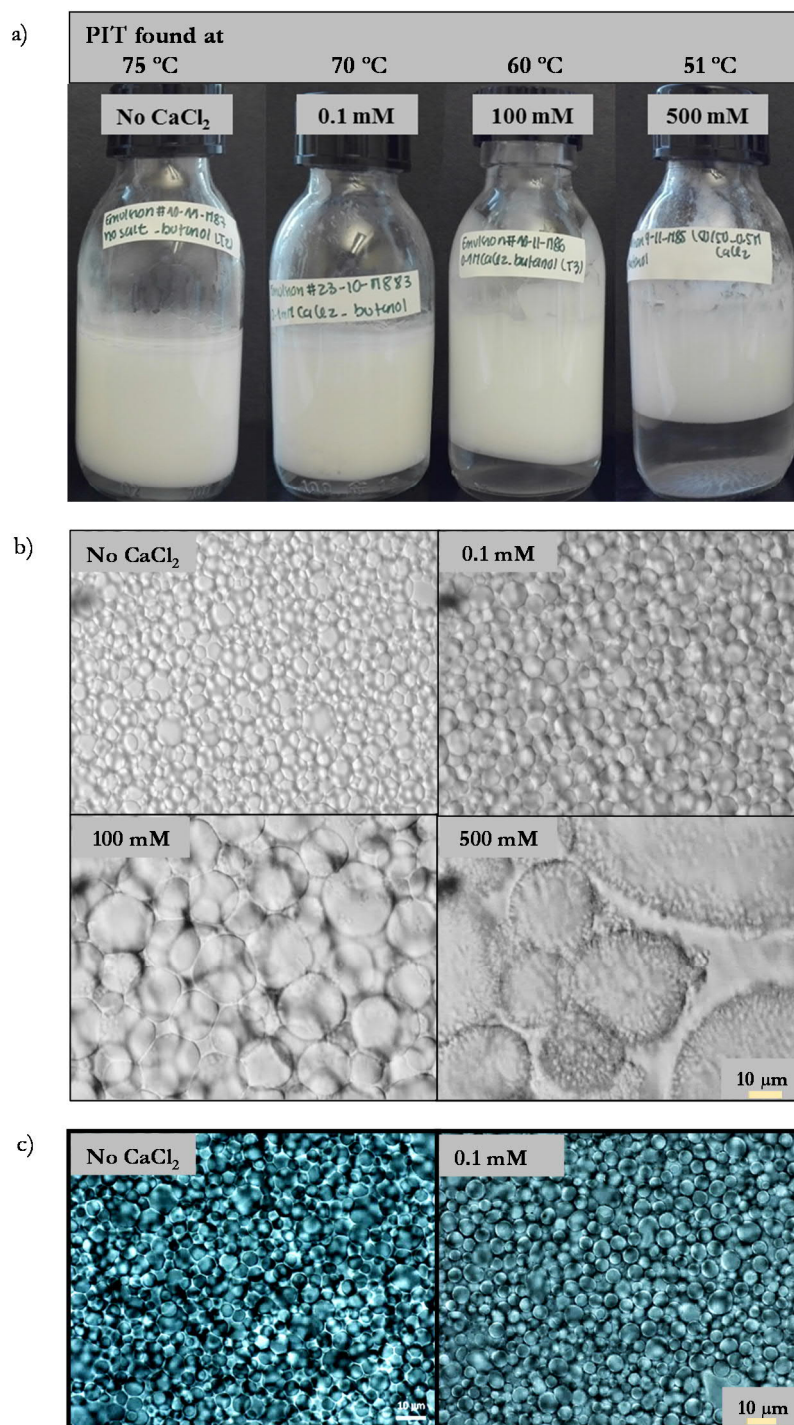


Figure 35. a): Pictures of emulsions at increasing CaCl<sub>2</sub> concentrations, taken one month after emulsification. b): Micrographs of the emulsions obtained, taken the day of emulsification, after the samples have been cooled to room temperature. c): Micrographs of emulsions obtained, taken 8 months after emulsification. The scale bars correspond to 10  $\mu\text{m}$ . Propyl<sub>0.93</sub>/mPEG<sub>0.27</sub>-SiNPs were used as emulsifiers and the emulsions were prepared at pH 4. The phase inversion temperature (PIT) values of these emulsion systems were found at 75  $\pm$  1 °C, 70  $\pm$  1 °C, 60  $\pm$  2 °C and 51  $\pm$  6 °C for no added CaCl<sub>2</sub>, for 0.1, 100 and 500 mM, respectively (averages of 2-4 experiments). Increasing the CaCl<sub>2</sub> concentration increases the creamed phase, results in larger emulsion droplets, but reduces the PIT.

The pH influences the PIT through effects on both the particle surface charge and the PEG-silica interactions where a reduced pH reduces the PIT, found at 92 °C, 76 °C and 48 °C, at pH 7, 4 and 2, respectively, without added CaCl<sub>2</sub>. At pH 9, where the silica surface charge is high, poor emulsification abilities are found and no phase inversions occurred. Emulsification with suspensions containing 100 mM CaCl<sub>2</sub> reduces the PIT to 60 °C, at pH 4 and 71 °C, at pH 7, but the salt has no effect on the PIT at pH 2. A salting out effect can be distinguished at high salt concentrations, going from 100 to 500 mM CaCl<sub>2</sub>. The results suggest that at high pH conditions, silica chemistry has an important influence, while at low pH conditions mPEG-silica interactions as well as the propyl and mPEG functionalities are dominating the behavior, through i.e. salting out of the PEG-chains.

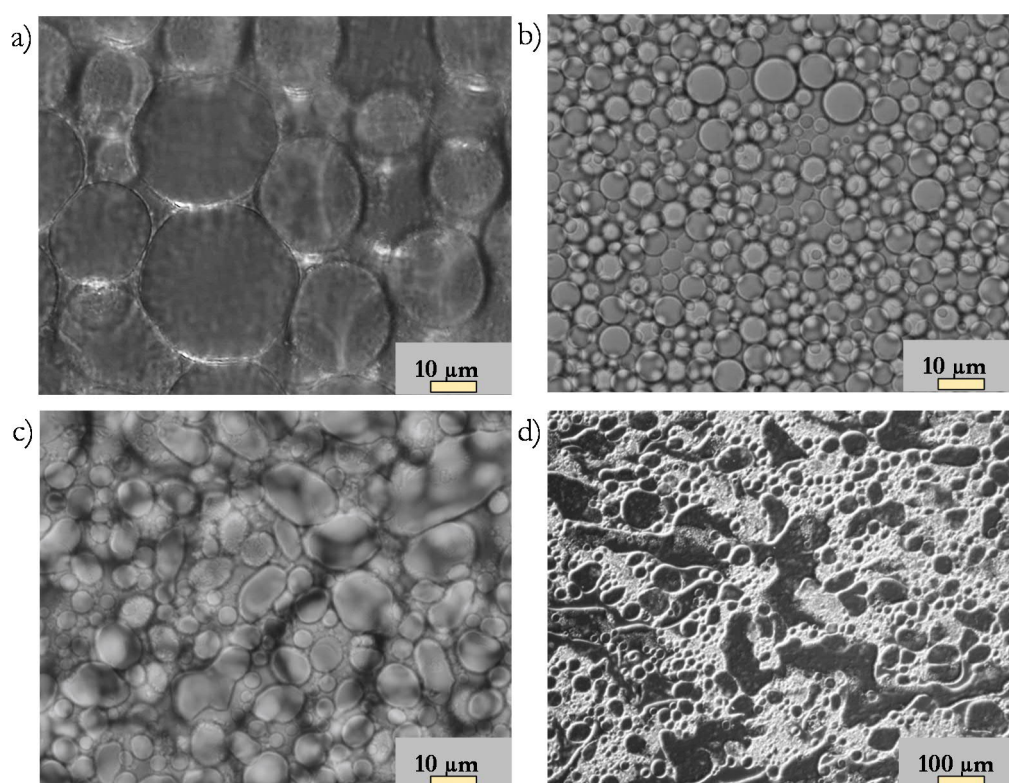


Figure 36. Micrographs of butanol emulsions, stabilized by propyl<sub>0.93</sub>/mPEG<sub>0.27</sub>-SiNPs, taken the day of emulsification, after being cooled to room temperature. a) Prepared at 45 °C, with the aqueous phase adjusted to pH 7, at 100 mM CaCl<sub>2</sub> (expected PIT 71 °C). b) Prepared at 80-90 °C, with the aqueous phase adjusted to pH 7, without added salt (expected PIT 92 °C). c) Prepared at 53 °C, with the aqueous phase adjusted to pH 2, without added salt (expected PIT 48 °C). d) Prepared at 43 – 67 °C, with the aqueous phase adjusted to pH 2, without added salt (expected PIT 48 °C).

Temperature can be used to impact the emulsion droplet size, and this was clearly seen at pH 7: poor emulsification performance is observed when emulsification is carried out at 45 °C; fast phase separation occurred without added salt and large emulsion droplets were observed at 100 mM CaCl<sub>2</sub>. An increase in temperature significantly reduces the emulsion droplet size, seen in Figure 36a) and b). Also the emulsion morphology is affected; emulsions prepared at pH 2 that were homogenized close their PIT observed at 48 °C, have large emulsion droplets which are poly-disperse (see Figure 36c). The emulsion prepared above PIT displays an appearance, after

being cooled to room temperature, resembling that of a bi-continuous phase observed in surfactant systems close to PIT (see Figure 36d).<sup>32, 37</sup>

### Reversibility and hysteresis effects

The possibility of switching back from w/o to o/w emulsions after PIT exists in surfactant systems, but it is not obvious that the same can occur in Pickering emulsions. A particle at an interface is viewed as a relatively static system with a desorption energy much higher than that of a surfactant. Hysteresis effects are normally present in surfactant systems undergoing catastrophic phase inversions, but not for transitional phase inversions. Transitional phase inversions are usually distinguished by the possibility to obtain stable emulsions on “both sides” of the inversion, in contrast to catastrophic phase inversions.<sup>77</sup>

For the emulsion systems studied in this work, it was possible to regain a stable o/w emulsion when an inverted w/o emulsion was cooled with homogenization applied. A hysteresis effect, of varying magnitude, was observed. Figure 37 shows that the hysteresis,  $\Delta T$ , is around 30 °C without added salt and when the silica surface charge is relatively high, e.g. at pH 7. Addition of salt reduces  $\Delta T$  and the smallest hysteresis effect, only 5 °C, is obtained when the pH is reduced to 2. Figure 38 shows how the conductivity changes when the temperature is altered during the PIT experiments, with the aqueous phase adjusted to pH 4, at varying salt concentrations. Hence, a high salt concentration leads to a reduced PIT, a smaller hysteresis, but large emulsion droplets.

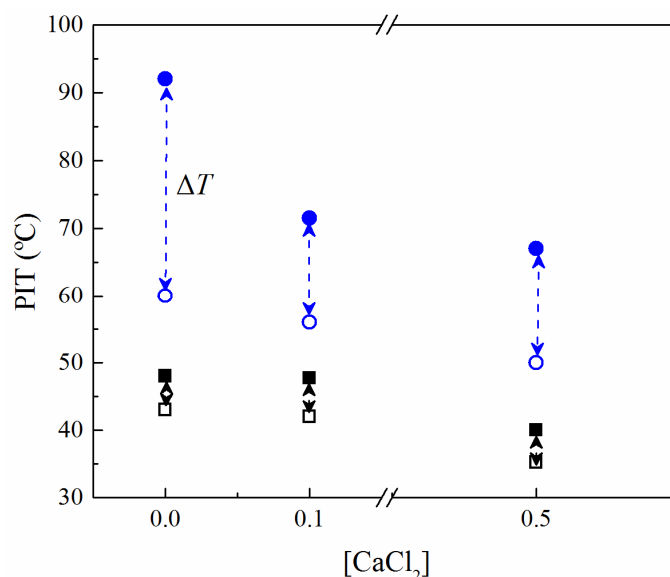


Figure 37. Phase inversion temperature (PIT) as a function of calcium chloride concentration, in M, for butanol emulsions prepared with the aqueous phase adjusted to pH 7 (●) and pH 2 (■). Solid symbols indicate inversion from o/w to w/o, open symbols show the temperature at which the emulsions revert back to o/w and the arrows indicate the hysteresis effect,  $\Delta T$ . The emulsions were stabilized by propyl<sub>0.93</sub>/mPEG<sub>0.27</sub>-SiNP and consisted of butanol and silica suspension at 50/50 vol%.



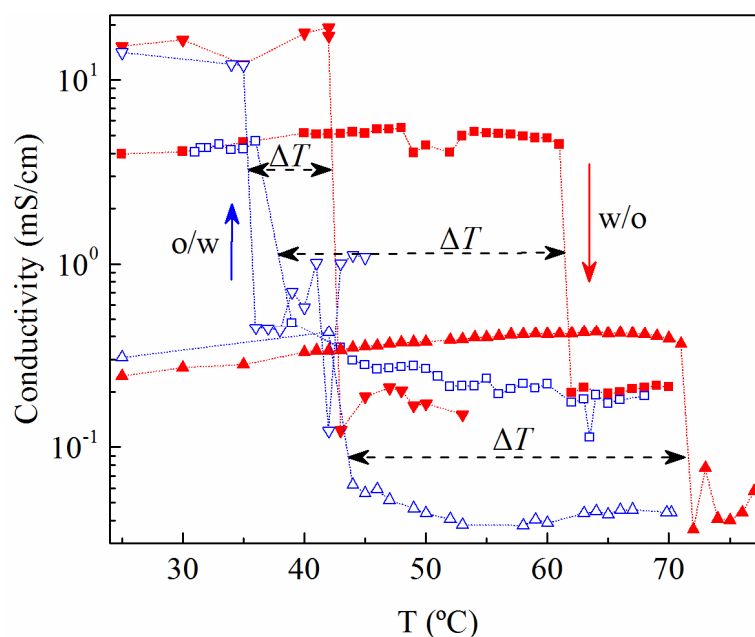


Figure 38. Conductivity as a function of temperature during emulsification of butanol in an aqueous phase adjusted to pH 4 and containing propyl<sub>0.93</sub>/mPEG<sub>0.27</sub>-SiNPs which act as emulsifiers. The emulsions have an aqueous phase containing 0.1 mM CaCl<sub>2</sub> (heating: red ▲, cooling: blue △), 100 mM CaCl<sub>2</sub> (heating: red ■, cooling: blue □) and 500 mM CaCl<sub>2</sub> (heating: red ▼, cooling: blue ▽). The system was heated during the homogenization (red solid symbols) and after the PIT had been observed the system was cooled with the homogenization running to achieve inversion back to o/w emulsions (blue open symbols). The hysteresis,  $\Delta T$ , is the difference between inversions from o/w to w/o and w/o to o/w.

The hysteresis phenomena and its dependence on salt concentration and pH can be explained by considering how the particle-covered droplets interact, and how it differs in the different media. Water has a higher dielectric constant than butanol, and the droplet-droplet repulsion is expected to be larger in an o/w emulsion, when the silica surface charge is high, compared to a w/o emulsion.<sup>33,35</sup> Repulsions can occur through the oil phase as well,<sup>19</sup> but these are expected to be weaker. The reduced hysteresis effect observed at high ionic strengths and low pH conditions could be a consequence of the screening of charges and the reduced silica surface charge, making o/w and w/o droplets behave more similar. In addition, inversions both to o/w and to w/o, could be facilitated by the larger and less stable emulsion droplets created at high CaCl<sub>2</sub> concentrations, a consequence of severe particle aggregation, leading to a poor surface coverage of the droplets. At pH 2, where the particle charge is low and the PEG-silica interaction is high, low PIT and small  $\Delta T$  are found. It is possible that a bi-continuous phase is created, which should facilitate droplet breakup and recreation. Such phase could also be present in the system at pH 4, with 500 mM CaCl<sub>2</sub>, since the conductivity increases stepwise, but has not yet been captured in a micrograph.

#### Other oil phases

Phase inversions from water-continuous to oil-continuous emulsions below 95 °C, using propyl<sub>0.93</sub>/mPEG<sub>0.27</sub>-SiNPs as emulsifiers, have only been achieved in butanol-emulsions at the conditions explored in this work. Still, an effect of the temperature on emulsification is observed also in o/w emulsions with other, less polar, oil-phases. Figure 39 shows how the droplet size of

an olive oil emulsion is reduced through increasing the temperature during the emulsification process (unpublished data). Prepared dodecane emulsions (results not shown) display the same – a reduction of emulsion droplet size occurs when homogenization is carried out at elevated temperatures, but no inversion occurs. This demonstrates the potential for opening new routes to tailoring properties of Pickering emulsions using functionalized silica sols as emulsion stabilizers, where thermo-stable emulsions can be prepared, and temperature can be used as a tool for controlling emulsion properties.

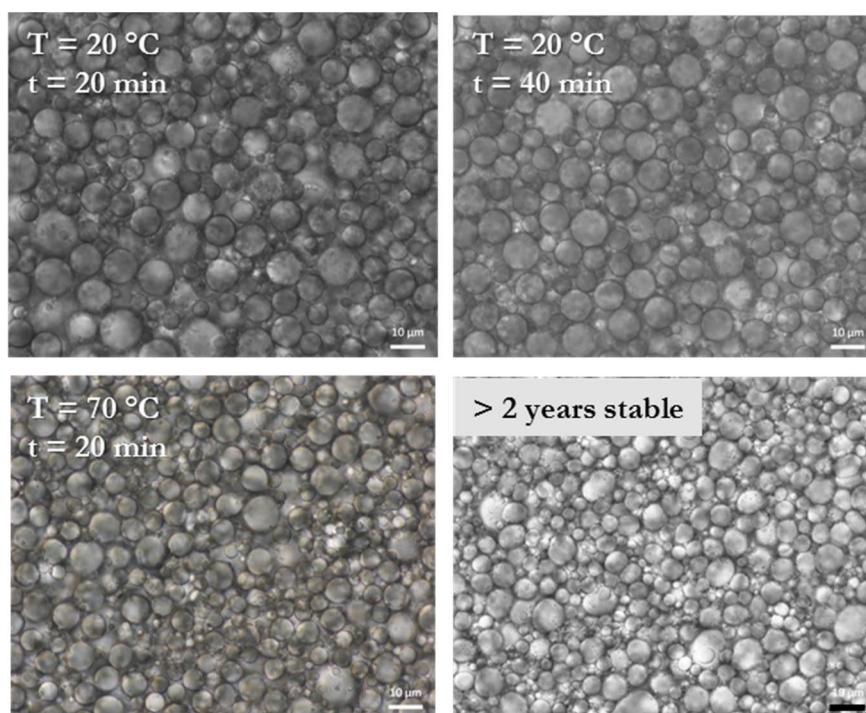


Figure 39. Olive oil emulsions stabilized by  $\text{propyl}_{0.93}/\text{mPEG}_{0.27}\text{-SiNP}$ , with the aqueous phase adjusted to pH 4. Increasing the temperature results in smaller emulsion droplets and an emulsion with very high stability towards coalescence was obtained: almost no change in emulsion droplet size was observed over the course of more than 2 years.





## DISCUSSION AND PERSPECTIVES

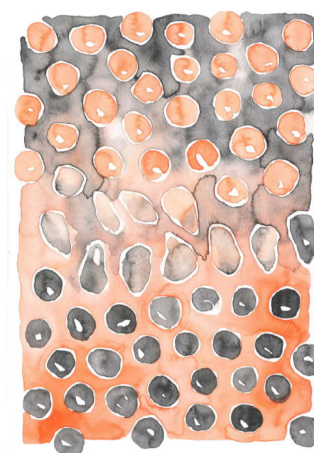
This work was carried out in close collaboration with a chemical company (Nouryon PPC AB), wherefore a short discussion with an industrial perspective is justified, and the use of functionalized colloidal silica as emulsifier are definitely of commercial interest. The silica starting sols utilized in the work presented in this thesis are commercially available, and the raw material (water-glass) is affordable and accessible. Functionalization with silane species requires an additional manufacturing step during the production process. However, commercially available silane-modified silica particles already exist, and implementation of the manufacturing process should therefore be quite straight forward. Since the silanes are relatively expensive, a significant increase in production cost, compared with the cost of non-modified silica sol is expected. Functionalized colloidal silica may therefore not become a cost efficient alternative to existing surfactant stabilized emulsion systems, but may have other benefits.

The chemical nature of the functionalized colloidal silica is beneficial from health, safety and environmental perspectives. The main constituent is  $\text{SiO}_2$ ; the propyl<sub>0.93</sub>/mPEG<sub>0.27</sub>-SiNP<sub>130</sub> sample employed in Paper IV contains, before dilution and purification, 34 wt%  $\text{SiO}_2$ , 1.4 wt% mPEG silane, 0.54 wt% propyl silane, around 1 wt% alcohol residues, 0.18 wt%  $\text{Na}_2\text{O}$  and the rest is water. Technical value may therefore be relevant in high end-value applications where health aspects are important. Research already exist that point to both the existing use and the potential of using Pickering emulsions e.g. in cosmetics,<sup>2</sup> in sunscreen,<sup>149</sup> for topical delivery of active substances,<sup>1, 61</sup> for biomedical applications<sup>18</sup> and in food applications,<sup>5</sup> including low calorie food.<sup>56</sup>

By knowing how to control clouding in particle stabilized emulsion systems, as well as phase inversion and emulsion destabilization, preparation of tailor-made particles is possible, where e.g. the degree of modification is determined by the application conditions. The unique hysteresis effect observed in the PIT experiments could open opportunities for developing stimuli-responsive emulsions. The studies also showed that the prepared emulsions possess a thermal stability and endure high temperature, while still maintaining high coalescence stability.



## CONCLUDING REMARKS



The studies presented in this thesis have been performed using surface functionalized silica nanoparticles, and the functionalization was achieved through a direct and water-based route. Different silanes with hydrophilic or hydrophobic organofunctional groups were attached to the silica particle surface, and colloidal properties as well as emulsification abilities were explored.

The hydrophilic surface functionalization employed was a silane with an mPEG functional group. NMR diffusometry proved to be an excellent method for quantification of the amount of mPEG attached, and the measurements also strongly indicate covalent binding to the silica surface. The surface properties of the silica particles are affected through the functionalization; the surface charge density is significantly reduced and the zeta potential moves closer to zero by the presence of bound mPEG. Surface active particles were obtained when the surface coverage was  $0.15 \mu\text{mol mPEG silane per m}^2 \text{ SiO}_2$  and above. At medium surface coverage, electrosteric stabilization of the particles was attained, and a pH dependent aggregation behavior was observed, where flocculation occurs below pH 6. It was concluded that this reversible phenomenon most likely originates from the attractive PEG-silica interaction. At high surface coverages steric stabilization towards flocculation, both at low pH conditions and at high salt concentrations, was achieved. In contrast to non-modified particles and particles with a low degree of surface functionalization, high concentrations of  $\text{CaCl}_2$  could therefore be added to particle-suspensions with high mPEG grafting density, without particle aggregation occurring at room temperature. This steric stabilization allowed studies of clouding behavior of the PEGylated particles; salting out effects reduced the cloud point temperatures of the particles and clouding could be observed below  $100 \text{ }^\circ\text{C}$ . Clouding is influenced by the interplay between particle-particle interaction, PEG-silica interaction and intramolecular effects. These are in turn influenced by salt concentration and pH, where an increase in salt concentration and a reduction of pH reduce the cloud points, as well as of free mPEG present in the suspensions. A synergistic effect was found, where, at high salt concentrations ( $1 - 1.5 \text{ M CaCl}_2$ ), presence of free mPEG silane allows reversible clouding, while purification of the samples results in irreversible aggregation of the particles at temperatures above their cloud points.

The hydrophilic mPEG functionalization provides several properties beneficial for studying the emulsification properties of the particles (i.e. controllable and pH dependent flocculation behavior through electrosteric stabilization, significant reduction of surface charge density, surface activity and clouding behavior). To render particles that efficiently can emulsify non-polar oils an increased hydrophobic character is required, since the emulsifying properties are

dependent on the wettability of the particle in both the water and oil phase of the emulsion. This was achieved by heterogeneous functionalization with hydrophobic groups such as propyl and methyl silanes. This functionalization process could be carried out in the water-based system, in concentrated silica sols. Silica sols functionalized with the combination of both hydrophilic and hydrophobic groups were found to be very efficient Pickering emulsifiers. Particles functionalized with mPEG and propyl silanes were used to stabilize Pickering emulsions of e.g. Exxsol D60, butanol and olive oil, and some emulsions were found stable to coalescence for more than 4.5 years. Several conditions govern the emulsification, such as the functionalization conditions, the degree of particle aggregation, the surface area  $\text{SiO}_2$ -to-oil ratio in the emulsion, and the salt concentration and pH of the silica suspension. Through adjusting these variables emulsion droplet formation may be facilitated through increased particle adsorption at an oil-water interface.

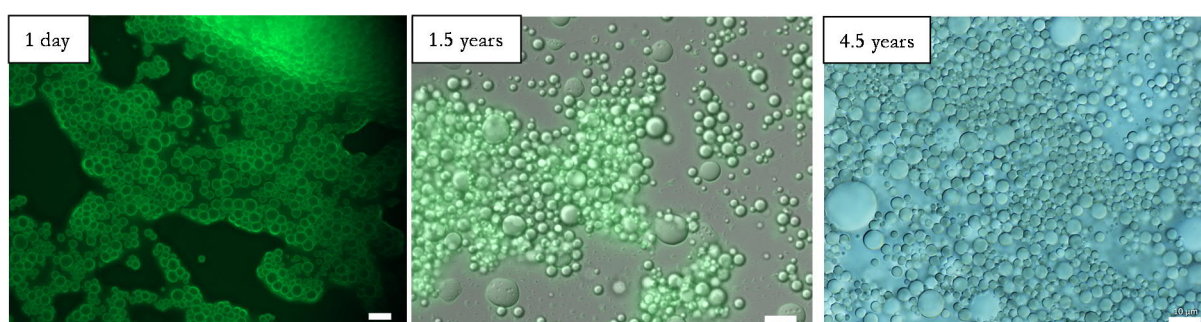


Figure 40. An o/w emulsion, with the oil phase colored with fluorescent dye, of Exxsol D60, stabilized with propyl/mPEG-SiNPs. Over the course of 4.5 years, low degree of coalescence occurs, where a few large droplets are created, while most remain intact with a median emulsion droplet size of around  $10\ \mu\text{m}$ , as measured with laser diffraction. The scale bars represent  $10\ \mu\text{m}$ .

The clouding behavior observed for mPEG-grafted particles could be exploited in phase inversion studies. Emulsions that were heated while homogenized displayed transitional phase inversion at specific phase inversion temperatures (PITs). The emulsification, and subsequently the PITs, could be affected by the salt concentration and the pH in the silica suspension. The phase inversion originates in the same thermo-responsiveness that causes clouding to occur; the PEG-polymer chain undergoes conformational changes to less polar conformations, increasing the hydrophobic character of the particle surface and the oil wettability. Thereby, the formation of w/o emulsions is possible. In agreement with the effects of clouding, reduced PITs are observed for high salt concentrations and low pH conditions. Effects that originate from silica chemistry and particle-particle interactions were found to most likely dominate the behavior at high pH. The high silica surface charge results in poor emulsifying properties, which may, at neutral pH, be partly improved by addition of salt. At low pH, effects attributed to electrosteric stabilization and salting-out effects of the PEG-chain almost certainly have a stronger effect. Simultaneously, the influence of surface charge screening effects is reduced at very low pH (i.e. pH 2). If an inverted emulsion is cooled with the homogenizer running, it reverts back to a stable o/w emulsion, but at a lower temperature compared to the inversion from o/w to w/o. The hysteresis is reduced by increased salt concentration and reduced pH. High salt concentration renders less stable, larger emulsion droplets, due to severe particle aggregation and less available surface area to stabilize the emulsion droplets. This could facilitate the inversions. In addition,

screening of the surface charge, or a reduced surface charge as obtained at pH values below 7, result in more similar behavior of o/w and w/o droplets, in turn reducing the hysteresis. Finally, a phase similar to bi-continuous systems present in surfactant microemulsions may be present close to the inversion points, pointing to one of the similarities between particulate and surfactant emulsifiers that exist.

The results presented in this thesis show the potential of using water-borne surface-functionalized silica nanoparticles as Pickering emulsifiers and for creating an improved understanding of Pickering systems. Particle characterization prior to emulsification studies is beneficial for exploiting the colloidal properties obtained, and studies of phase inversions may expand the use of Pickering emulsions and open possibilities of reducing the energy demand for emulsion preparation, through exploiting e.g. the PIT emulsification method. Surface modified silica particles have been successfully prepared, which may function as emulsifiers in a broad range of o/w systems; oils of varying polarity, e.g. from butanol to dodecane, have been successfully emulsified. The production of stable w/o emulsions would, however, require a particle of increased hydrophobic nature.



## Abbreviations

ASC	Apparent surface charge
CP	Cloud point
DLS	Dynamic Light Scattering
FID	Free Induction Decay
HLB	Hydrophilic-lipophilic balance
mPEG	methyl poly(ethylene glycol)
NMR	Nuclear Magnetic Resonance
PEG	Poly(ethylene glycol)
PEO	Poly(ethylene oxide)
PIT	Phase inversion temperature
PPC	Pulp and Performance Chemicals
SCD	Surface charge density
SiNP	Silica nanoparticle
ST	Surface tension
UV/Vis	Ultraviolet-visible
UF	Ultra filtration

## Acknowledgements

Firstly, the Swedish Research Council and Nouryon Pulp and Performance Chemicals AB are greatly acknowledged for funding this project.

Acknowledgements go also to the Swedish NMR Centre for providing splendid services, especially to Diana and Maxim for the help in front of the magnets during the first years of this project.

I would then like to express my deep gratitude to the following persons:

Anders Palmqvist, my main supervisor, thank you for your guidance in the academic world and for the freedom you have given me in my project, and your constant encouragement and reassurance have kept me on the right path. Lars Nordstierna, I could not have had a better my co-supervisor, thank you for endless patience with my NMR struggles and for being my friend. Martin Andersson, my examiner, thank you for always having your door open to me and for your support.

My mentors at Nouryon: Anders Törnecrona, thank you for always supplying me with input and for efficiently answering my various questions. Michael Persson, you have provided me with valuable feedback and ideas, for which I am very grateful.

Ylva Wildlock, my former boss, thank you for backing me up and for all our pleasant discussions. I am so grateful to have had the chance to work as an industrial PhD student, with lab- and office spaces both at Chalmers and at our Nouryon-site in Bohus, and for feeling welcome in both locations.

Andreas Sundblom, my colleague and co-author, thank you for your valuable inputs and for help with master-student supervisions.

Some strong women who I truly look up to; you are role models and you have supported me throughout this journey: Anne Farbot, my former colleague and friend, our lunch-dates really lifted my spirits more than once, I am so grateful for your consideration and your many wise reflections. Kristina Lundahl, my colleague and friend, I have so much enjoyed co-authoring an article with you, thank you for giving me of your time to have our long discussions about both science and life. Hanna Härelind, for your invaluable support, especially in the role as study dean, I am so happy to have you now as manager of Applied Chemistry. Anna Martinelli, you have inspired me since our first encounter during our struggles with finalizing the master thesis.

My former and present office-mates: Johanna, Björn, Ralph, Zeynep, Khalid and Säul; it has been a real pleasure to share room with you, thank you for being so supportive! My fantastic research group at Chalmers: Milene, Giulio, Gunnar, Yifei, Joakim, Andrey, Florian, Sam, Walter, I have been happy to belong in your group!

All the nice people who are working at Applied Chemistry, and all of you who have worked there during these years, thank you for creating such a nice environment and for all research- and life-related discussions, good times in the labs and fun division days. Special thank you to Caroline Janson, Anna-Karin Hellström, Frida Iselau, Simon Isaksson, Olesia Danyliv, and



Emma Westas, for being kind friends! And thank you Frida Andersson for providing solutions to all administrative problems!

Krister Holmberg, for introducing surface chemistry in such a nice way during my master studies, for accepting to be examiner of my master thesis, for giving input to this thesis as well, and for always answering my e-mails. Romain Bordes, for nice teaching experiences and for your help.

Zareen Abbas, for guiding me in the world of surface charge, Isabelle Simonsson and Christian Sögaard, for welcoming me into your lab.

All my colleagues at the Silica development department at Nouryon, for all our discussions, good company during experimental work and for all your encouraging words, especially Per Restorp for helping me with molecular conformations, Peter Hell for always helping out in the lab, Catarina Petersen for always knowing where to find things.

My colleagues in Deventer: BoenHo O for giving me input throughout these years, and Rudy Venderbosch for making my stay in Deventer a pleasure.

My two fantastic thesis workers, Maria Diaz, so productive in the experimental work, and Tazhan Faraj, for making me interested in pharmacology.

Alexandra, for your wonderful friendship, I am so glad that we have persistently supported one another even if this journey has been challenging at times, from nollningen the first year of Chalmers, through becoming mothers, and until now.

My lovely family: Mum, thanks for you unconditional support, for taking care of my children so that I have gotten time to work and for proof-reading my thesis. Dad, for inspiration and support in many ways. My wonderful brother Joel, sister Mirja, and brother-in-law Niklas, I am so glad to have you close in my life. Thank you Annika and Jan-Åke for all the love you give my daughters. My most beloved: Mattias, for your endless love, patience and unconditional kindness, and our "PhD babies", Emy and Agnes, you light up my life in the most extraordinary ways.



## References

1. Wahlgren, M., J. Engblom, M. Sjöö, and M. Rayner, The use of Micro- and nanoparticles in the stabilisation of Pickering-type emulsions for topical delivery. *Current Pharmaceutical Biotechnology*, 2013. 14(15): p. 1222-1234.
2. Yang, Y., Z. Fang, X. Chen, W. Zhang, Y. Xie, Y. Chen, Z. Liu, and W. Yuan, An Overview of Pickering Emulsions: Solid-Particle Materials, Classification, Morphology, and Applications. *Frontiers in Pharmacology*, 2017. 8(287).
3. Holmberg, K., B. Jönsson, B. Kronberg, and B. Lindman, *Surfactants and Polymers in Aqueous Solution*. 2 ed. 2003, Chichester, West Sussex: John Wiley & Sons.
4. Dickinson, E., Food emulsions and foams: Stabilization by particles. *Current Opinion in Colloid and Interface Science*, 2010. 15(1-2): p. 40-49.
5. Dickinson, E., Use of nanoparticles and microparticles in the formation and stabilization of food emulsions. *Trends in Food Science & Technology* 2012. 24: p. 4-12.
6. Vilchez, A., C. Rodríguez-Abreu, J. Esquena, A. Menner, and A. Bismarck, Macroporous Polymers Obtained in Highly Concentrated Emulsions Stabilized Solely with Magnetic Nanoparticles. *Langmuir*, 2011. 27(21): p. 13342-13352.
7. Esquena, J. and C. Solans, Highly Concentrated Emulsions as Templates for Solid Foams, in *Emulsions and emulsion stability*, J. Sjöblom, Editor. 2006, Taylor & Francis: Boca Raton. p. 245-260.
8. Holmberg, K., Organic Reactions in Emulsions and Microemulsions, in *Emulsions and emulsion stability*, J. Sjöblom, Editor. 2006, Taylor & Francis: Boca Raton. p. 263-278.
9. Ramsden, W., Separation of Solids in the Surface-Layers of Solutions and 'Suspensions' (Observations on Surface-Membranes, Bubbles, Emulsions, and Mechanical Coagulation). -- Preliminary Account. *Proceedings of the Royal Society of London*, 1903. 72(477-486): p. 156-164.
10. Pickering, S.U., CXCVI.-Emulsions. *Journal of the Chemical Society, Transactions*, 1907. 91(0): p. 2001-2021.
11. Briggs, T.R., Emulsions with Finely Divided Solids. *Journal of Industrial & Engineering Chemistry*, 1921. 13(11): p. 1008-1010.
12. Finkle, P., H.D. Draper, and J.H. Hildebrand, The theory of emulsification. *Journal of the American Chemical Society*, 1923. 45(12): p. 2780-2788.
13. Murray, B.S., Pickering emulsions for food and drinks. *Current Opinion in Food Science*, 2019. 27: p. 57-63.
14. Tang, J., P.J. Quinlan, and K.C. Tam, Stimuli-responsive Pickering emulsions: Recent advances and potential applications. *Soft Matter*, 2015. 11(18): p. 3512-3529.
15. Chevalier, Y. and M.A. Bolzinger, Emulsions stabilized with solid nanoparticles: Pickering emulsions. *Colloids and Surfaces A: Physicochemical and Engineering Aspects*, 2013. 439: p. 23-34.
16. Binks, B.P., Colloidal Particles at a Range of Fluid–Fluid Interfaces. *Langmuir*, 2017. 33(28): p. 6947-6963.
17. Binks, B.P. and T.S. Horozov, eds. *Colloidal Particles at Liquid Interfaces*. 1 ed. 2006, Cambridge University Press: New York.
18. Harman, C.L.G., M.A. Patel, S. Guldin, and G.L. Davies, Recent developments in Pickering emulsions for biomedical applications. *Current Opinion in Colloid and Interface Science*, 2019. 39: p. 173-189.
19. Binks, B.P., Particles as surfactants—similarities and differences. *Current Opinion in Colloid & Interface Science*, 2002. 7(1–2): p. 21-41.
20. Bergna, H.E., Colloid Chemistry of Silica: An Overview, in *Colloidal Silica Fundamentals and Applications*, H.E. Bergna and W.O. Roberts, Editors. 2006, Taylor & Francis Group. p. 9-37.
21. Albertsson, J., Kiseldioxid, in *Nationalencyklopedin*.
22. Bergna, H.E. and W.O. Roberts, eds. *Colloidal Silica Fundamentals and Applications*. surfactant science series. Vol. 131. 2006, Taylor & Francis Group.
23. Barthel, H., Surface interactions of dimethylsiloxy group-modified fumed silica. *Colloids and Surfaces A: Physicochemical and Engineering Aspects*, 1995. 101(2–3): p. 217-226.
24. Bridger, K. and B. Vincent, The terminal grafting of poly(ethylene oxide) chains to silica surfaces. *European Polymer Journal*, 1980. 16(10): p. 1017-1021.

25. Zhang, Z., A.E. Berns, S. Willbold, and J. Buitenhuis, Synthesis of poly(ethylene glycol) (PEG)-grafted colloidal silica particles with improved stability in aqueous solvents. *Journal of Colloid and Interface Science*, 2007. 310(2): p. 446-455.
26. Xu, H., F. Yan, E.E. Monson, and R. Kopelman, Room-temperature preparation and characterization of poly (ethylene glycol)-coated silica nanoparticles for biomedical applications. *Journal of Biomedical Materials Research Part A*, 2003. 66A(4): p. 870-879.
27. Graf, C., Q. Gao, I. Schütz, C.N. Noufele, W. Ruan, U. Posselt, E. Korotianskiy, D. Nordmeyer, F. Rancan, S. Hadam, A. Vogt, J. Lademann, V. Haucke, and E. Rühl, Surface Functionalization of Silica Nanoparticles Supports Colloidal Stability in Physiological Media and Facilitates Internalization in Cells. *Langmuir*, 2012. 28(20): p. 7598-7613.
28. Yagüe, C., M. Moros, V. Grazú, M. Arruebo, and J. Santamaría, Synthesis and stealthing study of bare and PEGylated silica micro- and nanoparticles as potential drug-delivery vectors. *Chemical Engineering Journal*, 2008. 137(1): p. 45-53.
29. Mukherjee, P., S.K. Padhan, S. Dash, S. Patel, and B.K. Mishra, Clouding behaviour in surfactant systems. *Advances in Colloid and Interface Science*, 2011. 162(1): p. 59-79.
30. Shinoda, K. and H. Arai, The Correlation between Phase Inversion Temperature In Emulsion and Cloud Point in Solution of Nonionic Emulsifier. *The Journal of Physical Chemistry*, 1964. 68(12): p. 3485-3490.
31. Marszall, L., HLB of Nonionic Surfactants: PIT and EIP Methods, in *Nonionic Surfactants: Physical Chemistry*, M.J. Schick, Editor. 1987, Marcel Dekker Inc.: New York.
32. Friberg, S.E., R.W. Corkery, and I.A. Blute, Phase Inversion Temperature (PIT) Emulsification Process. *Journal of Chemical & Engineering Data*, 2011. 56(12): p. 4282-4290.
33. Perazzo, A., V. Preziosi, and S. Guido, Phase inversion emulsification: Current understanding and applications. *Advances in Colloid and Interface Science*, 2015. 222: p. 581-599.
34. Shinoda, K. and H. Saito, The effect of temperature on the phase equilibria and the types of dispersions of the ternary system composed of water, cyclohexane, and nonionic surfactant. *Journal of Colloid and Interface Science*, 1968. 26(1): p. 70-74.
35. Yeo, L.Y., O.K. Matar, E.S. Perez De Ortiz, and G.F. Hewitt, Phase inversion and associated phenomena. *Multiphase Science and Technology*, 2000. 12(1): p. 51-116.
36. Anton, N. and T.F. Vandamme, The universality of low-energy nano-emulsification. *International Journal of Pharmaceutics*, 2009. 377(1): p. 142-147.
37. Brooks, B.W., H.N. Richmond, and M. Zerfa, Phase Inversion and Drop Formation in Agitated Liquid-Liquid Dispersions in the Presence of Nonionic Surfactants, in *Modern Aspects of Emulsion Science*, B.P. Binks, Editor. 1998, The Royal Society of Chemistry: Cambridge, UK. p. 175-205.
38. Walstra, P. and P.E.A. Smulders, Emulsion formation, in *Modern Aspects of Emulsion Science*, B.P. Binks, Editor. 1998, The Royal Society of Chemistry: Cambridge, UK. p. 56-99.
39. Horozov, T.S. and B.P. Binks, Particle-Stabilized Emulsions: A Bilayer or a Bridging Monolayer? *Angewandte Chemie International Edition*, 2006. 45(5): p. 773-776.
40. Midmore, B.R., Preparation of a novel silica-stabilized oil/water emulsion. *Colloids and Surfaces A: Physicochemical and Engineering Aspects*, 1998. 132(2): p. 257-265.
41. Tambe, D.E. and M.M. Sharma, Factors controlling the stability of colloid-stabilized emulsions. I. An experimental investigation. *Journal of Colloid And Interface Science*, 1993. 157(1): p. 244-253.
42. Tambe, D., J. Paulis, and M.M. Sharma, Factors controlling the stability of colloid-stabilized emulsions. IV. evaluating the effectiveness of demulsifiers. *Journal of Colloid And Interface Science*, 1995. 171(2): p. 463-469.
43. Tambe, D.E. and M.M. Sharma, Factors controlling the stability of colloid-stabilized emulsions II. A model for the rheological properties of colloid-laden interfaces. *Journal of Colloid And Interface Science*, 1994. 162(1): p. 1-10.
44. Midmore, B.R., Synergy between silica and polyoxyethylene surfactants in the formation of O/W emulsions. *Colloids and Surfaces A: Physicochemical and Engineering Aspects*, 1998. 145(1-3): p. 133-143.
45. Midmore, B.R., Effect of Aqueous Phase Composition on the Properties of a Silica-Stabilized W/O Emulsion. *Journal of Colloid and Interface Science*, 1999. 213(2): p. 352-359.
46. Binks, B.P. and S.O. Lumsdon, Stability of oil-in-water emulsions stabilised by silica particles. *Physical Chemistry Chemical Physics*, 1999. 1(12): p. 3007-3016.
47. Aveyard, R., B.P. Binks, and J.H. Clint, Emulsions stabilised solely by colloidal particles. *Advances in Colloid and Interface Science*, 2003. 100-102(SUPPL.): p. 503-546.

48. Binks, B.P. and S.O. Lumsdon, Effects of oil type and aqueous phase composition on oil-water mixtures containing particles of intermediate hydrophobicity. *Physical Chemistry Chemical Physics*, 2000. 2(13): p. 2959-2967.
49. Binks, B.P. and S.O. Lumsdon, Influence of Particle Wettability on the Type and Stability of Surfactant-Free Emulsions. *Langmuir*, 2000. 16(23): p. 8622-8631.
50. Binks, B.P. and S.O. Lumsdon, Catastrophic Phase Inversion of Water-in-Oil Emulsions Stabilized by Hydrophobic Silica. *Langmuir*, 2000. 16(6): p. 2539-2547.
51. Binks, B.P. and S.O. Lumsdon, Transitional Phase Inversion of Solid-Stabilized Emulsions Using Particle Mixtures. *Langmuir*, 2000. 16(8): p. 3748-3756.
52. Binks, B.P. and S.O. Lumsdon, Pickering Emulsions Stabilized by Monodisperse Latex Particles: Effects of Particle Size. *Langmuir*, 2001. 17: p. 4540-4547.
53. Binks, B.P. and J.A. Rodrigues, Double Inversion of Emulsions By Using Nanoparticles and a Di-Chain Surfactant. *Angewandte Chemie International Edition*, 2007. 46(28): p. 5389-5392.
54. Horozov, T.S., B.P. Binks, and T. Gottschalk-Gaudig, Effect of electrolyte in silicone oil-in-water emulsions stabilised by fumed silica particles. *Physical Chemistry Chemical Physics*, 2007. 9(48): p. 6398-6404.
55. Binks, B.P. and S.O. Olusanya, Phase Inversion of Colored Pickering Emulsions Stabilized by Organic Pigment Particle Mixtures. *Langmuir*, 2018. 34(17): p. 5040-5051.
56. Binks, B.P. and H. Shi, Phase Inversion of Silica Particle-Stabilized Water-in-Water Emulsions. *Langmuir*, 2019. 35(11): p. 4046-4057.
57. Binks, B.P. and J.H. Clint, Solid Wettability from Surface Energy Components: Relevance to Pickering Emulsions. *Langmuir*, 2002. 18(4): p. 1270-1273.
58. Binks, B.P., L. Isa, and A.T. Tyowua, Direct Measurement of Contact Angles of Silica Particles in Relation to Double Inversion of Pickering Emulsions. *Langmuir*, 2013. 29(16): p. 4923-4927.
59. Frelichowska, J., M.A. Bolzinger, and Y. Chevalier, Pickering emulsions with bare silica. *Colloids and Surfaces a-Physicochemical and Engineering Aspects*, 2009. 343(1-3): p. 70-74.
60. Frelichowska, J., M.-A. Bolzinger, and Y. Chevalier, Effects of solid particle content on properties of o/w Pickering emulsions. *Journal of Colloid and Interface Science*, 2010. 351(2): p. 348-356.
61. Frelichowska, J., M.-A. Bolzinger, J.-P. Valour, H. Mouaziz, J. Pelletier, and Y. Chevalier, Pickering w/o emulsions: Drug release and topical delivery. *International Journal of Pharmaceutics*, 2009. 368(1): p. 7-15.
62. Laredj-Bourezg, F., M.A. Bolzinger, J. Pelletier, and Y. Chevalier, Pickering emulsions stabilized by biodegradable block copolymer micelles for controlled topical drug delivery. *International Journal of Pharmaceutics*, 2017. 531(1): p. 134-142.
63. Brunier, B., N. Sheibat-Othman, Y. Chevalier, and É. Bourgeat-Lami, Effect of Pickering stabilization on radical entry in emulsion polymerization. *AIChE Journal*, 2018. 64(7): p. 2612-2624.
64. Murray, B.S., K. Durga, A. Yusoff, and S.D. Stoyanov, Stabilization of foams and emulsions by mixtures of surface active food-grade particles and proteins. *Food Hydrocolloids*, 2011. 25(4): p. 627-638.
65. Vignati, E., R. Piazza, and T.P. Lockhart, Pickering Emulsions: Interfacial Tension, Colloidal Layer Morphology, and Trapped-Particle Motion. *Langmuir*, 2003. 19(17): p. 6650-6656.
66. Xu, H.-N., Y. Liu, and L. Zhang, Salting-out and salting-in: competitive effects of salt on the aggregation behavior of soy protein particles and their emulsifying properties. *Soft Matter*, 2015. 11(29): p. 5926-5932.
67. Rodríguez-Abreu, C. and M. Lazzari, Emulsions with structured continuous phases. *Current Opinion in Colloid & Interface Science*, 2008. 13(4): p. 198-205.
68. Binks, B.P. and P.D.I. Fletcher, Particles Adsorbed at the Oil–Water Interface: A Theoretical Comparison between Spheres of Uniform Wettability and “Janus” Particles. *Langmuir*, 2001. 17(16): p. 4708-4710.
69. Casagrande, C., P. Fabre, E. Raphaël, and M. Veyslié, “Janus Beads”: Realization and Behaviour at Water/Oil Interfaces. *EPL (Europhysics Letters)*, 1989. 9(3): p. 251.
70. Glaser, N., D.J. Adams, A. Böker, and G. Krausch, Janus Particles at Liquid–Liquid Interfaces. *Langmuir*, 2006. 22(12): p. 5227-5229.
71. Takahara, Y.K., S. Ikeda, S. Ishino, K. Tachi, K. Ikeue, T. Sakata, T. Hasegawa, H. Mori, M. Matsumura, and B. Ohtani, Asymmetrically Modified Silica Particles: A Simple Particulate Surfactant for Stabilization of Oil Droplets in Water. *Journal of the American Chemical Society*, 2005. 127(17): p. 6271-6275.
72. Arditty, S., C.P. Whitby, B.P. Binks, V. Schmitt, and F. Leal-Calderon, Some general features of limited coalescence in solid-stabilized emulsions. *European Physical Journal E*, 2003. 11(3): p. 273-281.

73. Saleh, N., T. Sarbu, K. Sirk, G.V. Lowry, K. Matyjaszewski, and R.D. Tilton, Oil-in-Water Emulsions Stabilized by Highly Charged Polyelectrolyte-Grafted Silica Nanoparticles. *Langmuir*, 2005. 21(22): p. 9873-9878.
74. Haney, B., D. Chen, L.-H. Cai, D. Weitz, and S. Ramakrishnan, Millimeter-Size Pickering Emulsions Stabilized with Janus Microparticles. *Langmuir*, 2019. 35(13): p. 4693-4701.
75. Persson, K.H., I.A. Blute, I.C. Mira, and J. Gustafsson, Creation of well-defined particle stabilized oil-in-water nanoemulsions. *Colloids and Surfaces A: Physicochemical and Engineering Aspects*, 2014. 459(0): p. 48-57.
76. Vaessen, G.E.J., Predicting catastrophic phase inversion in emulsions, in *Technische Universiteit Eindhoven*. 1996: Eindhoven.
77. Binks, B.P., Emulsions - Recent Advances in Understanding, in *Modern Aspects of Emulsion Science*, B.P. Binks, Editor. 1998, The Royal Society of Chemistry: Cambridge, UK. p. 1-48.
78. Dickinson, E., Interpretation of emulsion phase inversion as a cusp catastrophe. *Journal of Colloid and Interface Science*, 1981. 84(1): p. 284-287.
79. Sundblom, A., A.E.C. Palmqvist, and K. Holmberg, Study of the pluronic-silica interaction in synthesis of mesoporous silica under mild acidic conditions. *Langmuir*, 2010. 26(3): p. 1983-1990.
80. Shinoda, K. and H. Kunieda, Chapter 5, in *Encyclopedia of Emulsion Technology*, P. Becher, Editor. 1983, Marcel Dekker: New York.
81. Mohlin, K., K. Holmberg, J. Esquena, and C. Solans, Study of low energy emulsification of alkyl ketene dimer related to the phase behavior of the system. *Colloids and Surfaces A: Physicochemical and Engineering Aspects*, 2003. 218(1): p. 189-200.
82. Rodríguez-Abreu, C., On the Relationships between the Hydrophilic-Lipophilic Balance and the Nanoarchitecture of Nonionic Surfactant Systems. *Journal of Surfactants and Detergents*, 2019. 0(0).
83. Schulman, J.H. and J. Leja, Control of contact angles at the oil-water-solid interfaces: Emulsions stabilized by solid particles (BaSO<sub>4</sub>). *Transactions of the Faraday Society*, 1954. 50: p. 598-605.
84. Herzig, E.M., K.A. White, A.B. Schofield, W.C.K. Poon, and P.S. Clegg, Bicontinuous emulsions stabilized solely by colloidal particles. *Nature Materials*, 2007. 6: p. 966.
85. Cates, M.E. and P.S. Clegg, Bijels: a new class of soft materials. *Soft Matter*, 2008. 4(11): p. 2132-2138.
86. Cai, D. and P.S. Clegg, Stabilizing bijels using a mixture of fumed silica nanoparticles. *Chemical Communications*, 2015. 51(95): p. 16984-16987.
87. Vilchez, A., C. Rodríguez-Abreu, A. Menner, A. Bismarck, and J. Esquena, Antagonistic effects between magnetite nanoparticles and a hydrophobic surfactant in highly concentrated pickering emulsions. *Langmuir*, 2014. 30(18): p. 5064-5074.
88. Jiang, J., Y. Zhu, Z. Cui, and B.P. Binks, Switchable Pickering Emulsions Stabilized by Silica Nanoparticles Hydrophobized In Situ with a Switchable Surfactant. *Angewandte Chemie International Edition*, 2013. 52(47): p. 12373-12376.
89. Zhu, Y., J. Jiang, K. Liu, Z. Cui, and B.P. Binks, Switchable Pickering Emulsions Stabilized by Silica Nanoparticles Hydrophobized in Situ with a Conventional Cationic Surfactant. *Langmuir*, 2015. 31(11): p. 3301-3307.
90. Malhotra, V., R. Pal, and S. Alhassan, Catastrophic phase inversion of emulsions stabilized by amphiphilic nanoparticles. *Journal of Nanofluids*, 2018. 7(1): p. 30-36.
91. Binks, B.P. and J.A. Rodrigues, Types of Phase Inversion of Silica Particle Stabilized Emulsions Containing Triglyceride Oil. *Langmuir*, 2003. 19(12): p. 4905-4912.
92. Cui, Z.G., L.L. Yang, Y.Z. Cui, and B.P. Binks, Effects of Surfactant Structure on the Phase Inversion of Emulsions Stabilized by Mixtures of Silica Nanoparticles and Cationic Surfactant. *Langmuir*, 2010. 26(7): p. 4717-4724.
93. Ngai, T., S.H. Behrens, and H. Auweter, Novel emulsions stabilized by pH and temperature sensitive microgels. *Chemical Communications*, 2005(3): p. 331-333.
94. Li, Z., W. Richtering, and T. Ngai, Poly(N-isopropylacrylamide) microgels at the oil-water interface: temperature effect. *Soft Matter*, 2014. 10(33): p. 6182-6191.
95. Binks, B.P., R. Murakami, S.P. Armes, and S. Fujii, Temperature-Induced Inversion of Nanoparticle-Stabilized Emulsions. *Angewandte Chemie International Edition*, 2005. 44(30): p. 4795-4798.
96. Iler, R.K., *The Chemistry of Silica*. 1979, New York: Wiley.
97. Stöber, W., A. Fink, and E. Bohn, Controlled growth of monodisperse silica spheres in the micron size range. *Journal of Colloid And Interface Science*, 1968. 26(1): p. 62-69.

98. Facal Marina, P., J. Xu, X. Wu, and H. Xu, Thinking outside the box: placing hydrophilic particles in an oil phase for the formation and stabilization of Pickering emulsions. *Chemical Science*, 2018. 9(21): p. 4821-4829.
99. Gautier, F., M. Destribats, R. Perrier-Cornet, J.-F. Dechézelles, J. Giermanska, V. Héroguez, S. Ravaine, F. Leal-Calderon, and V. Schmitt, Pickering emulsions with stimuable particles: from highly- to weakly-covered interfaces. *Physical Chemistry Chemical Physics*, 2007. 9(48): p. 6455-6462.
100. French, D.J., P. Taylor, J. Fowler, and P.S. Clegg, Making and breaking bridges in a Pickering emulsion. *Journal of Colloid and Interface Science*, 2015. 441: p. 30-38.
101. French, D.J., A.T. Brown, A.B. Schofield, J. Fowler, P. Taylor, and P.S. Clegg, The secret life of Pickering emulsions: particle exchange revealed using two colours of particle. *Scientific reports*, 2016. 6: p. 31401-31401.
102. Chuiko, A.A., V.V. Lobanov, and A.G. Grebenyuk, Structure of Disperse Silica Surface and Electrostatic Aspects, in *Colloidal Silica Fundamentals and Applications*, H.E. Bergna and W.O. Roberts, Editors. 2006, Taylor & Francis.
103. Binks, B.P. and D. Yin, Pickering emulsions stabilized by hydrophilic nanoparticles: in situ surface modification by oil. *Soft Matter*, 2016. 12(32): p. 6858-6867.
104. Binks, B.P., P.D.I. Fletcher, B.L. Holt, P. Beaussoubre, and K. Wong, Phase inversion of particle-stabilised perfume oil–water emulsions: experiment and theory. *Physical Chemistry Chemical Physics*, 2010. 12(38): p. 11954-11966.
105. Binks, B.P. and A.T. Tyowua, Oil-in-oil emulsions stabilised solely by solid particles. *Soft Matter*, 2016. 12(3): p. 876-887.
106. Macedo Fernandes Barros, F., C. Chassenieux, T. Nicolai, M.M. de Souza Lima, and L. Benyahia, Effect of the hydrophobicity of fumed silica particles and the nature of oil on the structure and rheological behavior of Pickering emulsions. *Journal of Dispersion Science and Technology*, 2019. 40(8): p. 1169-1178.
107. Griffith, C. and H. Daigle, Destabilizing Pickering emulsions using fumed silica particles with different wettabilities. *Journal of Colloid and Interface Science*, 2019. 547: p. 117-126.
108. Zang, D., A. Stocco, D. Langevin, B. Wei, and B.P. Binks, An ellipsometry study of silica nanoparticle layers at the water surface. *Physical Chemistry Chemical Physics*, 2009. 11(41): p. 9522-9529.
109. Roberts, W.O., Manufacturing and Applications of Water-Borne Colloidal Silica, in *Colloidal Silica Fundamentals and Applications*, H.E. Bergna and W.O. Roberts, Editors. 2006, Taylor & Francis Group. p. 131-175.
110. Yoshida, A., Silica Nucleation, Polymerization, and Growth Preparation of Monodispersed Sols, in *Colloidal Silica Fundamentals and Applications*, H.E. Bergna and W.O. Roberts, Editors. 2006, Taylor & Francis Group. p. 47-56.
111. Iler, R.K., *The Chemistry of Silica*. 1979, Wiley: New York. p. 173-461.
112. Saigal, T., H. Dong, K. Matyjaszewski, and R.D. Tilton, Pickering Emulsions Stabilized by Nanoparticles with Thermally Responsive Grafted Polymer Brushes. *Langmuir*, 2010. 26(19): p. 15200-15209.
113. Ridet, L., M.-A. Bolzinger, N. Gilon-Delepine, P.-Y. Dugas, and Y. Chevalier, Pickering emulsions stabilized by charged nanoparticles. *Soft Matter*, 2016. 12(36): p. 7564-7576.
114. Li, J. and H.D.H. Stöver, Doubly pH-responsive pickering emulsion. *Langmuir*, 2008. 24(23): p. 13237-13240.
115. Binks, B.P., J.A. Rodrigues, and W.J. Frith, Synergistic Interaction in Emulsions Stabilized by a Mixture of Silica Nanoparticles and Cationic Surfactant. *Langmuir*, 2007. 23(7): p. 3626-3636.
116. Zhuravlev, L.T., Concentration of hydroxyl groups on the surface of amorphous silicas. *Langmuir*, 1987. 3(3): p. 316-318.
117. Shaw, D., *Introduction to Colloid and Surface Chemistry*. [electronic resource]. 4th ed. ed. 2013: Butterworth-Heinemann [Imprint].
118. Pashley, M.R. and E.M. Karaman, *Applied Colloid and Surface Chemistry*. 2004, West Sussex: John Wiley & Sons, Ltd.
119. Israelachvili, J.N. and R.M. Pashley, Molecular layering of water at surfaces and origin of repulsive hydration forces. *Nature*, 1983. 306(5940): p. 249-250.
120. Iler, R.K., *The Chemistry of Silica*. 1979, Wiley: New York. p. 364-367.
121. Shaw, D., Colloid stability, in *Introduction to Colloid and Surface Chemistry*. [electronic resource]. 2013, Butterworth-Heinemann [Imprint]. p. 210-243.
122. Plueddemann, E.P., *Silane Coupling Agents*. 2 ed. 1991, New York Plenum Press.

123. Osterholtz, F.D. and E.R. Pohl, Kinetics of the hydrolysis and condensation of organofunctional alkoxysilanes: a review. *Journal of Adhesion Science and Technology*, 1992. 6(1): p. 127-149.
124. Sears, G.W., Determination of Specific Surface Area of Colloidal Silica by Titration with Sodium Hydroxide. *Analytical Chemistry*, 1956. 28(12): p. 1981-1983.
125. Greenwood, P. and B. Gevert, Aqueous silane modified silica sols: theory and preparation. *Pigment & Resin Technology*, 2011. 40(5): p. 275-284.
126. Lampman, G.M., D.L. Pavia, G.S. Kriz, and J.R. Vyvyan, *Spectroscopy*. 4 ed. 2010, Belmont, USA: Mary Finch.
127. Keeler, J., *Understanding NMR Spectroscopy*. 2 ed. 2010, West Sussex, UK: Wiley.
128. Tanner, J.E., Use of the stimulated echo in nmr diffusion studies. *The Journal of Chemical Physics*, 1970. 52(5): p. 2523-2526.
129. Wäsche, R., M. Naito, and V.A. Hackley, Experimental study on zeta potential and streaming potential of advanced ceramic powders. *Powder Technology*, 2002. 123(2): p. 275-281.
130. Lützenkirchen, J., T. Preočanin, D. Kovačević, V. Tomišić, L. Lövgren, and N. Kallay, Potentiometric titrations as a tool for surface charge determination. *Croatica Chemica Acta*, 2012. 85(4): p. 391-417.
131. Simonsson, I., C. Sögaard, M. Rambaran, and Z. Abbas, The specific co-ion effect on gelling and surface charging of silica nanoparticles: Speculation or reality? *Colloids and Surfaces A: Physicochemical and Engineering Aspects*, 2018. 559: p. 334-341.
132. Huh, C. and S.G. Mason, A rigorous theory of ring tensiometry. *Colloid and Polymer Science Kolloid Zeitschrift & Zeitschrift für Polymere*, 1975. 253(7): p. 566-580.
133. Schönhoff, M., NMR studies of sorption and adsorption phenomena in colloidal systems. *Current Opinion in Colloid & Interface Science*, 2013. 18(3): p. 201-213.
134. Eklund, D. and T. Lindström, Colloidal stability, in *Paper Chemistry: An introduction*. 1991, DT Paper Science Publications: Grankulla, Finland.
135. Iler, R.K., Colloidal Silica-Concentrated Sols, in *The Chemistry of silica*. 1979, Wiley: New York. p. 376-378.
136. Paunov, V.N., B.P. Binks, and N.P. Ashby, Adsorption of Charged Colloid Particles to Charged Liquid Surfaces. *Langmuir*, 2002. 18(18): p. 6946-6955.
137. Blute, I., R.J. Pugh, J. van de Pas, and I. Callaghan, Industrial manufactured silica nanoparticle sols. 2: Surface tension, particle concentration, foam generation and stability. *Colloids and Surfaces A: Physicochemical and Engineering Aspects*, 2009. 337(1-3): p. 127-135.
138. Okubo, T., Surface Tension of Structured Colloidal Suspensions of Polystyrene and Silica Spheres at the Air-Water Interface. *Journal of Colloid And Interface Science*, 1995. 171(1): p. 55-62.
139. Dong, L. and D.T. Johnson, The Study of the Surface Tension of Charge - Stabilized Colloidal Dispersions. *Journal of Dispersion Science and Technology*, 2005. 25(5): p. 575-583.
140. Malmsten, M., P. Linse, and T. Cosgrove, Adsorption of PEO-PPO-PEO block copolymers at silica. *Macromolecules*, 1992. 25(9): p. 2474-2481.
141. Rubio, J. and J.A. Kitchener, Mechanism of adsorption of poly(ethylene oxide) flocculant on silica. *Journal of Colloid and Interface Science*, 1976. 57(1): p. 132-142.
142. Lafuma, F., K. Wong, and B. Cabane, Bridging of colloidal particles through adsorbed polymers. *Journal of Colloid And Interface Science*, 1991. 143(1): p. 9-21.
143. Nozary, S., H. Modarress, and A. Eliassi, Cloud-point measurements for salt plus poly(ethylene glycol) plus water systems by viscometry and laser beam scattering methods. *Journal of Applied Polymer Science*, 2003. 89(7): p. 1983-1990.
144. Mohsen-Nia, M., H. Rasa, and H. Modarress, Cloud-point measurements for (water plus poly(ethylene glycol) plus salt) ternary mixtures by refractometry method. *Journal of Chemical and Engineering Data*, 2006. 51(4): p. 1316-1320.
145. Schantz Zackrisson, A., A. Martinelli, A. Matic, and J. Bergenholtz, Concentration effects on irreversible colloid cluster aggregation and gelation of silica dispersions. *Journal of Colloid and Interface Science*, 2006. 301(1): p. 137-144.
146. Light, T.S. and S.L. Licht, Conductivity and resistivity of water from the melting to critical point. *Analytical Chemistry*, 1987. 59(19): p. 2327-2330.
147. Sadeghi, R. and F. Jahani, Salting-In and Salting-Out of Water-Soluble Polymers in Aqueous Salt Solutions. *The Journal of Physical Chemistry B*, 2012. 116(17): p. 5234-5241.



148. Ananthapadmanabhan, K.P. and E.D. Goddard, A correlation between clouding and aqueous biphasic formation in polyethylene oxide/inorganic salt systems. *Journal of Colloid and Interface Science*, 1986. 113(1): p. 294-296.
149. Binks, B.P., P.D.I. Fletcher, A.J. Johnson, I. Marinopoulos, J.M. Crowther, and M.A. Thompson, Evaporation of Particle-Stabilized Emulsion Sunscreen Films. *ACS Applied Materials & Interfaces*, 2016. 8(33): p. 21201-21213.

148. Ananthapadmanabhan, K.P. and E.D. Goddard, A correlation between clouding and aqueous biphasic formation in polyethylene oxide/inorganic salt systems. *Journal of Colloid and Interface Science*, 1986. 113(1): p. 294-296.
149. Binks, B.P., P.D.I. Fletcher, A.J. Johnson, I. Marinopoulos, J.M. Crowther, and M.A. Thompson, Evaporation of Particle-Stabilized Emulsion Sunscreen Films. *ACS Applied Materials & Interfaces*, 2016. 8(33): p. 21201-21213.